The Integration of Higher Cognition and Internal State Across Development

A Thesis

Submitted to the Faculty

in partial fulfillment of the requirements for the

degree of

Doctor of Philosophy

in

Psychological and Brain Sciences

by

Craig Martin Bennett

DARTMOUTH COLLEGE

Hanover, New Hampshire

04/03/2008

Examining Committee:

_____

George L. Wolford II, Ph.D.

_____

Paul J. Whalen, Ph.D.

_____

Donna Coch, Ed.D.

_____

Abigail A. Baird, Ph.D.

_____

Charles K. Barlowe, Ph.D.
Dean of Graduate Studies

Abstract

For centuries scholars have debated the relationship between mind and body. Some have sought to unify these two entities as necessarily intertwined. Others have taken the view that the mind and body are separable objects that can exist independently. Modern cognitive neuroscience has provided evidence for the view that information from the body is critical for navigating our world. The new perspective of embodied cognition is that the neural systems supporting internal information processing are also uniquely suited to support higher cognitive functions, such as decision making and action planning. Further, it has been shown that the cortical areas supporting higher order integration of internal state information have a protracted developmental trajectory. This series of experiments was designed to improve our knowledge of internal state information processing in adulthood and characterize how this processing changes across the years of adolescence.

The results of these experiments highlight the unique role of internal state information in the brain. The first finding is that early sensory areas considered to be 'primary interoceptive cortex' are actually much more multimodal than previously thought. The second finding is that a distinction between interoceptive and exteroceptive information does exist at a higher, more abstract level of processing. The third finding is that there are few developmental differences between adolescents and adults in terms of first-order interoceptive sensory processing. Finally, the fourth finding is that areas involved in higher-order interoceptive processing do show marked developmental differences between adults and adolescents. The window of time between the onset of adolescence and young adulthood contains some of the greatest changes the body experiences after infancy. Areas of the brain supporting internal state processing must change as well.

Acknowledgements

"The lyf so short, the craft so long to lerne"

- Geoffrey Chaucer, "The Parliament of Fowls"

Graduate education has been one of the greatest adventures of my life. At once it has been the most frustrating and challenging thing I have ever done while simultaneously being one on the single greatest joys I have experienced. With the completion of this thesis I have now finished the first step in what I hope will be a long career in support of scientific truth.

I would first like to thank Abigail Baird, who has been nothing short of amazing over the last five years. Through all the trials and tribulations of my education she has never failed to be there when I needed her. She is one of the most loyal and loving people mentors I have ever had, which is one of the highest compliments I can give.

I would also like to recognize Daniel Ansari and George Wolford. These men were selfless in their support and gave freely of their time and energy when I needed their input. If this thesis has accomplished anything it is because of their assistance at critical periods along the way. I am also obliged to thank George's air compressor, per our 2007 agreement.

A special thanks goes out to my incredible wife Sarah. While graduate school has been an amazing adventure, it pales in comparison to my marriage to her. I cannot wait to see where our travels will take us in the future Finally, I would like to thank my mother and father. It has been a long road of 25 years since they first enrolled me in preschool to the day I received my PhD. I literally couldn't have done it without you – I love you both.

Table of Contents

List of Tables

List of Figures

General Introduction

I. Background and Significance

Each second, an incredible amount of information regarding the internal state of your body is made available to your brain. Through receptors that observe the internal milieu, visceral, vestibular, and musculoskeletal systems a complete picture of the current state of the body can be assembled. How the brain assembles this diverse set of sensation into a coherent picture of homeostatic state remains a mystery. Further, while internal state information seems to be a critical part of higher cognition, we know very little about how this information is accessed and integrated across diverse regions of the brain. Therein lies the heart of this thesis: to better understand how internal state information is represented in the brain and integrated with higher cognitive processes. By adopting a developmental approach we hope to not only gain knowledge related to internal information processing, but to also map out the maturation of the mind-body relationship from adolescence to adulthood.

Mind-Body Dualism

Throughout history scientists and philosophers alike have pondered the nature of mind and body. What are they made of? How are they related? For Descartes the mind and body were composed of entirely different substances, one of mechanical clockwork and the other of the ethereal soul (Baker & Morris, 2002; Descartes, 1990). In other perspectives the mind and body were as one, with each specially adapted to support the other (Della Rocca, 1996; Spinoza, Boyle, & Parkinson, 1989). For a thousand years the duality of mind and body has been debated in this manner. Over time some measure of truth has accrued. For instance, we now recognize that cognition and emotion are not reciprocal functions that exist only at the expense of the other. We now believe that they are synergistic and heavily intertwined, both supporting effective navigation of the world (Antonio R. Damasio, 1994).

Still, many questions remain. Even with the power of modern cognitive neuroscience much of the relationship between mind and body remains unexplored.

While early philosophers could only conjecture about the inner workings of the mind, today an impressive set of tools and methods enable us to reveal what was previously hidden. To approach the issue of dualism from a scientific point of view it is necessary to examine the point where the body and mind are thought to meet: the brain. While some degree of information processing goes on in the peripheral nervous system outside the brain, the vast majority of operations occur in the brainstem and cerebral cortex in the central nervous system (Craig, 2002). It is here that the diverse signals from the body are processed and first made into representations of body state. It is also here that the first major division of afferent information from the body takes place (Critchley, 2005). This division is made by the separation of all incoming sensations as either originating from within the body [interoceptive] or from the external environment [exteroceptive]. It is this foundation of internal, interoceptive information that is relevant to the discussion of dualism. From this wealth of internal sensation the first abstracted representations of the current body state are created. These representations are also the foundation of emotion, which may well be construed as the unique link between mind and body.

Historical Perspectives on Interoception & Emotion

The modern study of emotion traces its roots back to Charles Darwin, who first examined the common elements of emotional expression. Darwin was attempting to better understand why some animals engage in behaviors that have no known purpose, behaviors we would now perhaps call genetically driven. Why do dogs circle the floor several times before lying down to sleep? Why do older cats still knead a warm, soft surface as if preparing to feed from their mother? For Darwin these habitual movements were vestiges of the animal's evolutionary past (Darwin, 1872). True to his theory of natural selection in "The Origin of Man", emotion must have conveyed a survival advantage to a distant

evolutionary ancestor for it to be so pervasive in animals and man today (Darwin, 1859).

After observing the behavior and reactions of numerous species Darwin came to the conclusion that the emotional behaviors seen in animals are homologues for the human expression of affect. Thus, when a dog bares his teeth to show anger it is the same as when a human snarls to do the same. Darwin was also one of the first to look at emotional expression across cultures, determining that some expressions are universal across human experience. One emotion that Darwin saw to be common between individuals was grief, which he found to be similar around the world. From these investigations he postulated that there are a limited set of 'basic' emotions upon which more complex constructions are based (Dalgleish, 2004; Darwin, 1872).

Following shortly after Darwin was another scientist who had a profound impact on the study of emotion, William James. While Darwin focused heavily on the expression of emotion across species, James was chiefly interested in the experience of emotion in humans. In trying to understand the genesis of emotion James was increasingly drawn toward the body as the foundation for emotional experience. He saw emotion as the bridge connecting the current state of the body and the present cognitive state. In his classic quote from the Principles of Psychology (James, 1890):

"If we fancy some strong emotion and then try to abstract from our consciousness of it all the feelings of its characteristic bodily symptoms, we find we have nothing left behind, no 'mind-stuff' out of which the emotion can be constituted, and that a cold and neutral state of intellectual perception is all that remains."

It is this focus on the body that is the hallmark of James' theory on emotion. James argued against the common sense view, which is that we have a perception, experience an emotion, and only then perceive a bodily response. He argued that we instead have a perception, experience changes in the body consequent to the perception, and only then experience the emotion. James stated that "the bodily changes follow directly the perception of the exciting fact, and that our feeling of the same changes as they occur is

emotion." (James, 1890). In this manner sweaty hands would lead to the perception of moisture on the palms, which would lead to the feeling of being anxious.

As a thought experiment James considered what emotion would be without its physical manifestation. He came to the conclusion that, "a purely disembodied human emotion is a nonentity" (James, 1890). This position has strong implications for dualism, with the body and mind considered inseparable with regard to emotion. Carl Lange proposed similar ideas concurrently with the work by William James, yielding the complete James-Lange theory of emotion (Lange, James, & Haupt, 1922). While many have since criticized the theory as incomplete (Antonio R. Damasio, 1994) or just plain wrong (W. Cannon, 1914, 1927), this theoretical construct gave the scientific world a standard against which to judge other proposed theories of emotional experience. A common thread has emerged from this research: that aspects of the original James-Lange may have been correct. Areas of the brain necessary for emotional experience are also areas that are heavily tied to the processing of bodily sensation.

Modern Theories of Interoception & Emotion

Beginning in the 1960s a new generation of neo-Jamesean researchers began to again examine the role of the body in the generation of emotion. One important figure of this period was Stanley Schachter. Schachter's Two Factor Theory of Emotion stated that there are two components of emotional experience: physiological arousal and contextual cognition (Schachter & Singer, 1962). Schachter agues that physiological arousal alone is not sufficient for the production of emotion. It is the context provided by cognition that is the key to emotional experience. This is a notable addition to the original James-Lange theory as it adds an evaluative component to the changes that occur in the body. This addition helps to accommodate one of Walter Cannon's main critiques of the James-Lange theory: that identical changes occur in the viscera for many different emotional states (W. Cannon, 1927). According to Schachter's theory it is the cognitive context that

differentiates them.

The evidence Schachter cited for his theory came from altering the physiological state of the body while varying the context in which changes occur. One such experiment (Schachter & Wheeler, 1962) began by giving some subjects an injection of epinephrine. In this manner researchers could reliably elicit a sympathetic nervous system response throughout the body. The researchers also varied the amount of information the subjects had on the injection, with some subjects knowing the shot would give rise to sympathetic effects and others being ignorant of the effects or uninformed. The subjects were then placed in conditions of contextual anger or euphoria. The results of the study showed that euphoria and anger were elevated only when the subject did not know the injection was the cause of the sensations. For Schachter this was strong evidence of multiple factors in the generation of emotion.

In the years since Schachter first proposed his theory many problems have arisen. Issues stemming from the theoretical foundation and the method of investigation have been extensively discussed (see Reisenzein, 1983). The primary criticism levied against the theory is that Schachter and Singer were not entirely successful in creating emotions purely based on contextual differences. Experiments attempting to replicate Schachter and Singers experiments would often result in effects opposite to what Schachter reported. Also, effect sizes were rather small when the experiments did work as planned. It is for reasons such as this that Cotton (1981) remarked that "time has not been charitable" to Schachter's theory. Still, the fundamental contribution of Schachter remains: that cognitive context plays a critical role in emotional experience.

During the last 20 years many researchers have sought to combine the expanding knowledge of information processing in the brain with historical emotion theory. One scientist with this approach is Antonio Damasio. Together with his colleagues in Iowa he created what is commonly known as the Somatic Marker Hypothesis of Decision-Making (Antonio R. Damasio, 1994). While it is not strictly a theory of emotional experience, it

does elaborate on how emotion is processed in the brain and subsequently used in higher cognition. For Damasio there was a clear distinction between emotion and feeling. Emotion is the brain's representation of internal body states. These representations may be taken from the current state of the body or the result of a brain-based prediction mechanism. Feelings, on the other hand, are the conscious awareness of the present emotional state. These are more highly abstracted, and represent the summation of underlying emotions.

The most important contribution of the Somatic Marker Hypothesis was the assertion that emotional information is used throughout the brain to assist higher cognitive processes, such as problem solving, learning, and decision-making. This position was contrary to the more typical belief that emotional experience interfered with successful 'cold' cognition (Loewenstein & Lerner, 2003). Damasio's position was that emotional information is important as a biasing agent in decision-making, or when the task at hand becomes very complex or uncertain. In a world of infinite possibility the emotional valence of each option can quickly reduce the amount of information to be processed. Much of Damasio's evidence came from lesion studies, collected at the University of Iowa and elsewhere. In patients who exhibited a missing "somatic marker" there was often damage in areas of the brain known to have access to both internal state information and executive working memory (Bechara, Damasio, & Damasio, 2000; A. R. Damasio, 1996). Damasio cited areas of cingulate, insula, and especially ventromedial prefrontal cortex as necessary for the Somatic Marker to operate.

A final theory of emotional experience to consider is the combined work of Arthur Craig and Hugo Critchley. While their ideas have generally been voiced separately, when put together their work is highly complimentary. Craig's research focuses on the representation and experience of internal visceral information in the brain and Critchley's research centers on how autonomic states interact with higher cognition. While the foundation of their approaches are not fundamentally different from other theories of emotion, their focus on the neurobiology of emotional experience is quite novel. For example, Craig has studied

interoceptive experience from the cellular level on up to the level of cortical regions. Both scientists have used a variety of psychophysiological tools to probe the generation, experience, and effects of emotion.

Three points are important to note about the Craig-Critchley approach. First is that interoceptive information has a privileged status in the human brain. A disproportionate amount of cortical and subcortical tissue is devoted to the processing of interoceptive information in homo sapiens (Craig, 2002). When compared to other great apes humans have the capacity to possess a much more complete representation of internal state (Blomqvist, Zhang, & Craig, 2000). For Craig, differences in emotional experience arise from the ability to process that information and bring it into awareness. The second point of Craig and Critchley to consider is that there are multiple levels of emotion representation in the brain (Craig, 2004b; Critchley, Mathias, & Dolan, 2001). First-order representations are close to what Damasio meant in his definition of emotion. They are the first depiction of the present body state in the brain. Second-order representations are abstracted from first-order information for integration with higher cognitive processes. This is where emotions come into conscious awareness and are elaborated on by the current cognitive context. The third point of Critchley and Craig is that the mind and body are tied together not only in the parsing of afferent internal state information, but also in the efferent regulation of arousal states. Critchley postulates that the setting of autonomic state in the body is directly tied to the current cognitive demands of the task at hand (Critchley, Mathias et al., 2003; Critchley, Tang, Glaser, Butterworth, & Dolan, 2005). Through the ideas of Craig and Critchley a sort of grand-unified-theory of mind-body information processing emerges. Interoception, emotion, and autonomic responses can be seen as different facets of the same mechanism, set up to monitor and control body state for optimal performance.

Recent theories of emotion have added much to the historical views of earlier scientists and philosophers. It is important to note that the more we understand about emotion in general the more important a role it seems to play in the brain. In the last century we have

seen emotion move from a scientific curiosity to sharing a central role in higher cognition. From this research it is also apparent that the body influences the mind in ways not thought possible several decades ago.

Afferent Mechanisms: Interoceptive Input

It was in 1906 that Sir Charles Sherrington first coined the term 'interoceptor' to describe the group of sensory cells that provide information on internal body state (Sherrington, 1906). As originally defined the term meant only the production of visceral sensation. Today that definition has expanded to include the current homeostatic condition of the entire body and the ability for this information to reach conscious awareness (Craig, 2003b). An important aspect of contemporary interoception is the intimate link between internal state and emotion. Virtually all interoceptive sensations have a motivational, affective component to their perception. This is largely due to the prominent role of interoception in homeostasis. Homeostasis, as first termed by Cannon (W. B. Cannon, 1932), is the dynamic equilibrium of processes aimed at an organism's survival. The interoceptive feeling of hunger would lead an organism to food-seeking behavior, and the feeling of cold thermal distress would lead one to seek warmth. A simplified schematic diagram of interoceptive afferent input to cortical areas is presented in Figure 1.

Evidence for the broader view of interoception comes from studies illustrating that multimodal internal state information is conveyed and processed together in the spinal cord and brainstem. Early processing of pain, temperature, itch, muscle burn, hunger, thirst, taste, and sensual touch are all conducted in similar cortical and subcortical regions (Craig, 2002; Saper, 2002). Studies have also shown that the transmission of bundled interoceptive information is anatomically separate from information related to the external environment. For instance, at the level of the spinal cord pain and temperature pathways are resident in the contralateral spinothalamic projection and fine touch discrimination resident in ipsilateral lemniscal projections (Iannetti et al., 2003). In the thalamus a viscerotopically

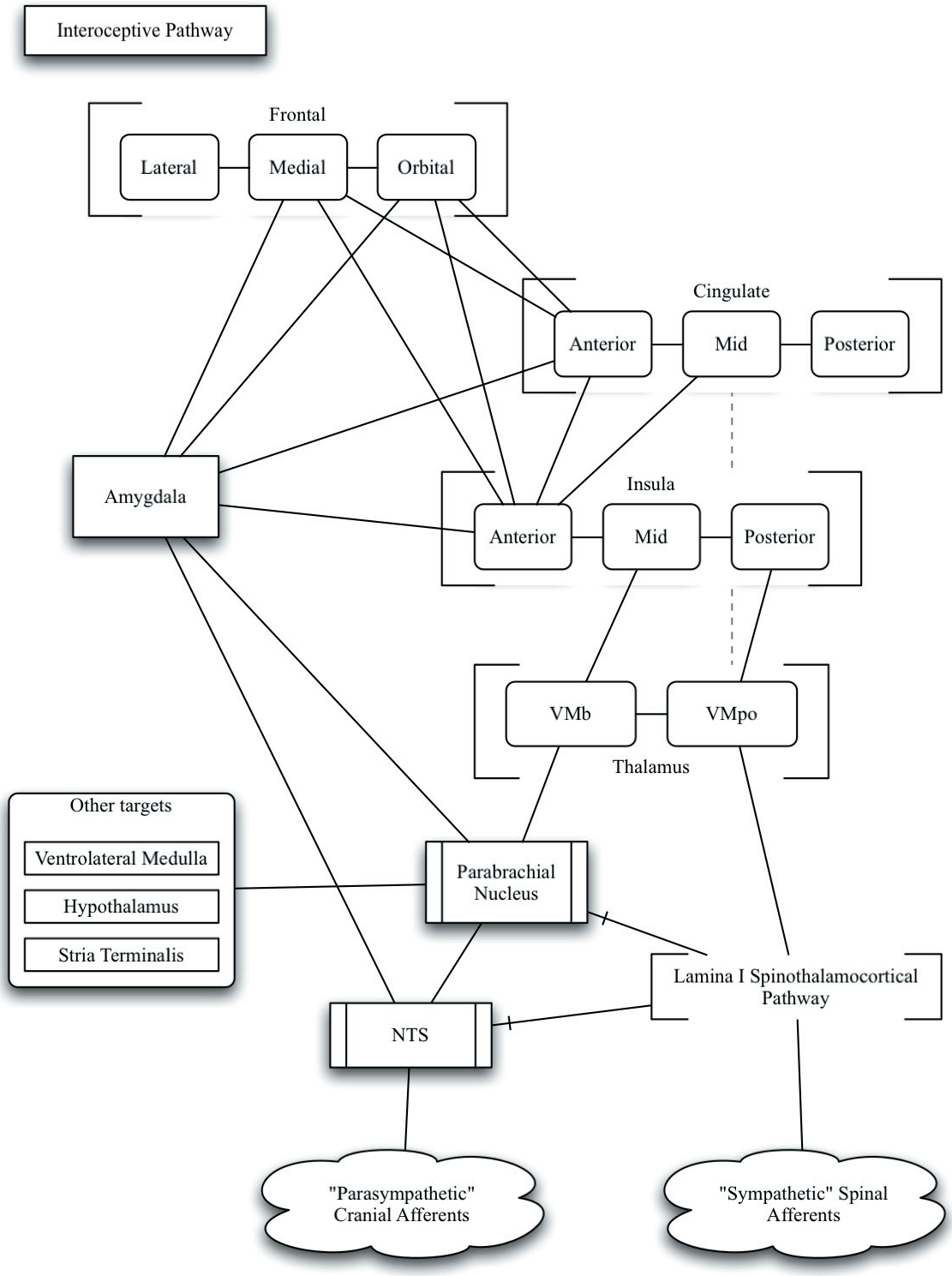

Figure 1. Schematic representation of the interoceptive afferent system. The majority of sympathetic afferents from the body are conveyed by way of the lamina I spinothalamocortical pathway. While this pathway projects to major brainstem regions its primary target is the thalamus, which relays the information to interoceptive cortex in the insula and mid cingulate.

organized region of the ventroposterior medial nucleus conveys body state information to cortical regions (Craig, 2004a; Craig, Bushnell, Zhang, & Blomqvist, 1994). At the level of the cortex internal state information continues to be segregated. In both primates and humans bilateral posterior insula and areas of SII somatosensory cortex are the locus of first-order interoceptive information processing (Brooks, Zambreanu, Godinez, Craig, & Tracey, 2005; Frot, Magnin, Mauguiere, & Garcia-Larrea, 2006; Hua le, Strigo, Baxter, Johnson, & Craig, 2005). Beyond these cortical centers internal sensory information becomes abstracted and cannot be considered distinctly interoceptive.

There is an increasing amount of evidence that the cortical representation and re-representation of body state is the foundation for conscious awareness of 'how you feel'. The general feeling of homeostatic condition is not made up of myriad hunger pangs, temperature sensations, and thoughts of blood pressure magnitude. Instead it is an abstracted integration of all these sensations, and more. While debate continues regarding the information processing necessary to create this abstracted perception, there is a fair degree of certainty regarding which cortical regions are involved. Areas that are known to play a role in the higher-order processing of interoceptive information include anterior insula, anterior cingulate, medial prefrontal cortex, and orbitofrontal cortex. It is in these areas that the motivational value of interoceptive information comes to influence conscious will. The second-order interaction of interoceptive information and higher-order cognition is a major piece of the experiments of this thesis.

Efferent Mechanisms: Autonomic Output

The autonomic nervous system represents the primary method of efferent internal state regulation in the human body. It not only maintains a positive homeostatic condition throughout the body but also sets the body state to suit environmental challenges. While most theories of emotion detail how incoming information influences emotional experience, overall very little attention is paid to how the brain sets the state of the body

to accommodate internal and environmental demands. Much of this function falls to the efferent mechanisms of the autonomic nervous system. The autonomic system is divided into two efferent branches, the sympathetic and parasympathetic. Generally these branches act in reciprocal opposition to each other, with each serving a role in energy balance throughout the body. The sympathetic branch involves behaviors and actions that involve energy expenditure. Examples of sympathetic responses include increased heart rate, dilated pupils, and increased blood flow to skeletal muscles. Fight-or-flight responses are sympathetic in nature, as they require a dramatic increase in energy use to run or defend. In contrast, the parasympathetic branch involves behaviors and actions that involve energy conservation. Conservative behaviors include decreased heart rate, constricted pupils, and increased blood flow to the gastrointestinal tract. The shorthand for parasympathetic responses is "rest and digest", which refers to the conservation and regeneration of energy involved in behaviors of this axis.

There are numerous subcortical areas that play a role in sympathetic and parasympathetic autonomic control. Most basic autonomic reaction patterns are generated by nuclei in the hypothalamus, pons, and brainstem. Several of these nuclei, especially in the brainstem and pons, serve functionally distinct roles. One example is the rostral medullary raphe in the brainstem, which is considered to be a thermoregulatory pattern generator (Saper, 2002). A second example is the ventrolateral medulla, which regulates arterial perfusion of tissues throughout the body (Morrison, 2001). Through the combination of multiple basic response patterns a larger set of more complex autonomic responses can be assembled. These highly integrated responses are usually generated at the level of the hypothalamus, which can use its connections to compose coherent autonomic responses (Saper, 2002). A good analogy would be the brainstem nuclei as musicians in a symphony orchestra able to be directed by a single conductor. While each player creates music individually, it is the sum of the responses that make up differentiable autonomic states that we associate with emotions. An example of this mechanism at work would be a coordinated fight-or-

flight response initiated by the amygdala, coordinated by the hypothalamus, and fulfilled in lower brainstem autonomic regions.

While much of the second-to-second regulation of homeostatic state is controlled by subcortical structures it is known that regions of cerebral cortex can also strongly influence autonomic state. Areas of anterior insula, anterior cingulate, medial prefrontal, and orbitofrontal cortex all have strong autonomic connections to the hypothalamus and lower brainstem areas (Nauta, 1971; Neafsey, Hurley-Gius, & Arvanitis, 1986; Terreberry & Neafsey, 1983). While the anatomical connections between these areas have been thoroughly mapped very little is known regarding when top-down control of autonomic state is engaged. The best theory states that cognitive effort of any kind evokes autonomic arousal. Activity in the dorsal anterior cingulate has shown to covary with many sympathetic measures, such as heart rate (Critchley, Rotshtein et al., 2005), blood pressure (Critchley, Corfield, Chandler, Mathias, & Dolan, 2000), and electrodermal response (Critchley, Elliott, Mathias, & Dolan, 2000). From this evidence a larger role for the anterior cingulate may be in order, with autonomic control occurring in the midcingulate, an area known to project to receive body state information form the thalamus and project to subcortical autonomic centers.

The Insula

Critical to the understanding of interoception is a discussion of insula anatomy and function. The *lobus insularis* is an isolated region of cortex just outside the extreme capsule of subcortical white matter fibers that is typically hidden by frontal, parietal, and temporal opercula (see Figure 2). The insula was first described by Reil (1890), who characterized it as an island of cortex buried deep within the Sylvian fissure. Even today some researchers reference the insula as the 'Island of Reil'. Following Reil there was much debate regarding whether the insula was a center for speech or taste. Penfield and Faulk (1955) tested this by using direct electrical pulses in conscious participants to map

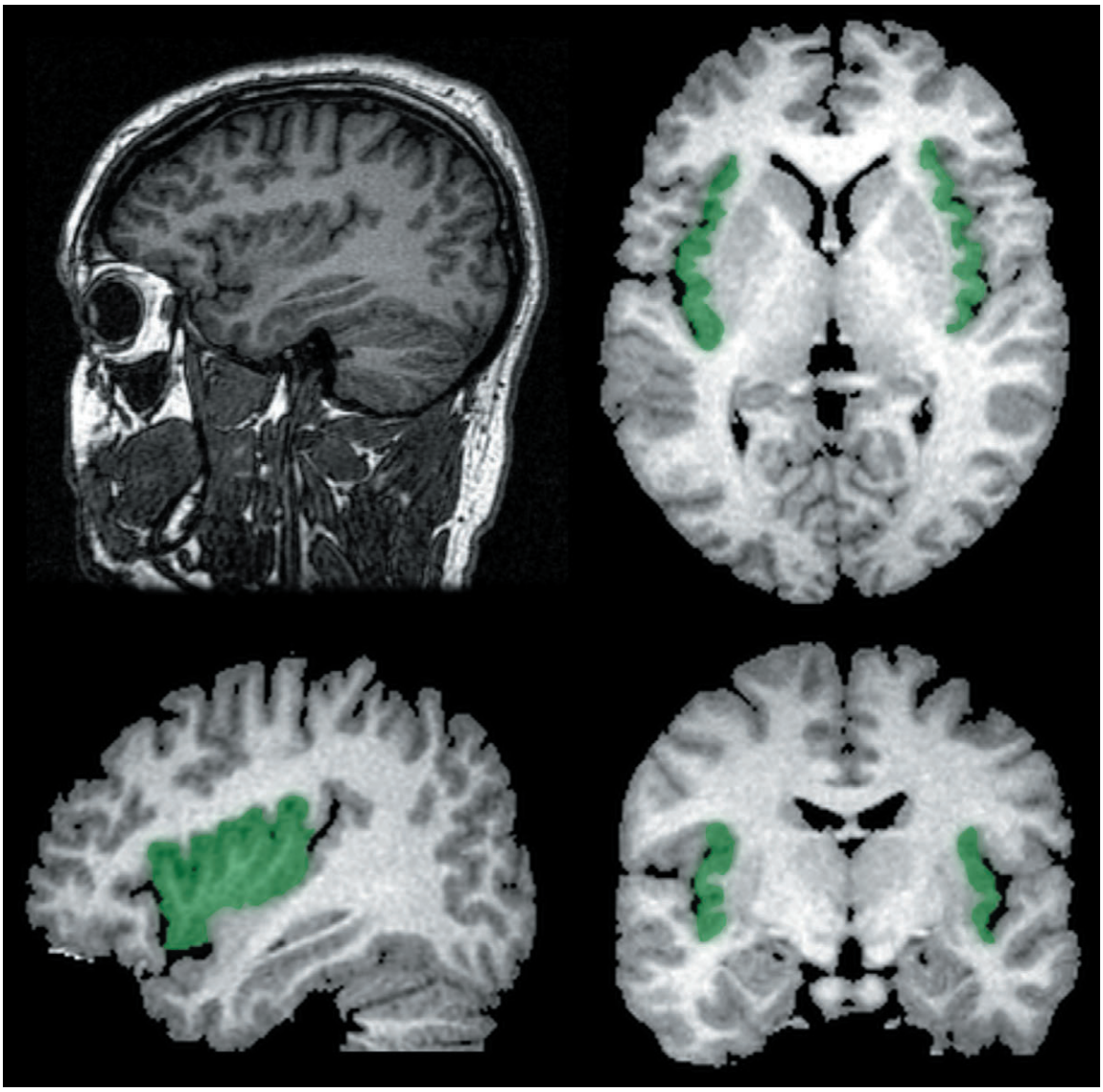

Figure 2. Anatomical location of the insula. The insula is depicted as the green shaded region in the sagittal plane (bottom left), axial plane (top right), and coronal plane (bottom right). A whole-head sagittal plane is shown in the top left for reference.

out the effects of insula stimulation. They found that the insula included areas of viscero-sensory and viscero-motor control, but they could not separate these functions out into separable sensory and motor regions. Today we find that the insula has been implicated in an unusually wide range of cognitive abilities. For example, the insula is known to play a role in language production, motor association, selective visual attention, and verbal working memory (Augustine, 1996). Even with this wide array of functions the insula is still best known for its role in visceral representation, gustation, and olfaction.

There are two traditional methods used to anatomically subdivide insular cortex. The first method is based on insular gyrification and involves the dividing the region into two parts based on the insular central sulcus. This forms an anterior aspect and a posterior aspect of the insula that my be further subdivided if pre- or post-central sulci exist (Naidich et al., 2004). However, further subdivision is rarely done due to the highly variable number of gyri observed across individuals. The number ranges from four to seven with an average number of five gyri (Ture, Yasargil, Al-Mefty, & Yasargil, 1999; Varnavas & Grand, 1999). The number of insular gyri can even vary by hemisphere within the same individual (Naidich et al., 2004). A better approach has been to divide the insula into more general subregions based on cytoarchitectonics. Using this method, regions of anterior, mid, and posterior insula emerge based on the granular appearance of stellate cells in its cortical layers (Augustine, 1985, 1996). Posterior insula has a granular structure, mid insula is defined as dysgranular, and anterior regions of the insula are said to be agranular (E. G. Jones & Burton, 1976; Mesulam & Mufson, 1982; Shi & Cassell, 1998). These divisions seem to more closely mirror regional connectivity and functional divisions across insular cortex (Augustine, 1996; Dupont, Bouilleret, Hasboun, Semah, & Baulac, 2003).

Taken as a whole the insula possesses a wide range of connections to almost every part of cortex in addition to many major subcortical areas. Still, the specific pattern of connectivity varies a great deal across the cytoarchitectonic divisions of the insula. The posterior granular areas of the insula receive a large amount of sensory information from

ventromedial thalamus and primary somatosensory cortex (Allen, Saper, Hurley, & Cechetto, 1991; Augustine, 1985; Craig, 2004a). It is also the target of afferent connections from areas of the superior temporal sulcus, dorsolateral striatum, and the basolateral amygdala (Chikama, McFarland, Amaral, & Haber, 1997). Efferent projections of the posterior insula connect to areas of frontal cortex, temporal pole, secondary somatosensory cortex, and ventral striatum (Dupont et al., 2003). Many scientists describe the posterior insula as primary interoceptive cortex, owing to the number of visceral afferents terminating there (Craig, 2003b). This has been supported by a number of functional imaging studies showing that the posterior insula is involved in thermal change (Craig, Chen, Bandy, & Reiman, 2000; Frot, Magnin, Mauguiere, & Garcia-Larrea, 2007), painful electric shock (Christmann, Koeppe, Braus, Ruf, & Flor, 2007), and rectal distention (Eickhoff et al., 2006). There is evidence that the layout of visceral processing in the posterior insula is somatotopic, with lower body structures in posterior areas and upper body structures in anterior areas (Brooks et al., 2005; Hua le et al., 2005).

The dysgranular mid insula straddles the area between posterior and anterior areas of the insula and has strong reciprocal connections to both. It also receives afferents from primary somatosensory cortex, superior temporal sulcus, and ventral thalamus (Augustine, 1996). It has projections to supplementary motor cortex, frontal operculum, orbital cortex, superior temporal sulcus, secondary somatosensory cortex, basolateral and corticomedial amygdala, and entorhinal cortex (Dupont et al., 2003). Because of its 'in-between' location very little is known specifically about the mid insula. It appears to play a role in secondary sensory integration and multisensory processing, making abstract representations of sensory stimuli available to the anterior insula and other areas of higher-order cortex (Leone et al., 2006).

The agranular anterior insula is a higher-order integration area that takes abstracted information from the mid and posterior insula and combines it with higher-order operations such as executive control. It receives afferents from entorhinal cortex, ventral striatum,

hypothalamus, and the thalamus (Augustine, 1996). It then projects to areas of the anterior cingulate, entorhinal cortex, ventral striatum, and periamygdaloid cortex (Dupont et al., 2003). One important function of the anterior insula the generation of generalized motivational states. These states are usually based on current homeostatic needs such as food or water (McKinley, Denton, Oldfield, De Oliveira, & Mathai, 2006 ; Rolls, 2006), but can also be constructed from more abstract desires or wants. A recent lesion study by Naqvi et al. (2007) demonstrates this concept through the lens of addiction. The authors found that damage to areas of left or right anterior insula disrupted the addictive desire for nicotine in chronic smokers. One subject in the study smoked up to 40 cigarettes a day before experiencing an insular stroke. After they were admitted to the hospital they never had another cigarette, with one patient commenting "I forgot I was a smoker" and "my body forgot the urge to smoke".

The anterior insula is also thought to play a role in the initiation of executive control. Recent functional imaging evidence has shown that the anterior insula/frontal operculum is part of a regional network that shifts the brain out of the default mode of processing and into a state of active executive control. Using metrics of resting state functional connectivity the insula/operculum was shown to initiate task control and also provide for the maintenance of cognitive sets during executive manipulation (Dosenbach et al., 2007; Dosenbach et al., 2006). Finally, the insula is thought to play a role in decision-making, risk perception, and consequence representation. A critical aspect of this ability is the representation of negative outcomes in decision-making (Berns et al., 2006; Paulus, Feinstein, Leland, & Simmons, 2005). While areas of orbital prefrontal cortex represent the positive outcomes of a decision based on their hedonic value (Bechara et al., 2000; Kringelbach, 2005), the insula can represent negative outcomes based on their negative emotional valence (Paulus, Rogalsky, Simmons, Feinstein, & Stein, 2003).

II. Disorders of Interoceptive Experience

Alexithymia

In Greek alexithymia literally means "without words for feeling". Sifneos (1972) first used the term to describe a group of individuals with a similar disturbance in their affective functioning. This group was unable to relate their somatic sensations to higher order cognitions, such as past memories, present thoughts, and future planning. In short, while they have first-order interoceptive information available they are unable to integrate it into second-order cognitive representations. While there are some individual differences in the manifestation of alexithymia several core aspects of this disorder are consistent across cases. Taylor, Bagby, and Parker (1997) characterize Alexithymia as [i] difficulty identifying feelings and distinguishing between feelings and the bodily sensations of emotional arousal; [ii] difficulty describing feelings to other people; [iii] constricted imagination, as evidenced by a paucity of fantasies; and [iv] a stimulus-bound, externally oriented cognitive style.

Much of the past research on alexithymia has been focused on individual deficits in emotional experience. However, several recent studies have demonstrated higher-order cognitive deficits in alexithymics. Lane et al. (1996; 2000) found that both verbal and nonverbal recognition of emotional stimuli was impaired in alexithymics. Bydlowski et al. (2005) found that alexithymic patients had difficulty describing the emotional experience of others in hypothetical situations. Other research follows a similar pattern, with alexithymic patients showing deficits in internal state discrimination and emotion recognition (Aleman, 2005).

The etiology of alexithymia is unidentified, but much is known about the resulting abnormalities in the structure and function of the brain. One structure that seems to play a prominent role in the interoceptive dysfunction of alexithymia is the cingulate. Mantani et al. (2005) found that when engaging in emotional mental imagery alexithymia patients

showed significantly reduced regional activity in the posterior cingulate when compared to normal controls. Similar activity differences have also been observed bilaterally in the anterior cingulate (Berthoz et al., 2002) and mid-insula (Kano et al., 2003). As mentioned earlier, these are regions known to integrate current body state and current cognitive goals. Together these results reinforce the importance of abstracted internal state information and illustrate the effects of having interoceptive information poorly integrated with higher cognition.

Pain Asymbolia

The normal experience of pain is created through the combination of separable sensory and affective components. Pain asymbolia refers to deficits in the affective component of pain, leaving the sensory component as the sole cortical processor of nociceptive sensation (Schilder & Stengel, 1931). Patients with asymbolia can perceive that painful stimuli exist and can accurately report the spatial location of the stimulation. However, they lack the emotional and motivational responses that accompany pain. For example, an asymbolia patient would be able to report that a dinner plate was painfully hot, but would not feel compelled to remove their hand from the plate. Some patients even smiled or laughed when given painful stimulation (Berthier, Starkstein, & Leiguarda, 1988). These affective deficits seem to arise from damage to areas of the anterior insula and anterior cingulate (Price, 2002). These structures are considered aspects of the medial pain system and are critical in assigning motivational significance to internal state sensations (Coghill, Sang, Maisog, & Iadarola, 1999; Craig, 2003a; Vogt, 2005). The results of lesion work have been validated in normal participants through the use of functional imaging. Studies have found that the unpleasantness of pain was encoded by areas of the dorsal mid-insula (Schreckenberger et al., 2005) and the anterior cingulate (Fulbright, Troche, Skudlarski, Gore, & Wexler, 2001).

It is also possible to have damage to the sensory component of pain while sparing

the affective component. A patient was described by Ploner et al. (1999) who had a right postcentral lesion affecting areas of primary and secondary somatosensory cortex. The patient was unable to experience painful sensations along their left side. When thermal stimulation was increased to painful levels the patient was able to report a 'clearly unpleasant' feeling during stimulation, but they were unable to identify its source or location. These results combine with those of asymbolia to illustrate the contributions of different cortical regions on interoceptive information. Somatosensory cortex and posterior insula seem to play a role in the primary decoding of interoceptive sensations, providing information on stimulus intensity and location. Areas of the anterior insula are more closely related to the motivational and affective aspects of interoceptive processing. In the case of pain, the insula is the avenue through which future action planning can be influenced.

Pure Autonomic Failure

Pure autonomic failure [PAF] is a condition wherein the autonomic nerves of the peripheral nervous system cease to conduct information. Specifically, connections within the autonomic ganglia break down, leaving the central and peripheral systems disconnected. This type of damage to the autonomic system appears to be quite specific, as other sensory and motor pathways remain intact (Bannister, 1988). While PAF has no known cause, the autonomic degeneration has been associated with the presence of Lewy bodies and abnormal alpha-synuclein in autonomic ganglia (Hague, Lento, Morgello, Caro, & Kaufmann, 1997; Kaufmann, Hague, & Perl, 2001). These are features usually found in Parkinson's disease, which may help explain why PAF is almost exclusively diagnosed in middle age or later (Bannister, Mathias, & Polinsky, 1988). The most consistent symptom in PAF is orthostatic hypotension, a significant drop in blood pressure with standing (Bannister et al., 1988). Other common symptoms of PAF include the absence of thermoregulatory sweating (Collins, 1988) and the absence of a galvanic skin response (Magnifico, Misra, Murray, & Mathias, 1998). All are due to the disconnection of autonomic centers in the

brain and the effector organs in the periphery.

While PAF and related autonomic disorders have been identified for decades it is a relatively rare disorder, which makes large-scale experimentation difficult. For this reason it is only recently that PAF has been examined with modern neuroimaging tools. Voxel-based-morphometry has been used to compare the anatomical structure of PAF brains with those of age-matched controls. Reductions in gray matter volume were observed in the left anterior cingulate, right anterior insula, and right inferior prefrontal gyrus (Critchley, Good et al., 2003). Additionally, the severity of PAF symptoms was correlated with the amount of left cingulate gray matter volume. Functionally, task-independent differences in BOLD activity have been found in the pons, hypothalamus, somatosensory cortex, and insula (Critchley et al., 2001). During tasks that require cognitive or physical effort, tasks that would ordinarily elicit a sympathetic autonomic response, increased BOLD activity was observed in the anterior cingulate and decreased BOLD activity was observed in the posterior cingulate.

The impact of PAF on higher cognition is still under debate. An early study by Heims et al. (2004) found that PAF had no significant impact on tests of motivational decision-making, recognition of emotional facial expressions, and tests of social cognition. However, a more recent study by Heims et al. (2006) found that around 40% of patients diagnosed with PAF exhibit one or more cognitive deficits. It is still unknown if the observed cognitive deficits are due to a lack of autonomic feedback information or resulting from reduced blood pressure found in almost all cases of PAF. It seems likely, however, that cingulate gray matter atrophy seen in PAF patients may play a role in potential cognitive decline.

Schizophrenia

Schizophrenia is a complex disorder affecting a wide array of cognitive and emotional abilities. One of the most commonly documented negative symptoms of schizophrenia is

the flattening of affect and anhedonia (Bleuler, 1950; Horan, Kring, & Blanchard, 2006). It is seen as a hallmark of the disease; even to the degree that flat affect in normal individuals can be seen as a risk factor for schizophrenia (Mason et al., 2004). Flat affect is often accompanied by impairments in facial affect recognition (Edwards, Pattison, Jackson, & Wales, 2001), general emotion identification (Kohler, Bilker, Hagendoorn, Gur, & Gur, 2000), and social ability (Green, Kern, Braff, & Mintz, 2000). Together this indicates that a diverse set of emotional recognition and production skills are impacted, with more severely blunted affect indicating increased damage to emotional brain systems. The symptoms of flattened affect and anhedonia are associated with morphological differences in the insula (Saze et al., 2007), anterior cingulate (Job et al., 2002), and orbitofrontal cortex (Lacerda et al., 2007). While schizophrenia is associated with diverse damage to areas throughout the brain, damage to these areas specifically may have much to do with the emotional deficits observed in the disease.

III. The Developmental Perspective

Development of the brain during the first twenty years of life is not a straightforward, linear process. Instead, individual brain regions exhibit a large degree of variance in the timecourse of their maturation. Some cognitive milestones are reached quickly, while other processes take decades to fully mature. In adolescence development is often nonlinear, with abilities such as emotional integration adolescence actually degrading in performance before showing further maturation (McGivern, Andersen, Byrd, Mutter, & Reilly, 2002). Even when individual regions have reached maturity there is still a degree of coordination that must take place between maturing regions, something Luna et al. (2004) referred to as 'the emergence of collaborative function'.

Anatomical Brain Development Between Childhood and Adulthood

Post-mortem studies were the first to reveal that development in the central nervous system begins during gestation and continues well into the third decade of life (Benes, Turtle, Khan, & Farol, 1994; Brody, Kinney, Kloman, & Gilles, 1987; Hunter, Leavitt, & Rodriguez, 1997; Yakovlev & Lecours, 1967). These findings have been supported by work using positron emission tomography [PET], which can provide regional measures of baseline glucose metabolism. Using this method, cortical metabolic activity across the brain has been shown to reach stable, adult-like, levels in the mid-twenties (Van Bogaert, Wikler, Damhaut, Szliwowski, & Goldman, 1998). More recently, studies using magnetic resonance imaging have confirmed that brain maturation continues throughout adolescence and into young adulthood. Specifically, white matter volume increases linearly during this time and continues to increase into midlife (Bartzokis et al., 2001; Giedd et al., 1999). Further, gray matter volume has been shown to have a quadratic developmental trajectory, with volume increasing during childhood, peaking during adolescence, and then decreasing once more during late adolescence and young adulthood (Gogtay et al., 2004; Reiss, Abrams, Singer, Ross, & Denckla, 1996; Sowell, Thompson, Tessner, & Toga,

2001). The gray volume peak of each region differs temporally, with frontal and temporal lobes having the latest apex points (Giedd et al., 1999; Gogtay et al., 2004; Reiss et al., 1996). Spatially, the dorsal, medial, and lateral areas of prefrontal cortex and posterior areas of temporal cortex are the last cortical regions to develop, with the perisylvian region of the posterior temporal lobe having a characteristic late maturational pattern (Gogtay et al., 2004; Sowell et al., 2001). Changes in subcortical gray matter during adolescence and young adulthood have also been noted to occur in putamen, globus pallidus, and caudate (Sowell, Thompson, Holmes, Jernigan, & Toga, 1999; Thompson et al., 2000). Taken together, the aforementioned results converge to suggest that there are still notable changes in brain structure that occur between late childhood and adulthood.

Areas of second-order interoceptive integration are typically regions that take the longest amount of time to fully mature. In general, brain development follows a coherent pattern, with less abstracted information processing areas maturing before areas known to operate on higher-order information streams (Chiron et al., 1992; Flechsig, 1920; Guillery, 2005). Thus, primary visual, motor, and somatosensory cortex stabilizes early, usually during the first decade of life. Areas of higher-order association cortex, such as dorsolateral prefrontal and frontal pole regions, are then last to develop. This is parsimonious, as association cortex would undoubtedly require stable input from lower cortical areas before its own maturity could be established. Anterior insula, anterior cingulate, and medial prefrontal cortex are all regions of higher-order cortex that exhibit such a late developmental trajectory (Bennett & Baird, 2006; Gogtay et al., 2004; Sowell, Thompson, & Toga, 2004). Given the importance of these areas to interoception and given their extended development it is logical to believe that interoception is a high-level process critical to abstract association and complex cognition.

Functional Brain Development Between Childhood and Adulthood

While changes in anatomy are easily quantified and reported, differences in the

regional function of the brain over time are much harder to research. Between adolescence and adulthood virtually every area of the brain, including primary cortices, exhibits some measure of nonlinear functional change (Cross, Bennett, Grafton, & Baird, 2006; Luna & Sweeney, 2004). From recent research several patterns of functional change have emerged. First is the observation that activation patterns in children and adolescents are typically more diffuse than those of adults (Adleman et al., 2002). This is thought to be the result of additional tissue being recruited to make up for inefficiencies in information processing (Rypma et al., 2006). A second observation is that signal change in adults tends to be equivalent in magnitude to children (Kang, Burgund, Lugar, Petersen, & Schlaggar, 2003). A final observation is that there are occasions when the first two observations simply don't apply. In some tasks children, adolescents, and adults show wholly different patterns of activity for the same tasks. One task may show greater prefrontal activity in younger subjects (Baird, Fugelsang, & Bennett, in press) and in other tasks younger subjects may show greater subcortical activity (Ciesielski, Lesnik, Savoy, Grant, & Ahlfors, 2006). Because so little research has been done focusing on second-order interoception across development it is difficult to know what differences between adolescents and adults will look like. It is most probable that differences will manifest in line with the first two observations: that activations will be equivalently strong, but that the adolescent group will show a more diffuse activation pattern.

Brain Development and Interoceptive Emotion Processing

We are born with little capacity to understand or control our internal state. An infants crying is the signal that their homeostatic condition needs attention. When an infant's body state needs cannot be met by internal mechanisms an adult will have to step in to examine the infant's behavior and understand through external cues what the cause of discomfort is. With development the child will gradually grow to have greater internal state discrimination and autonomic control. The anatomical development of regions across the brain is thought

to have a direct impact on this ability to integrate cognitive and emotional processes. Not only are purported second-order integration centers showing anatomical change (Gogtay et al., 2004), but also primary interoceptive cortex has been shown to develop into the early twenties (Bennett & Baird, 2006). Still, very little is known about the developmental progression of higher-order interceptive and autonomic processes.

IV. Integration and Theoretical Questions

The cortical representation and re-representation of body state is critical to efficient higher-order cognition. Individuals with damage to regions that play a role in interoceptive integration can show marked deficits in problem solving, learning, and decision-making. Yet, to date, there has not been a comprehensive study investigating the development of interoception and internal state information processing within the brain. We know that between adolescence and adulthood marked anatomical changes take place in regions important to internal state processing. Are there functional changes in interoceptive processing as well? This dissertation proposes to answer this question, along with the following, more specific hypotheses:

1. Does the simple detection of interoceptive sensation change across development? While the overarching goal of this thesis is the investigation of higher-order integration it must first be established that the early processing of interoceptive and exteroceptive information is equivalent across the age groups under investigation. If the output of primary sensory areas is changing over time then the interpretation of differences in higher-order cortex is impossible. Experiments one and two examine this question.

2. Where is interoceptive information distinct from exteroceptive information in the brain and where is it not distinct? Many leading theories of interoceptive processing argue for a strong distinction between interoceptive and exteroceptive information in the brain (Craig, 2002; Critchley et al., 2001). We know these modalities are differentiable through the peripheral nervous system, spinal cord, brainstem, and thalamus (O. G. Cameron, 2001; Craig, 2003b). Still, little work has been done on the separability of internal/external information at cortical level. Experiments two, three, four, and five all examine this question.

3. Does ongoing neurodevelopment impact cognitive/interoceptive integration? This is the fundamental question that this thesis aims to address. This will be accomplished in two parts. First will be the identification of brain regions supporting interoceptive

integration in adults. This will be done to examine hypotheses of the anterior insula being a major integration center for internal state information. Second will be the examination of how adolescents differ from adults in terms of interoceptive integration. Experiments three, four, and five all examine these questions.

4. Does the top-down influence on interoceptive state change across development? The majority of this thesis examines the bottom-up perception and integration of internal state information. This leaves an outstanding question: what of top-down influences on internal state perception? Do the same structures that generate abstract representations of internal state also allow for abstract representations to be created in a top-down manner? Experiment five examines this question.

Together these hypotheses add up to become one of the first comprehensive examinations of interoceptive development. We hope to test several aspects of this system by beginning with experiments of basic sensory processing and moving up the cognitive ladder to examinations of interoceptive integration and executive control. Through this stepwise approach we hope to provide a rich set of new information on how the internal state of the body is represented in the brain.

Experiment One

Rationale and hypothesis

A fundamental problem in the study of interoception has been establishing a measure that accurately quantifies the interoceptive sensitivity of an individual. While many methods have been attempted, few have wholly succeeded in the ability to effectively discriminate those with high and low ability. Perceptual discrimination tasks are thought to be the best available measure of interoceptive ability (G. Jones, 1994; Reed, Harver, & Katkin, 1990). Of perceptual discrimination tasks the most popular by far has been heartbeat detection (O. G. Cameron, 2001). As a measure it is exceedingly easy to obtain heartbeat data and there is a great deal of scientific knowledge related to cardiovascular operation to draw upon. Heartbeat detection has successfully been used to index normal variability to emotional stimuli (Pollatos, Herbert, Matthias, & Schandry, 2007; Pollatos, Kirsch, & Schandry, 2005) and abnormal variability in anxiety (Pollock, Carter, Amir, & Marks, 2006; Stewart, Buffett-Jerrott, & Kokaram, 2001), depression (Dunn, Dalgleish, Ogilvie, & Lawrence, 2007), and panic disorder (Ehlers & Breuer, 1996; Zoellner & Craske, 1999). From this research it is clear that there are individual differences in the ability to perceive internal sensation. What remains uncertain is the direction and magnitude of developmental changes in heartbeat detection.

Of the handful of studies to address developmental changes in heartbeat detection most have examined comparisons between young children and adults. Others have primarily focused on the relationship between anxiety disorders and heartbeat detection in children. In general there is very little developmental data on heartbeat detection and almost none encompassing the adolescent age range (Oliver G. Cameron, 2002). The goal of this experiment is to quantify the amount of developmental change from adolescence to adulthood. It will also address whether developmental differences between the adolescents and adult groups are larger than the within-group individual differences.

Another question that has not been addressed is what the psychometric curve of

heartbeat detection looks like. While a number of experiments involving heartbeat detection have been completed, the design of these experiments has primarily been the use of a single delay condition, usually around 500ms (Oliver G. Cameron, 2002; G. Jones, 1994; Reed et al., 1990). How does accuracy vary across a range of delay values? Is there a performance drop-off somewhere between 0ms and 500ms? Does performance vary linearly or does it have a sigmoidal shape? By using several intermediate delay values this experiment will investigate these questions.

The main hypothesis for this experiment is that older participants will perform better than adolescents. Adults will be able to respond more quickly and accurately to internal sensation when compared to the adolescent sample. It is also hypothesized that the shape of the psychometric curve will be linear, with accuracy increasing and reaction times decreasing as the delay gets longer.

Methods

Participants. Nineteen healthy right-handed adults (13 female, 6 male, mean age = 28.1, age range = 22.3 to 39.3 years) recruited from the local community and fifteen healthy right-handed adolescents (10 female, 5 male, mean age = 11.9 years, age range = 9.4 to 13.8 years) recruited from local schools participated in experiment one. All subjects completed an informed consent procedure approved by the Committee for the Protection of Human Subjects at Dartmouth College and were compensated for their time.

Experimental design**.** The experiment was set up as a heartbeat detection task with feedback delay [0ms, 125ms, 250ms, 375ms, 500ms] as a principal factor. The dependent measures for the task were reaction time and discrimination accuracy. Each subject completed 10 trials of each condition. Several self-report measures of anxiety, current emotional state, and clinical states were administered after the heartbeat detection task was complete. Total duration of the experiment was 16 minutes, including instructions.

Apparatus**.** A custom microcontroller system was used for the administration of this experiment [see Figure 3]. A Nonin Xpod pulse oximiter [Nonin Medical, Plymouth, MN] was used to obtain measures of blood oxygenation [SpO2], plethysmographic pulse value, and heart rate. The oximiter probe was placed on the left index finger. Oximiter information was output to a Basic Stamp II microcontroller (Model BS2pe; Parallax Inc., Rocklin, CA) by way of serial data connection. A custom parsing program then translated the proprietary Nonin data format into raw plethysmographic data. A peak signal detection algorithm then processed the raw data and identified individual heartbeats. The half-maximum rise point was used as the trigger for synchrony due to delays in pulse propagation and signal processing time. A large LED display would either blink in synchrony with the heartbeat or delayed by a specified amount.

Figure 3. The heartbeat detection apparatus. The heart-shaped ring of LEDs would flash either in sync or out of sync with the participant's heart.

Self-Report measures. Participants completed the State/Trait Anxiety Scale [STAI; Spielberger, 1983], Behavior Rating Inventory of Executive Function [BRIEF; Guy, Isquith, Gioia, 2000], the Multidimensional Empathy Scale [MES; Baird and Marsh, 2003], and the Positive and Negative Affect Schedule for state ratings [PANAS; Watson, Clark et al. 1988].

Experimental procedure and task detail. The subject was seated in front of the device with both hands flat on a table. Response buttons [no delay, delay] were available under the

right hand while the left hand remained immobile on a rest to ensure oximiter data quality. All trials began with a high-pitched [1760 Hz] preparatory tone and red LED flash as a trial onset cue. A yellow LED would then illuminate while the oximiter sampled four seconds of data to calibrate the half-maximum plethysmographic value used to signal heartbeat onset. After calibration a green LED would illuminate and the primary LED display would begin to flash. During each trial the subject had to determine if the flashing was synchronous or asynchronous with their heartbeat. Participants were given rest periods after 18 and 36 trials. At the end of the experiment the subject was interviewed to determine their perceived difficulty in making the circle and heart judgments.

Statistical analysis. A signal detection analysis of participant accuracy was completed on the response data. Sensitivity and response criterion for heartbeat asynchrony detection were calculated as d-prime and Xc (Macmillan & Creelman, 1991). A larger d-prime value indicates a better ability to discriminate between synchronous and asynchronous events while d-prime values of zero indicate no discrimination ability. The response criterion value indicates the degree of bias that a participant has in responding. Negative values indicate a lax criterion for determining synchrony while positive values indicates a more strict synchrony criterion. Adjustments to the hit rate (HR) and false alarm rate (FAR) were completed according to the method of Corwin (1994) to avoid issues of zero division. A one-sample t-test was applied to the d-prime values of each feedback delay condition to determine if the group d-prime was significantly different from zero. A one-sample t-test was also applied to the response criterion values of each feedback delay condition to determine if the group response bias was significantly different from zero. The Bonferroni-corrected significance cutoff for these comparisons was $p = 0.0025$.

Reaction time data was transformed using a reciprocal [1/x] calculation to satisfy assumptions of data normality in the linear analysis. Transformed reaction times were submitted to a one-way repeated-measures analysis of variance (ANOVA) with the five

levels of feedback delay [0ms, 125ms, 250ms, 375ms, 500ms] input as a within-subjects factor. The Pearson product-moment correlation [r] was used to examine linear relationships between d-prime and self-report measure results. The average d-prime and response criterion for each participant was compared to their score on subscales of the PANAS, STAI, and MES. Results are reported with values corrected ($p = 0.0063$) and uncorrected ($p = 0.05$) for multiple comparisons.

Results

Response Accuracy. Boxplots of d-prime values by feedback delay level are shown in Figure 4. Results of the one-sample t-tests on group d-prime values indicated that no feedback delay levels had d-prime values significantly different from zero, even with a significance cutoff uncorrected for multiple comparisons. This indicates that the group was, on average, unable to discriminate between the synchronous and asynchronous conditions. While all conditions had a negative mean response criterion only the 125ms delay and 375ms delay conditions had values significantly different from zero. Boxplots of response criterion values by feedback delay level are shown in Figure 5. The negative criterion values indicate the participants were generally more likely to respond that there was no delay.

Reaction Time. Bar plots of raw reaction time data are depicted in Figure 6. The one-way repeated-measures ANOVA results indicated a significant effect of feedback delay ($F(4,48) = 4.65$, $p = 0.003$, partial $\eta^2 = 0.279$). Polynomial contrasts were completed for the feedback delay factor and indicated that the change across delay values was linear ($F(1,12) = 14.38$, $p = 0.003$, partial $\eta^2 = 0.545$).

Self-Report Correlations. Differences in average d-prime across subjects were correlated with the negative subscale of the PANAS ($r = 0.711$, $p = 0.006$) and the general

emotional sensitivity subscale of the MES (r = 0.586, p = 0.035). Only the negative PANAS subscale survived the more stringent multiple comparisons threshold of $p = 0.0063$. Differences in average response criterion values across subjects were correlated with both state ($r = 0.598$, $p = 0.031$) and trait ($r = 0.588$, $p = 0.035$) subscales of the STAI. Neither correlation survives multiple comparisons correction.

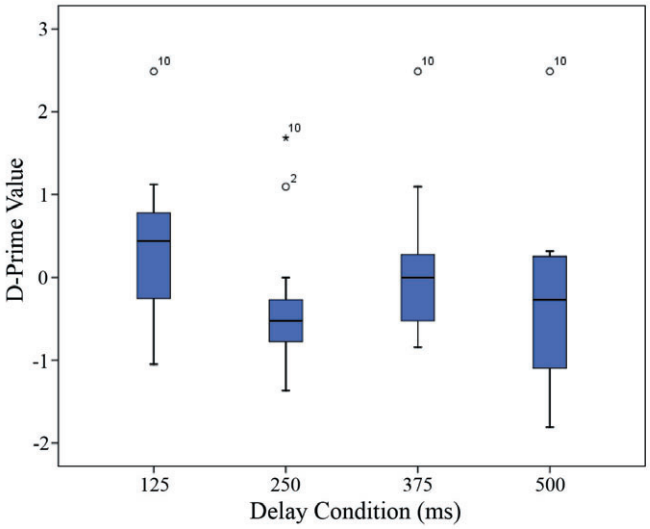

Figure 4. Plots of group d-prime values by delay condition. No values were significantly different from zero, indicating zero sensitivity to detecting synchrony.

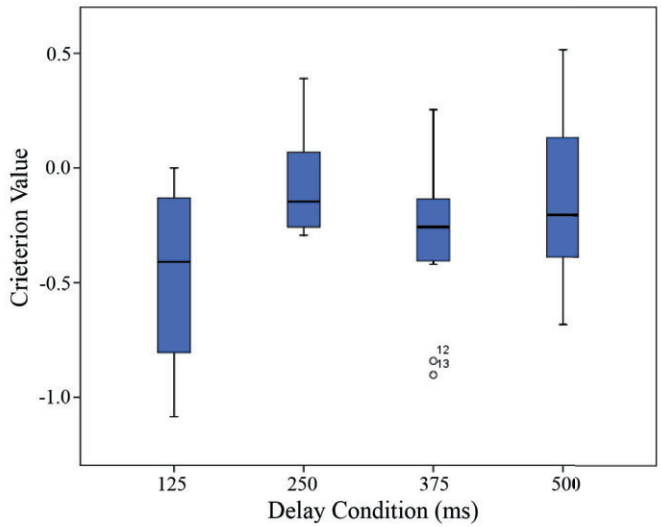

Figure 5. Plots of group criterion values by delay condition. The 125ms and 375ms delay conditions were significantly different from zero, indicating a group bias to respond that there is synchrony.

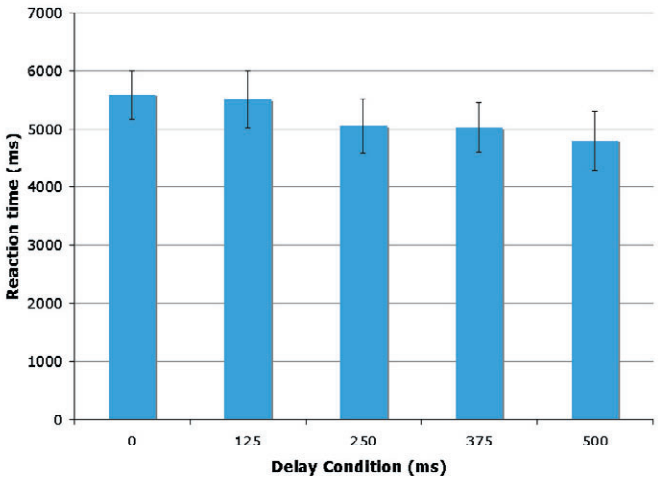

Figure 6. Plots of group reaction time values by delay condition. There was a significant linear differece in response time across the delay conditions, with larger delays leading to faster reaction times.

Discussion

This experiment was halted before the adolescent group of participants could be run. As the number of subjects rose to levels appropriate for statistical inference it became clear from the signal detection analysis that participants were simply unable to discriminate between delay and no-delay conditions. While some subjects were able to make successful discriminations (d-prime = 2.49), the majority of scores were clustered around zero. This is illustrated by the results of the one-sample t-tests on d-prime values, which showed that no condition had values significantly different from zero. There are three potential influences that may give rise to these results. One possibility may be that the apparatus was not functioning properly. Another is that the experimental design was inappropriate in some way. A final possibility is the existence of other sources of variability on the results. Each possibility will be discussed in turn.

While there is some variability contributed by the apparatus several pieces of information argue against it as the source of error. The most important validation point is that other research groups have successfully used a similar apparatus in their heartbeat detection experiments (Critchley, Wiens, Rotshtein, Ohman, & Dolan, 2004; Stewart et al., 2001). One source of error may have been the delay between when the heart beats and when the pressure wave arrives at the finger to be detected (Murray & Foster, 1996). However, this effect was quantified and accommodated by the use of the rising half-maximum of the pressure wave to trigger the LED display. As a final qualification synthetic data was input into the device to test total processing delay. This delay, while present, was negligible (~15ms). These arguments summate in favor of the device being an effective experimental tool.

If the device was working properly then another possibility is that the experimental design may be problematic. The majority of other studies have used a single delay condition in contrast to the no-delay condition (Oliver G. Cameron, 2002; G. Jones, 1994; Reed et al., 1990). This experiment deviated from these previous studies in the use of multiple

delay conditions. This was done with the goal of constructing psychometric curves of performance across varying values of delay. Still, having so many levels of feedback delay may have made the task much more difficult. While the decision is still a binary choice [delay, no-delay] the present experiment lacks the larger delay contrast that traditional heartbeat detection task possess. For example, one trial having a medium amount of delay [250ms] may precede a trial with the maximum amount of delay [500ms]. Anecdotal evidence from previous studies (Oliver G. Cameron, 2002) indicates that heartbeat detection tasks are already quite difficult with two conditions. Qualitative reports from participants in the present study indicate that was indeed very difficult, with many subjects believing they were guessing at random. The difficult experimental design may account for the poor d-prime discrimination values.

One last possibility to consider is the effect of another source of variability on the results. In this case it would be prudent to consider the influence of individual differences on the ability to make effective decisions based on heartbeat. Previous studies have shown that numerous state and trait values impact heartbeat detection. Variables such as participant weight (Oliver G. Cameron, 2002), anxiety (Eley, Stirling, Ehlers, Gregory, & Clark, 2004; Pollatos, Traut-Mattausch, Schroeder, & Schandry, 2007), panic (Ehlers & Breuer, 1996; Zoellner & Craske, 1999), depression (Dunn et al., 2007), and personality traits (Ludwick-Rosenthal & Neufeld, 1985) have all been shown to influence detection ability. It may be that increased task difficulty acts as a subtraction factor on individual d-prime values. This is evidenced by the fact that, while a majority of participants did quite poorly, the top 10% of participants still did acceptably well. While there were not enough participants in the study to warrant population generalization from the correlation results, it is important to note that the relationship of d-prime to self-report values indicated that some variability may be explained by individual difference factors.

A final point to consider is the interpretation of reaction time results. While the signal detection analysis showed that subjects could not effectively discriminate between delay

and no-delay conditions, there was a strong linear effect of reaction time as it decreased with larger delay values. This is counterintuitive, as there should be some relationship between response time and accuracy. It may be that with lower delay values the participants are sampling more heartbeats before making their final decision. It could also be an effect of the participants imposing an additional response delay during conditions with little feedback delay. Given the poor accuracy of the participants it is difficult to determine the source of the reaction time effect.

A future experiment should test the different delay levels separately to determine if the results of this experiment are due to the effects of testing in a single run. By restoring the contrast between delay and no-delay conditions it might make the task easy enough to complete without becoming swamped by the number of parametrically-varied delay levels. It may be that inserting additional feedback cues would make the task easier and allow effective discrimination. Feedback could be delivered by auditory and visual modalities simultaneously to increase the amount of information available for use in decision-making.

Experiment Two

Rationale and hypothesis

Second-order integration of interoceptive sensation is a critical transformation in the processing of internal state information. It is a difficult cognitive process to study since it requires the experimental manipulation of an individual's internal state. Most early studies used injected chemicals to alter the internal milieu in an effort to produce internal state changes. An example of this practice was the use of epinephrine to increase heart rate (Schachter & Wheeler, 1962). The results of these studies were inconclusive, as the resulting effects could be ascribed to the chemicals themselves or the interaction of altered body state and cognitive appraisal (Cotton, 1981). Since this early work many recent neuroimaging studies have evaluated methods of inducing uniquely visceral sensations in a subject. The results of these studies indicate that painful stimulation and thermal change are both effective means of producing interoceptive sensations (Craig, 2003b). The pattern of activity they produce in the brain is not dominated by somatosensory activity, but is instead marked by responses throughout the insula and anterior cingulate. This experiment investigates the role of thermal change as an interoceptive sensation to examine the integration of internal state information and higher cognitive processes.

It is apparent from anatomical tracing studies that thermal and tactile stimuli are conveyed to the brain along different routes. Pathways conveying temperature are resident in the contralateral spinothalamic projection while tactile discrimination is resident in ipsilateral lemniscal projections (Iannetti et al., 2003). This segregation of information continues though brainstem areas and the thalamus until the information is projected to separate cortical targets (Oliver G. Cameron, 2002; Craig, 1995; Craig et al., 1994). After the thalamus somatosensory stimulation is first processed by primary somatosensory cortex (Rowe, Turman, Murray, & Zhang, 1996) and thermal stimulation is processed by posterior insular cortex (Craig et al., 2000; Moulton, Keaser, Gullapalli, & Greenspan, 2005). Still, the modalities do begin to overlap after these initial cortical areas. Regions

of secondary somatosensory cortex have demonstrated activity for both tactile stimulation (Nelson, Staines, Graham, & McIlroy, 2004) and for thermal stimulation (K. L. Casey, Minoshima, Morrow, & Koeppe, 1996). The question becomes how much overlap there is in the cortical representation of the thermal and tactile modalities.

While thermal and tactile stimulation have both been completed during functional imaging a number of questions still exist regarding these basic perceptual processes. For example, studies investigating temperature have primarily examined thermal changes applied to only one hand, yielding no knowledge related to differences in the laterality of thermoception (Craig, 1995; Hua le et al., 2005). This is a fundamental question, as other studies have identified laterality differences in tactile stimuli (Coghill, Gilron, & Iadarola, 2001). Additionally, thermal and tactile changes have never been directly compared, producing no knowledge of how these systems are similar or different. The theories of interoception put forth by Craig (Craig, 2002, 2003b) draw a sharp distinction between somatosensory and interoceptive processes in the brain. He argues that the posterior insula should be considered as a region of primary interoceptive cortex, with activity unique to interoceptive information. While studies have provided support for the brain regions involved in interoception, a direct comparison to somatosensory stimuli has not been made.

This experiment uses a passive experience task to examine early areas of processing involved in thermal and tactile sensation. It uses a new MR-compatible stimulation device to parametrically apply thermal and tactile stimulation to the hands of study participants. The hypothesis for this experiment is that activity for tactile stimulation will be seen primarily in primary and secondary somatosensory cortex while activity for thermal stimulation will be seen in areas of posterior and mid-insula. In general, it is thought that the two modalities will be functionally segregated.

Methods

Participants. Twenty healthy right-handed adults (11 female, 9 male, mean age = 27.7, age range = 23.1 to 39.3 years) recruited from the local community and sixteen healthy right-handed adolescents (7 female, 9 male, mean age = 11.7 years, age range = 8.1 to 13.8 years) recruited from local schools participated in experiment two. One female and one male adolescent were excluded from further analysis due to excessive movement (1mm/TR) in their fMRI data. All participants completed an informed consent procedure approved by the Committee for the Protection of Human Subjects at Dartmouth College and were compensated for their time.

Experimental design. The experiment was set up as an event-related 2x2 factorial design with principal factors of presentation hand [left and right] and sensory modality [thermal and tactile]. Each subject completed one event-related fMRI session consisting of eleven events of each condition. Each event lasted 650ms and had between 5.5s and 8.2s of rest between each event. Events were 3-back counterbalanced across the run to avoid order effects. Large blocks of rest lasting 15s were placed at the beginning, middle, and end of the task. Total scan time was 5 minutes.

Apparatus. Experiment 3 utilized the thermotactile stimulation apparatus described in appendix B. Briefly, the apparatus allowed for the parametric application of thermal and tactile stimuli to the palms of each hand.

Experimental procedure and task detail**.** Upon arrival the participant was first asked to go through a thermal and tactile calibration procedure. This was done to ensure that stimulation would encompass the entire dynamic range of perception without inducing discomfort or pain. A stepwise progression of increasing temperature proceeded until the subject reported excessive heat. Each step added roughly 5º F to the presented value. The calibration value was the last level of thermal application without discomfort. A

similar procedure was used for tactile calibration, with air pressure increasing until it was uncomfortable. The calibration value was then 5 psi below that level.

Instructions for the experiment were to passively experience the thermal and tactile stimuli. Participants were told that no responses would be necessary, but to remain vigilant throughout the scanning session. A fixation cross was presented for 500ms at the beginning of each trial to signal the onset of each thermal or tactile stimulation. At the end of the scan the subject was asked how effectively they could feel the stimulation of each modality and if there were any unexpected events during the scan, such as attention lapses.

Preprocessing of imaging data. Preparation of the data involved global artifact detection, realignment of the functional images, coregistration to the high-resolution anatomical image, normalization to the ICBM-152 atlas space, and smoothing using a Gaussian kernel of 8mm FWHM. Details of the fMRI preprocessing strategy can be found in appendix A.

General linear model analysis of imaging data**.** A two-level mixed-effects methodology was used to analyze the functional imaging data. The first level consisted of a multiple regression analysis estimated using ordinary least squares (OLS) in SPM2 (Statistical Parametric Mapping, www.fil.ion.ucl.ac.uk/spm/). Predictors were created using an impulse function based the stimulus onset times convolved with a canonical hemodynamic response function. Four predictors of interest were generated according to the modality-hand pairings: thermal-left, thermal-right, tactile-left, and tactile-right. Other nuisance predictors were also created to account for low-frequency noise and subject head movement.

For each participant a set of four volumes was generated corresponding to the voxelwise beta estimates of each condition. These images were input into a multiple regression at the second level for final hypothesis testing. The second level was estimated using restricted

maximum likelihood (ReML) to account for dependencies and unequal variance among the levels of each repeated measure. Additional details regarding statistical analysis of the fMRI data can be found in appendix A.

Contrasts of interest were generated at the second level to test *a priori* hypotheses. Contrasts were created to test for similarities and differences between thermal and tactile stimulation. These contrasts collapsed across presentation hand to examine effects of modality regardless of presentation site. Another contrast was made to test specifically for laterality differences in handedness. Two final contrasts were made to separately test for developmental differences in thermal and tactile stimulation.

Independent components analysis (ICA) of imaging data. The data from each participant was also analyzed using Probabilistic Independent Component Analysis (Beckmann & Smith, 2004) as implemented in MELODIC (Multivariate Exploratory Linear Decomposition into Independent Components) Version 3.05 (FMRIB Centre, University of Oxford, www.fmrib.ox.ac.uk/fsl). The following data pre-processing steps were applied to the input data: masking of non-brain voxels; voxel-wise de-meaning of the data; and normalization of the voxel-wise variance. Pre-processed data were whitened and projected into a 35-dimensional subspace using probabilistic Principal Component Analysis where the number of dimensions was estimated using the Laplace approximation to the Bayesian evidence of the model order (Minka, 2000). The whitened observations were decomposed into sets of vectors which describe signal variation across the temporal domain (time-courses), the session/subject domain and across the spatial domain (maps) by optimizing for non-Gaussian spatial source distributions using a fixed-point iteration technique (Hyvarinen & Pajunen, 1999). Estimated Component maps were divided by the standard deviation of the residual noise and thresholded by fitting a mixture model to the histogram of intensity values (Beckmann & Smith, 2004). Finally, the resulting ICA components were subjected to a fingerprinting process (Tohka et al., 2008) based on spatial

and temporal characteristics to determine sources of signal or noise.

Results

Similarity between thermal and tactile conditions. A conjunction analysis was preformed to identify regions responding strongly to both thermal and tactile stimulation. The parameters for this comparison were $t^2(60) > 3.23$, $p < 0.001$, 8 voxel extent threshold. From this analysis several areas of somatosensory and insular cortex had responses to both modalities (Table 1 and Figure 7). Multiple significant clusters were found in bilateral areas of the insula, including regions in the posterior (Figure 8a, b) and mid insula (Figure 8c, d). Bilateral areas of secondary somatosensory cortex (Figure 8e, f) were also active for both modalities.

Differences between thermal and tactile conditions. A directional *t*-contrast was used to test for regions activating preferentially to one modality over the other. The parameters for this comparison were $t(60) > 3.23$, $p < 0.001$, 8 voxel extent threshold. Most significant regions were found to preferentially respond to the tactile condition. Generally, these areas were found across bilateral regions of somatosensory, superior parietal, and premotor cortex (Table 2, Figure 9). Both primary (Figure 10a, b) and secondary (Figure 10c, d) somatosensory cortex showed preferential activity for tactile stimuli, as did regions within the dorsal premotor cortex (Figure 10e, f) and intraparietal sulcus (Figure 10g,h). Relatively few regions were shown to preferentially respond to the thermal condition (Table 2, Figure 9). The medial prefrontal cortex (Figure 11a, b), substantia nigra (Figure 11c), and bilateral areas of lateral occipital cortex (Figure 11d, e, f) all showed preferential activity to thermal stimulation.

Developmental changes in thermal and tactile responses. Two directional *t*-contrasts were used to test for regions showing differences in activity between adolescence

and adulthood. Each comparison had parameters of $t(116) > 3.16$, $p < 0.001$, 8 voxel extent threshold. The first contrast tested for developmental changes within the thermal modality. The primary finding from this comparison was an increased response in the parietal operculum within the adult group (Table 3, Figure 12). These bilateral areas of deep secondary somatosensory cortex showed a net signal decrease relative to zero in the adolescents and signal increases in the adults (Figure 13c, d). There were no significant regions of greater adolescent activity. The second contrast tested for developmental changes within the tactile modality. Several clusters of increased adult response were found in parietal cortex (Table 4 and Figure 12). Bilateral areas of intraparietal sulcus (Figure 13e, f) and superior parietal lobule (Figure 13g, h) showed increased activity for the adults. The adolescents showed increased activity in medial prefrontal cortex (Figure 13i) and posterior cingulate (Figure 13j).

Independent Components Analysis of the Passive Experience Data. A total of 27 independent components were estimated to be present in the data. Using an ICA fingerprinting process (Tohka et al., 2008) 15 of those components were found to account for sources of noise. Of the remaining 12 components only four had significant voxels within somatosensory or insular cortex: components 1, 2, 6, and 24 (Figure 14). Two components were found to correspond to stimulation of the left hand [1,2] and two components were found to correspond to stimulation of the right hand [6,24]. Components 1 and 6 contained areas of bilateral primary and contralateral secondary somatosensory cortex in addition to contralateral posterior insula and dorsal anterior cingulate. Components 2 and 24 contained areas of contralateral somatosensory, lateral parietal, lateral frontal, and rostral anterior cingulate.

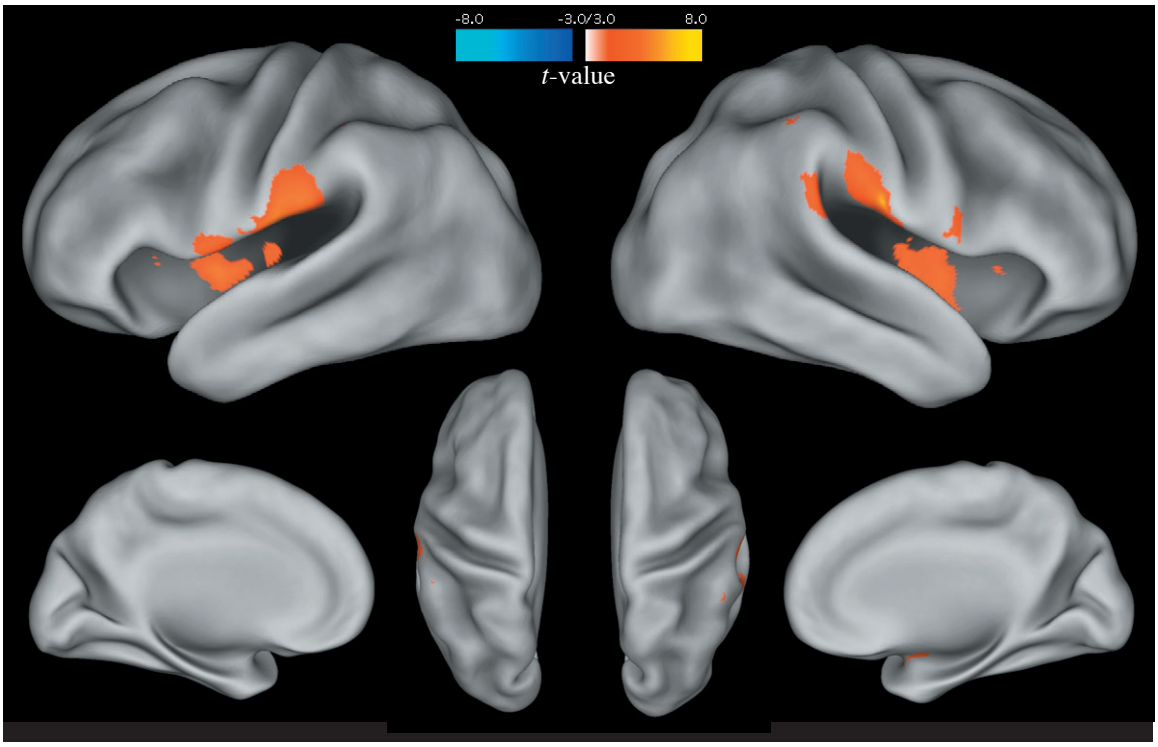

Figure 7. Regions showing significant activity in both passive thermal and passive tactile conditions. The parameters for this comparison were $t^2(60) > 3.23$, $p < 0.001$, 8 voxel extent threshold. From this analysis several areas of bilateral somatosensory and insular cortex responded to both modalities.

Table 1
Regions showing significant activity in both passive thermal and passive tactile conditions

Region Name	HEM	BA	Area Notes	MNI Coordinates x	y	z	*z*-value	*p*(uncorr)	*p*(FDR)
Frontal									
Inferior Frontal Gyrus	L	44	Broca's Area	-57	9	18	3.84	< 0.0001	0.006
Inferior Frontal Gyrus	R	44	Broca's Area	60	12	15	4.86	< 0.0001	< 0.0001
Temporal									
Insula	R	13	Ventral Mid Insula	36	6	-18	3.99	< 0.0001	0.004
Insula	L	13	Ventral Mid Insula	-39	0	-15	4.38	< 0.0001	0.001
Insula	R	13	Ventral Mid Insula	36	3	-12	3.91	< 0.0001	0.005
Insula	L	13	Mid Insula	-42	-3	3	5.57	< 0.0001	< 0.0001
Insula	R	13	Mid Insula	42	-6	3	5.31	< 0.0001	< 0.0001
Middle Temporal Gyrus	R	21		60	-54	6	4.06	< 0.0001	0.003
Parietal									
Parietal Operculum	L	OP1	Secondary Somatosensory	-60	-24	18	6.02	< 0.0001	< 0.0001
Parietal Operculum	R	OP1	Secondary Somatosensory	66	-18	21	7.29	< 0.0001	< 0.0001
Subcortical									
Amygdala	R			21	0	-15	4.78	< 0.0001	< 0.0001
Cerebellum									
Superior Cerebellum	L			-24	-66	-27	5.19	< 0.0001	< 0.0001

Table lists significant areas of activation ($p < 0.001$, extent threshold 6 voxels).
HEM = hemisphere in which cluster was located; BA = approximate Brodmann area of cluster;
p(uncorr) = uncorrected cluster probability; *p*(FDR) = cluster probability under false discovery rate

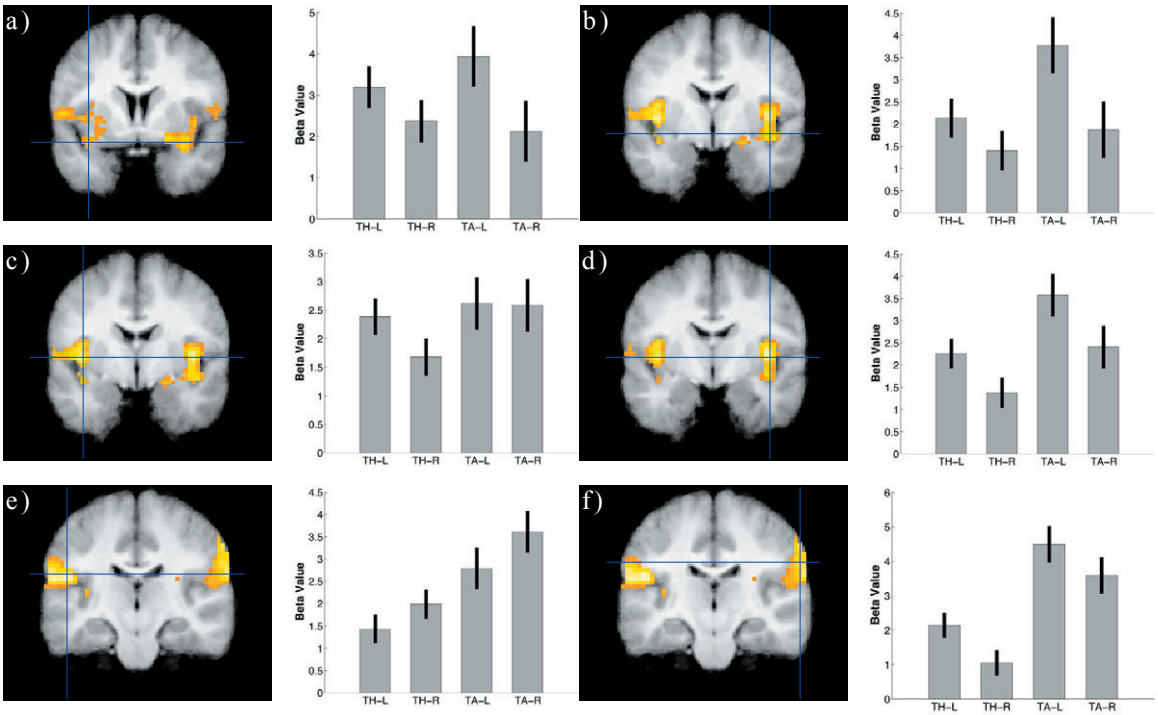

Figure 8. Parameter graphs for regions responding to both passive thermal and tactile stimulation. From left to right bars represent thermal-left, thermal-right, tactile-left, and tactile-right conditions. Multiple significant clusters were found in bilateral areas of the insula, including regions in the posterior (a,b) and mid insula (c,d). Bilateral areas of secondary somatosensory cortex (e,f) were also active for both modalities.

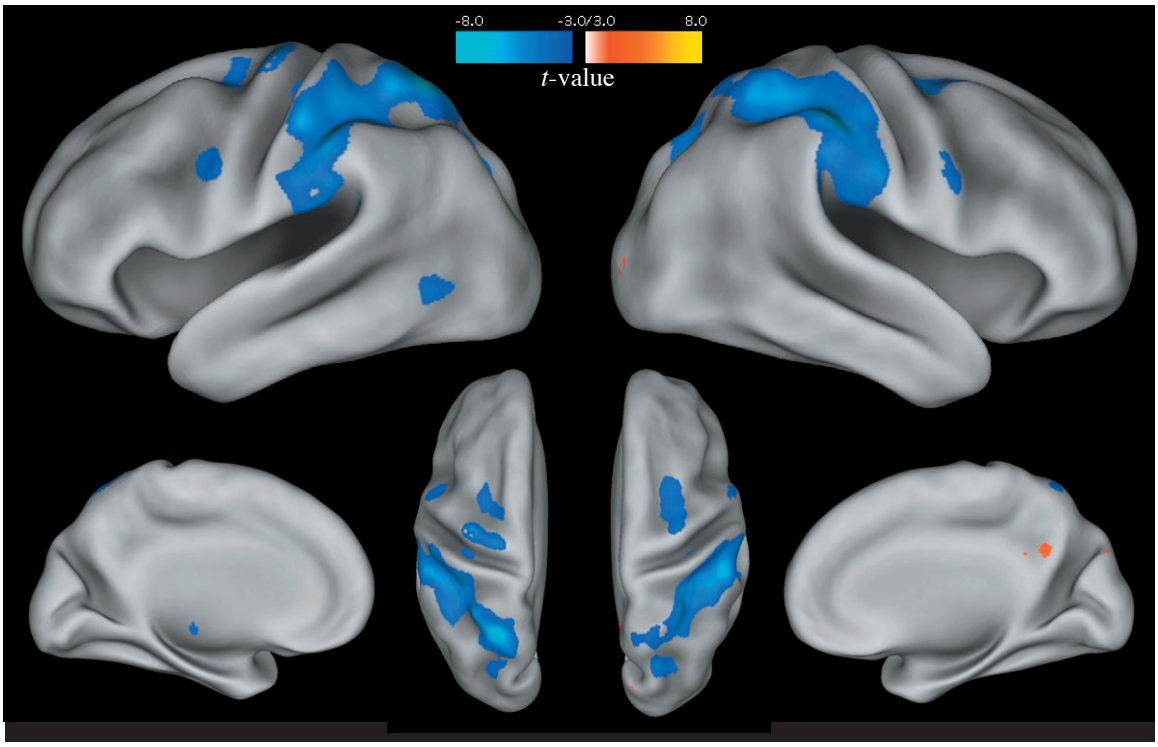

Figure 9. Regions showing preferential activity to either passive thermal (red) or passive tactile (blue) stimulation. The parameters for this comparison were $t(60) > 3.23, p < 0.001$, 8 voxel extent threshold. Most regions were found to preferentially respond to the tactile condition. These areas were found across bilateral regions of somatosensory, superior parietal, and premotor cortex.

Table 2
Regions showing a main effect of modality in the passive task

Region Name	HEM	BA	Area Notes	MNI Coordinates x	y	z	*z*-value	*p*(uncorr)	*p*(FDR)
Thermal > Tactile									
Temporal									
Superior Temporal Sulcus	L	19		-36	-57	21	3.64	<0.0001	0.0066
Parietal									
Precuneus	R	7		9	-57	33	3.49	<0.0001	0.0093
Occipital									
Lateral Occipital Cortex	L	19		-24	-84	-3	3.58	<0.0001	0.0078
Lateral Occipital Cortex	R	19		27	-90	0	4.25	<0.0001	0.0015
Subcortical									
Substantia Nigra	Mid			-6	-9	-18	3.53	<0.0001	0.0086
Tactile > Thermal									
Frontal									
Precentral Gyrus	L	6	Premotor	-54	6	33	4.79	<0.0001	<0.0001
Precentral Gyrus	R	6	Premotor	60	9	30	4.56	<0.0001	<0.0001
Superior Frontal Gyrus	R	9	Medial Prefrontal	9	48	33	3.77	<0.0001	0.0049
Precentral Gyrus	L	6	Premotor Cortex	-27	-3	57	4.28	<0.0001	0.0014
Precentral Gyrus	R	6	Premotor Cortex	33	-3	51	4.02	<0.0001	0.0027
Temporal									
Fusiform Gyrus	R	37	Inferior Temporal	36	-3	-33	3.60	<0.0001	0.0072
Middle Temporal Gyrus	L	19		-45	-60	0	4.15	<0.0001	0.0036
Parietal									
Supramarginal Gyrus	L	40		-60	-36	27	4.73	<0.0001	<0.0001
Supramarginal Gyrus	R	OP1	Secondary Somatosensory	51	-24	21	4.16	<0.0001	0.0019
Intraparietal Sulcus	R	hIP1		24	-69	42	3.99	<0.0001	0.0029
Intraparietal Sulcus	L	hIP1		-21	-60	60	5.21	<0.0001	<0.0001
Postcentral Gyrus	L	2	Primary Somatosensory	-39	-48	57	5.16	<0.0001	<0.0001
Postcentral Gyrus	L	2	Primary Somatosensory	-51	-30	45	4.73	<0.0001	<0.0001
Postcentral Gyrus	R	2	Primary Somatosensory	39	-39	54	5.74	<0.0001	<0.0001
Postcentral Gyrus	R	2	Primary Somatosensory	54	-21	48	6.05	<0.0001	<0.0001
Subcortical									
Medial Dorsal Thalamus	R			12	-18	12	3.39	<0.0001	0.0117
Medial Dorsal Thalamus	L			-18	-18	12	4.13	<0.0001	0.0021
Fornix	Mid			-3	-30	12	4.36	<0.0001	0.0011
Cerebellum									
Superior Cerebellum (VI)	R			30	-54	-27	3.94	<0.0001	0.0033

Table lists significant areas of activation ($p < 0.001$, extent threshold 6 voxels).
HEM = hemisphere in which cluster was located; BA = approximate Brodmann area of cluster;
p(uncorr) = uncorrected cluster probability; *p*(FDR) = cluster probability under false discovery rate

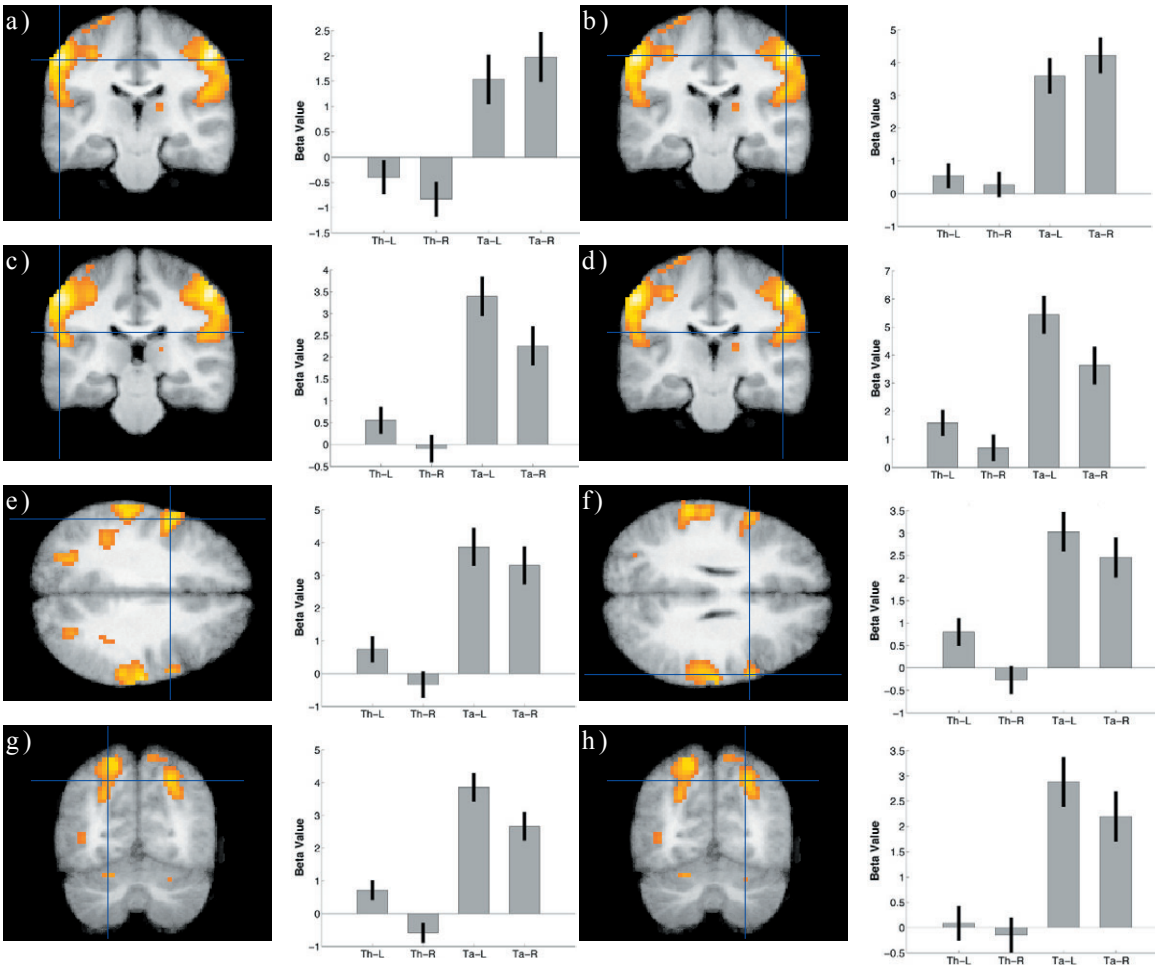

Figure 11. Parameter graphs of the passive tactile > thermal contrast. From left to right bars represent thermal-left, thermal-right, tactile-left, and tactile-right conditions. Both primary (a,b) and secondary (c,d) somatosensory cortex showed preferential activity for tactile stimuli, as did regions within the dorsal premotor cortex (e,f) and intraparietal sulcus (g,h).

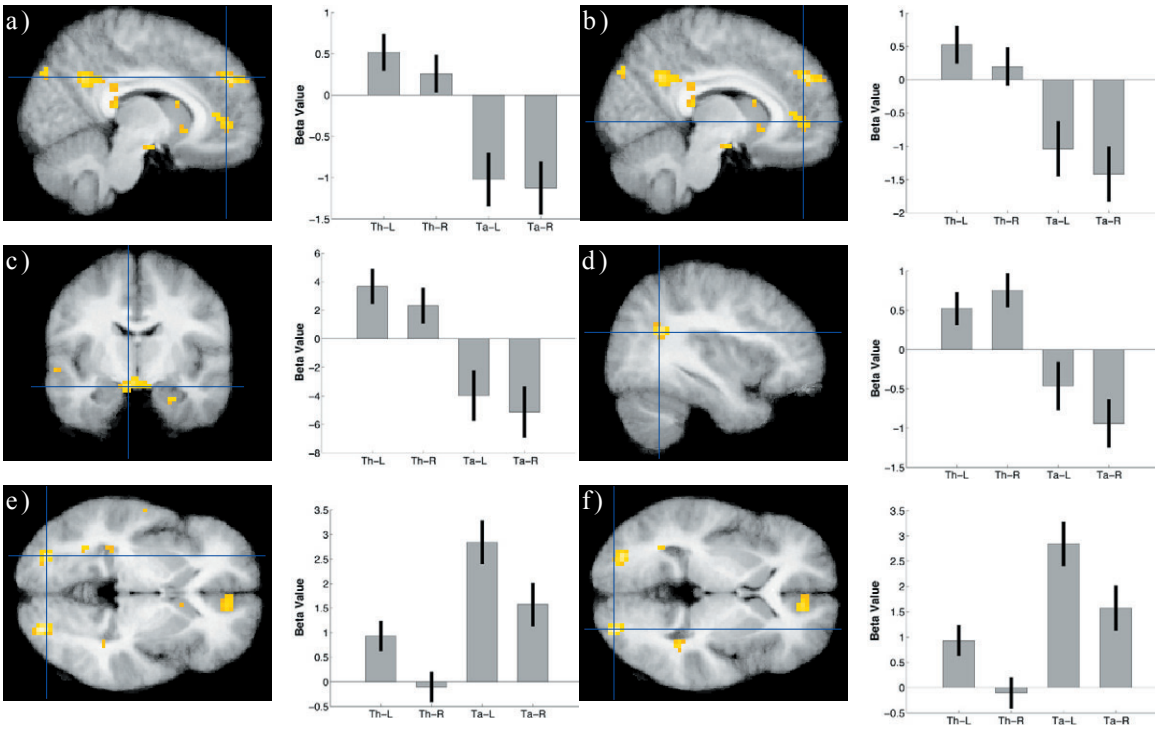

Figure 10. Parameter graphs of the passive thermal > tactile contrast. From left to right bars represent thermal-left, thermal-right, tactile-left, and tactile-right conditions. The medial prefrontal cortex (a,b), substantia nigra (c), and bilateral areas of lateral occipital cortex (d,e,f) all showed preferential activity to thermal stimulation.

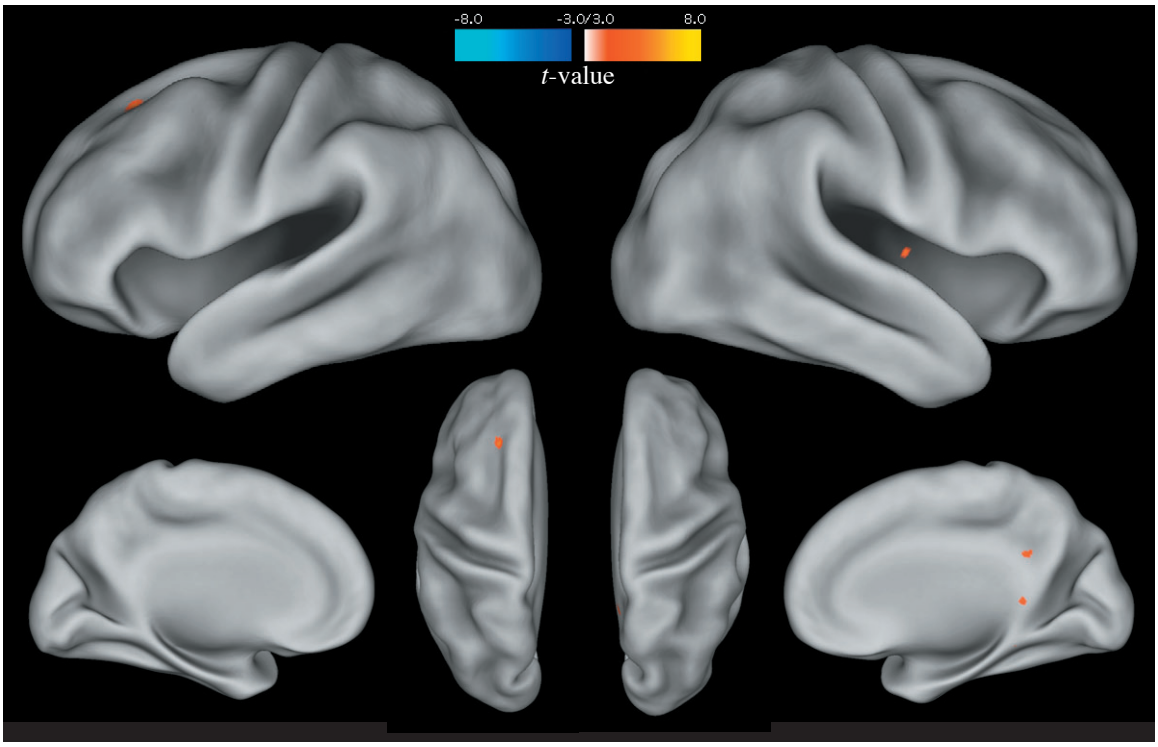

Figure 11. Regions showing developmental changes in activity to passive thermal stimulation. Greater activity in adults is represented in red and greater activity in adolescents is represented in blue. The parameters for this comparison were $t(116) > 3.16$, $p < 0.001$, 8 voxel extent threshold. The primary finding from this comparison was an increased response in the mid insula and parietal operculum (hidden) in the adult group.

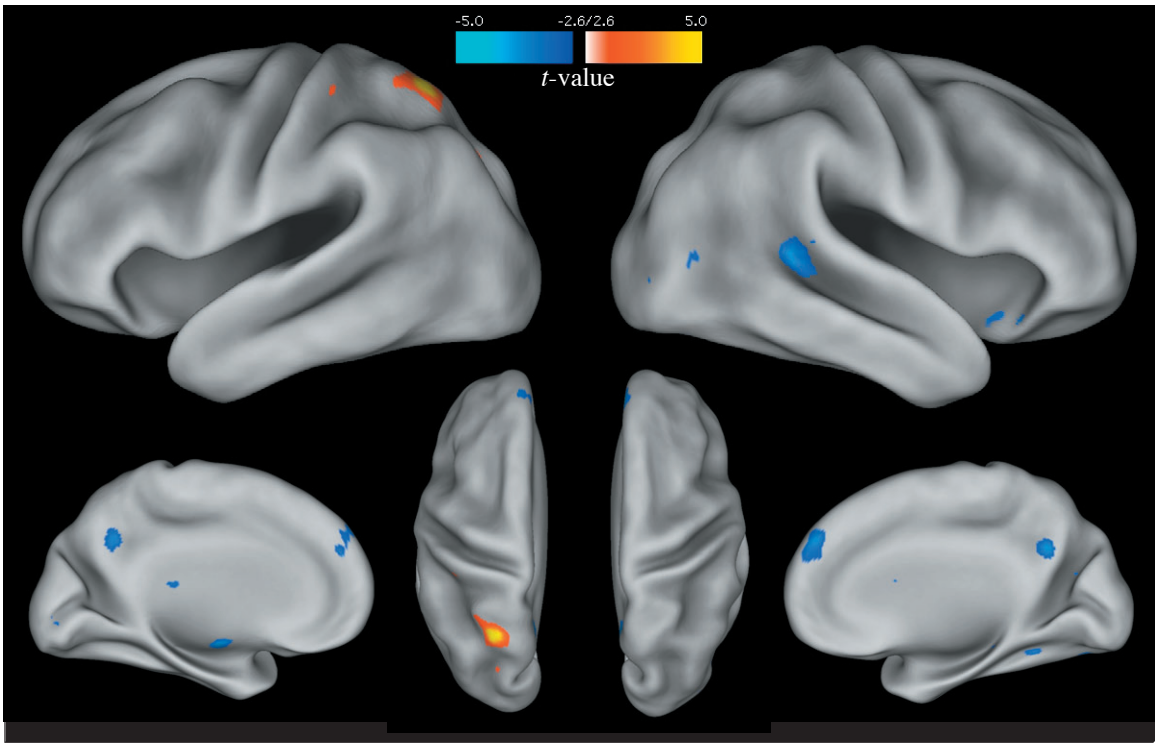

Figure 13. Regions showing developmental changes in activity to passive tactile stimulation. Superior activity in adults is represented in red and superior activity in adolescents is represented in blue. The parameters for this comparison were $t(116) > 3.16$, $p < 0.001$, 8 voxel extent threshold. Several clusters of increased adult response were found in parietal cortex while the adolescent group showed greater medial prefrontal, posterior cingulate, and lateral temporal activity.

Table 3
Regions showing developmental changes in activity for the passive thermal condition

Region Name	HEM	BA	Area Notes	MNI Coordinates x	y	z	*z*-value	*p*(uncorr)	*p*(FDR)
Adults > Adolescents									
Frontal									
Cingulate Gyrus	R	32	Dorsal Cingulate	18	15	30	3.54	< 0.0001	0.521
Superior Frontal Gyrus	L	6		-15	24	45	3.87	< 0.0001	0.521
Parietal									
Parietal Operculum	L	OP1	Secondary Somatosensory	-27	-33	21	3.68	< 0.0001	0.521
Parietal Operculum	R	OP1	Secondary Somatosensory	27	-24	21	3.3	< 0.0001	0.521
Occipital									
Intracalcarine Cortex	L	17	Visual Cortex	-27	-69	3	3.94	< 0.0001	0.521
Cingulate Gyrus	R	29	Posterior Cingulate	9	-45	9	3.15	0.001	0.521
Subcortical									
Brainstem	R		Substantia Nigra	15	-24	-18	3.22	0.001	0.521
Cerebellum									
Superior Cerebellum	R			21	-69	-24	3.73	< 0.0001	0.521

Table lists significant areas of activation ($p < 0.001$, extent threshold 6 voxels).
HEM = hemisphere in which cluster was located; BA = approximate Brodmann area of cluster;
p(uncorr) = uncorrected cluster probability; *p*(FDR) = cluster probability under false discovery rate

Table 4
Regions showing developmental changes in activity for the passive tactile condition

Region Name	HEM	BA	Area Notes	MNI Coordinates x	y	z	*z*-value	*p*(uncorr)	*p*(FDR)
Adults > Adolescents									
Parietal									
Intraparietal Sulcus	L	hIP1		-33	-48	33	3.28	0.001	0.346
Intraparietal Sulcus	R	hIP2		33	-42	36	3.79	< 0.0001	0.114
Superior Parietal Lobule	L	2	Primary Somatosensory	-24	-60	60	5.20	< 0.0001	0.005
Superior Parietal Lobule	R	2	Primary Somatosensory	48	-42	57	3.32	< 0.0001	0.322
Occipital									
Lateral Occipital	L	19		-39	-63	0	3.77	< 0.0001	0.118
Adolescents > Adults									
Frontal									
Superior Frontal Gyrus	Both	6	Medial Prefrontal Cortex	3	51	33	3.57	< 0.0001	0.331
Temporal									
Insula	R	13	Inferior Mid Insula	33	21	-15	3.43	< 0.0001	0.331
Fusiform Gyrus	L	37		-33	-54	-12	3.37	< 0.0001	0.331
Supramarginal Gyrus	R	22		51	-39	9	3.59	< 0.0001	0.331
Parietal									
Precuneus	Both	31		9	-54	33	3.71	< 0.0001	0.331
Occipital									
Lateral Occipital Cortex	R	19		42	-66	9	3.17	0.001	0.331
Subcortical									
Striatum	L			-12	-9	-6	3.76	< 0.0001	0.331
Hippocampus	L			-36	-27	-12	3.73	< 0.0001	0.331

Table lists significant areas of activation ($p < 0.001$, extent threshold 6 voxels).
HEM = hemisphere in which cluster was located; BA = approximate Brodmann area of cluster;
p(uncorr) = uncorrected cluster probability; *p*(FDR) = cluster probability under false discovery rate

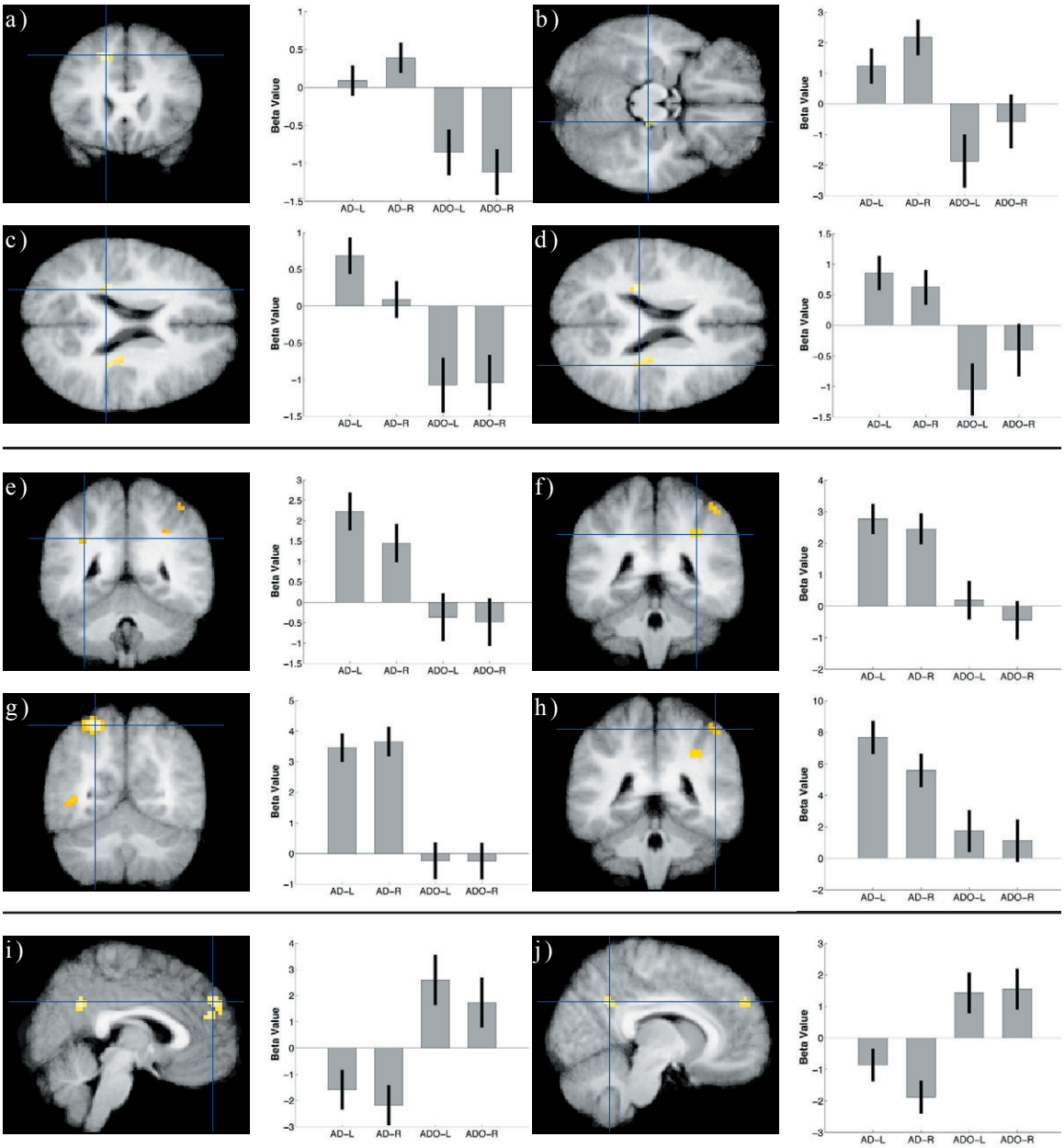

Figure 13. Parameter graphs of developmental differences in passive stimulation. From left to right bars represent thermal-left, thermal-right, tactile-left, and tactile-right conditions. For thermal stimulation adults showed increased activity in areas of dorsal frontal cortex (a), lateral substantia nigra (b), and bilateral secondary somatosensory cortex (c,d). There were no significant regions of greater adolescent activity. For tactile stimulation bilateral areas of intraparietal sulcus (e,f) and superior parietal lobule (g,h) showed increased activity for the adults. The adolescents showed increased activity in medial prefrontal cortex (i) and posterior cingulate (j).

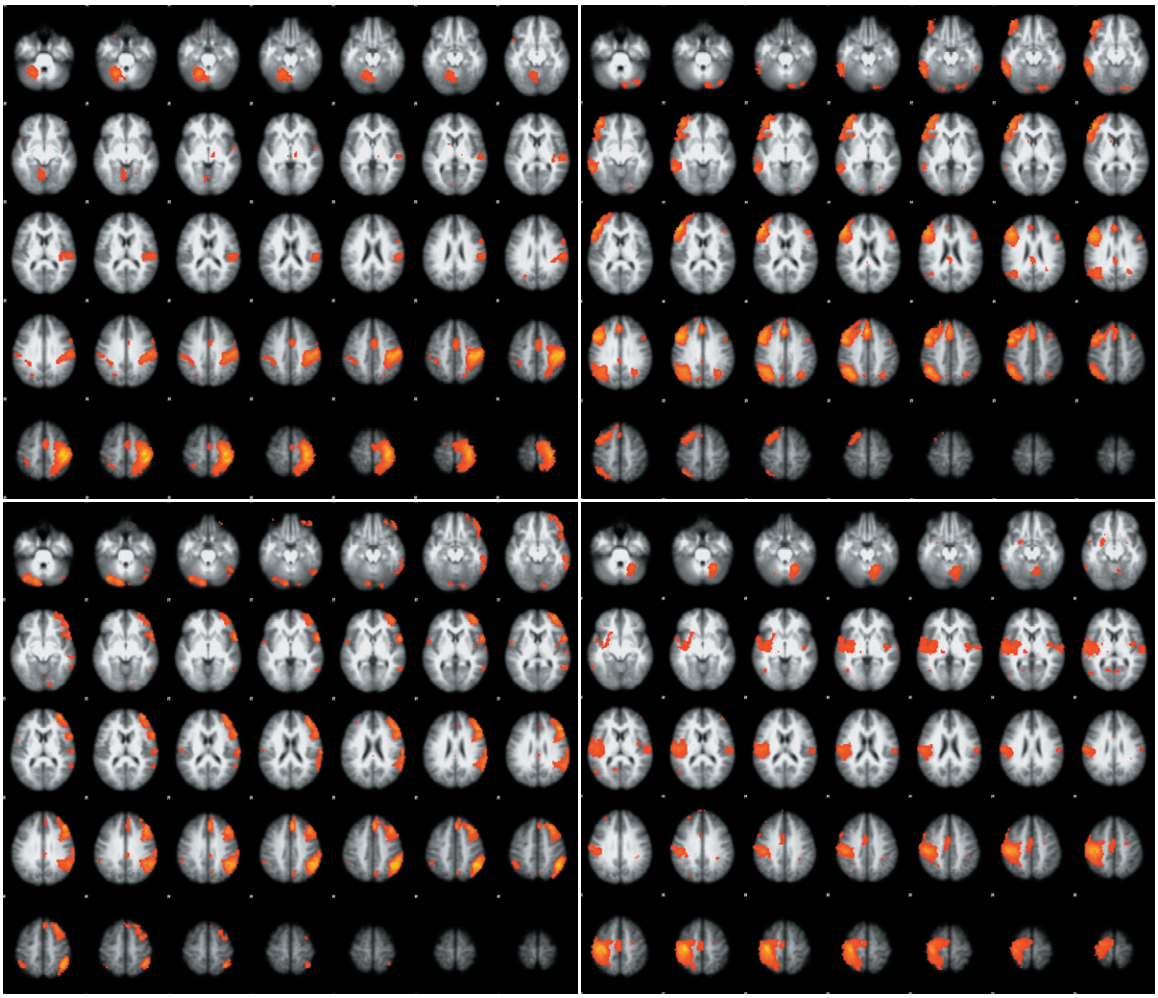

Figure 14. Independent component analysis results of the passive experience data. The left column represents components associated with left hand stimulation and the right column represents components associated with right hand stimulation. These are the only components to include areas of somatosensory cortex and the insula.

Discussion

Effects of passive stimulation. The most important finding from this experiment is the fact that thermal and tactile stimuli share a network of areas to process stimulus features. This result reaffirms previous findings by demonstrating that thermal changes drive activity in regions of secondary somatosensory cortex and posterior insula. This pattern of activity has now been shown across a range of interoceptive modalities and methods. Namely, thermal changes using Peltier thermoelectric devices (Craig et al., 2000), thermal laser stimulation (Frot et al., 2007), painful electric shock (Christmann et al., 2007), and rectal distention (Eickhoff et al., 2006). Still, these studies are limited in that none of them directly compared interoceptive stimulation to other modalities. Conspicuously absent has been a direct comparison to somatosensory stimulation.

It is clear from the results of this experiment that thermal and tactile information are not separable modalities with dissociable regions of primary sensory cortex. This speaks strongly against the assertions of Craig (2002, 2003b) who posits that the posterior insula should be considered as primary interoceptive cortex. By definition, areas of primary sensory cortex should respond in a unimodal fashion to stimuli (Hendry, Hsiao, & Brown, 2003). For example, primary visual cortex will respond uniquely to afferent visual information, but not to auditory input. While primary visual cortex activity can still be modulated by other areas of the brain, it is not chiefly responsible for modalities beyond the scope of vision. This cannot be said for areas of secondary somatosensory cortex, posterior insula, and mid insula. Thermal stimulation generated increased activity across both somatosensory and insular cortex. These same areas showed an equivalent or greater response during tactile stimulation. The only *a priori* area of interest to show a statistically significant unimodal response was bilateral primary somatosensory cortex (BA 2) in response to tactile stimulation.

Conclusions from the general linear model analysis are bolstered by the inclusion of an independent components analysis of the data. Only two statistically separable influences

on somatosensory and insula activity were found per hemisphere. The spatial pattern of each component indicates that somatosensory cortex and posterior/mid insula can operate in a highly correlated fashion regardless of whether the stimulus was thermal or tactile. This speaks further in favor of a network view of primary interoceptive and somatosensory information processing.

It is important to note that there is little developmental change in areas that process the primary and secondary features of somatosensory and internal state information. Few developmental changes were observed in the functional network supporting thermal and tactile information processing. While there were isolated clusters showing developmental differences none of these clusters was located in the primary or secondary sensory areas involved in the early processing of thermal and tactile information. This is logical, given the overall pattern of cortical maturation beginning in early sensory and motor areas and then proceeding over time to higher order areas of association cortex (Giedd et al., 1999; Gogtay et al., 2004; Sowell et al., 1999). It is also critical to note for follow-on studies, as the outright perception of thermal and tactile stimuli is not dramatically changing between early adolescence and adulthood. If any developmental differences are to be found between these age groups they will most likely be in areas of the brain that integrate secondary interoceptive information with higher-order areas of association cortex.

Methodological findings. Of primary importance to further experimentation is validation of the thermotactile apparatus. If the device were to prove impractical due to issues of implementation, MR artifact generation, or poor stimulation capacity it would be critical to uncover such problems before other experiments have begun. Several shortcomings of the device were identified during the planning and construction process and were rectified while still on the benchtop. Additional tuning was completed during an extensive verification, validation, and calibration process [see appendix B for more information]. Still, this was the first full fMRI experiment to utilize the new apparatus.

The results demonstrate that the thermotactile device works very effectively, providing a reliable method of parametrically applying both thermal and tactile stimuli. The qualitative feedback from study participants was that the device was user friendly, intuitive, and rather enjoyable to experience.

An important note for other experiments is that investigation of ventromedial and orbitofrontal areas of prefrontal cortex will be impossible given current echo-planar T2* acquisition parameters. There is a large amount of B0 field inhomogeneity in orbital areas of prefrontal cortex due to the air/fluid interface present in the sphenoid/ethmoid sinus and the long TE times necessary for functional imaging. This causes signal loss due to intravoxel spin dephasing (Deichmann, Gottfried, Hutton, & Turner, 2003). Some research groups have had success using diamagnetic shims in the roof of the mouth to reduce differences in regional magnetic susceptibility (Wilson, Jenkinson, & Jezzard, 2002). Other groups have utilized new acquisition parameters and pulse sequences that are less affected by the differences in susceptibility (Stenger, Boada, & Noll, 2000). For the other planned experiments it may be difficult to acquire quality data from ventromedial prefrontal cortex without the use of new imaging methods or devices.

Finally, it can be concluded from this experiment that to uncover areas of the brain that are preferentially sensitive to internal state information a more advanced experimental paradigm is necessary. Form the current results it has been shown that in tasks involving passive experience the line between interoception and exteroception is a tenuous one at best. Potential differences, if they exist at all, are likely to involve higher-order processing, which would necessitate a more complex experimental design involving the manipulation of higher-order integration.

Experiment Three

Rationale and hypothesis

An idea central to this thesis is that interoceptive information is useful for cognitive processes involved in decision-making. To investigate higher-order processing of interoceptive information it is necessary to create a paradigm that will be able to experimentally manipulate the demand for interoceptive information in the decision making process. To accomplish this end a magnitude comparison task was chosen as the foundation for experiment four. Magnitude comparison enables the partitioning of activity related to primary stimulus features, such as intensity, and abstract stimulus features, such as stimulus distance. This investigation will focus on regions that are modulated by demand for abstract stimulus features.

Few studies have attempted to investigate higher-order interoceptive integration. One reason is carried over from experiment three: it is very difficult to create uniquely interoceptive stimulation. Most major research investigating higher-order effects have used pain as an internal state stimulus. Studies have also used electric shock (Christmann et al., 2007), laser stimulation (Frot et al., 2007), and other forms of nociceptive stimulation. The results of these studies are difficult to interpret from an internal state point of view because they activate a matrix of brain regions involved in not only internal state perception but also action preparation, homeostatic control, and sympathetic up-regulation (Craig, 2003a; Perl, 2007; Vogt, 2005). A better stimulus for the investigation of everyday internal state decision-making would be interoceptive in nature but not painful or uncomfortable. Thermal stimulation is, again, an excellent candidate.

Tactile stimulation will continue to be used as a control modality. This will build on the findings of experiment two, which showed that primary processing of thermal and tactile modalities are highly complementary. While the initial sensory processing may be intermingled, there may still be regions coding specifically for abstract internal state features. It is hoped that higher-order effects in this experiment will be due to the abstract

stimulus features unique to each modality. The main hypothesis for this experiment is a distinction between regions operating on exteroceptive and interoceptive information within somatosensory cortex and the insula. Specifically, activity in the right anterior insula would be modulated as thermal discrimination becomes more difficult. It was also expected that activity in secondary somatosensory cortex would be modulated as tactile discrimination becomes more difficult.

The developmental hypothesis of this experiment is that younger subjects will have a more difficult time on the interoceptive integration task, which requires the use of higher-order cortex to integrate interoceptive stimulus features. Reaction times were predicted to be higher for younger subjects and accuracy scores were predicted to be lower. Regions of interest for all developmental analyses will include bilateral anterior insula, anterior cingulate, and ventromedial prefrontal cortex. These regions are chosen due to their late developmental trajectory (Gogtay et al., 2004) and putative role in higher-order interoceptive processing (Craig, 2002).

Methods

Participants. Twenty healthy right-handed adults (11 female, 9 male, mean age = 27.7, age range = 23.1 to 39.3 years) recruited from the local community and sixteen healthy right-handed adolescents (7 female, 9 male, mean age = 11.7 years, age range = 8.1 to 13.8 years) recruited from local schools participated in experiment three. One female and one male adolescent were excluded from further analysis due to excessive movement (1mm/TR) in their fMRI data. All participants completed an informed consent procedure approved by the Committee for the Protection of Human Subjects at Dartmouth College and were compensated for their time.

Experimental design**.** The experiment was set up as an event-related magnitude comparison task with three modalities: tactile, thermal, and combined thermal/tactile. Within

each modality there were five levels of stimulus distance that were varied throughout the task. Stimulus distance was defined as the absolute difference between the stimulus value of the left and right hands. Each subject completed three event-related fMRI sessions with each consisting of 42 events of a single modality. Each event lasted 650ms and had between 4.5s and 7.0s of rest between each event. Large blocks of rest lasting 15s were placed at the beginning, middle, and end of the task. The order of presentation for stimulus distance was 3-back counterbalanced across the task to avoid order effects. The presentation order of thermal and tactile sessions was counterbalanced across subjects. The combined modality condition was always presented last due to the necessity of previous experience with the stimulus levels. Reaction time and accuracy of responses were both recorded as dependent measures. Functional magnetic resonance imaging data was collected throughout the experiment. Total scan time was approximately 15 minutes.

Apparatus. Experiment four utilized the thermotactile stimulation apparatus described in appendix B. Briefly, the apparatus allowed for the parametric application of thermal and tactile stimuli to the palms of each hand.

Experimental procedure and task detail. Upon arrival the participant was first asked to go through a thermal and tactile calibration procedure. This was done to ensure that stimulation would encompass the entire dynamic range of perception without experiencing discomfort or pain. A stepwise progression of increasing temperature proceeded until the subject reported excessive heat. The calibration value was then the last level of thermal application without discomfort. A similar procedure was used for tactile calibration, with air pressure increasing until it was uncomfortable. The calibration value was then 5 psi below that level.

The participants were told that they would be presented with a magnitude comparison task and what the range of values for each modality would be. For the tactile condition

the participants were told that there would be from 1-5 pegs in contact with their hand and that the correct response would be to press the button on the side that had the greatest number of pegs. If less than five pegs were active a random subset of pegs would be selected to avoid using peg configuration as a cue. For the thermal condition they were told that there would be five discrete levels of temperature ranging from cold to hot and that the correct response would be to press the button on the side [left, right] that had the warmest temperature. To best mimic the tactile condition five different temperatures were used: cold, cool, neutral, warm, and hot. For the combination condition the participants were told to use their previous knowledge of the five temperature levels and the five peg levels to make judgments about which modality was higher on its unique measurement scale. For example, if the left hand had 3 pegs in contact with it (level 3) and the right hand had a warm temperature applied (level 4) the correct response would be to press the right button.

Before being placed in the scanner the participants received task instructions and completed a practice task consisting of four presentations of thermal and four presentations of tactile stimulation. For the practice task the participant was asked if they could clearly discern the stimuli on each hand and what the correct response to each trial would have been. If an individual reported difficulty perceiving the stimuli the apparatus calibration parameters were adjusted to ensure consistent stimulus perception.

Analysis of performance. Reaction time data was transformed using a reciprocal [1/x] calculation to satisfy assumptions of data normality in the linear analysis. Reaction time data for the adult group was analyzed using a one-way multivariate analysis of variance (MANOVA) with stimulus distance [1, 2, 3, 4] as a within-subjects factor. Mean reaction time data from each subject for all thermal, tactile, and mixed condition stimulus distances were input as separate dependent variables. To examine developmental changes in thermal response data a two-way analysis of variance (ANOVA) was calculated. A within-subjects

factor of thermal distance [1, 2, 3, 4] and a between-subjects factor of age group (adult, adolescent) was used.

Preprocessing of imaging data. Data were preprocessed using the methods detailed in appendix A. Preparation of the data involved global artifact detection, realignment of the functional images, coregistration to the high-resolution anatomical image, normalization to the ICBM-152 atlas space, and smoothing using a Gaussian kernel of 8mm.

General linear model analysis of imaging data. A two-level mixed-effects methodology was used to analyze the functional imaging data. The first level consisted of a multiple regression analysis estimated using ordinary least squares (OLS) in SPM2 (Statistical Parametric Mapping, www.fil.ion.ucl.ac.uk/spm/). Predictors were created using an impulse function based the stimulus onset times convolved with a canonical hemodynamic response function. Six predictors of interest were generated according to the modality and distance: thermal-stimulus, thermal-distance, tactile-stimulus, tactile-distance, combination-stimulus, and combination-distance. The stimulus regressors were included to account for the overall effect of stimulation while the distance regressors accounted for any parametric effect of distance within the data. Only trials containing correct magnitude comparisons were included. Incorrect trials for all conditions were modeled as a separate regressor of no interest. Other nuisance predictors were also created to account for low-frequency noise and subject head movement.

For each participant a set of six volumes was generated corresponding to the voxelwise beta estimates of each condition. These images were input into a multiple regression at the second level for final hypothesis testing. The second level was estimated using restricted maximum likelihood (ReML) to account for dependencies and unequal variance among the levels of each repeated measure. Additional details regarding statistical analysis of the fMRI data can be found in appendix A.

Contrasts of interest were generated at the second level to test a priori hypotheses. One contrast was made to test for similarities between thermal and tactile stimulation. Another contrast was setup to examine parametric differences between thermal and tactile stimulation. A contrast was made to test for parametric differences between the combination condition and the unimodal conditions. Finally, one contrast was made to test for potential developmental differences in the parametric response to thermal stimuli.

Results

Analysis of behavior. Adult group response data for the thermal, tactile, and mixed conditions is depicted in Figure 15. A within-subjects multivariate analysis yielded a significant effect of stimulus distance across thermal, tactile, and mixed modalities ($F(9,68.295) = 8.565$, Wilks' Lambda = 0.159, $p < 0.001$, partial $\eta^2 = 0.458$). Follow-on univariate analyses indicated a significant effect of distance in the thermal modality ($F(3,30) = 21.19$, $p < 0.001$, partial $\eta^2 = 0.679$), tactile modality ($F(3,30) = 23.472$, $p < 0.001$, partial $\eta^2 = 0.701$), and mixed modality condition ($F(3,30) = 8.586$, $p < 0.001$, partial $\eta^2 = 0.462$). Polynomial contrasts were completed for each modality and indicated that the stimulus distance factor was strongly linear for thermal ($F(1,10) = 39.19$, $p < 0.001$, partial $\eta^2 = 0.797$), tactile ($F(1,10) = 36.04$, $p < 0.001$, partial $\eta^2 = 0.783$) and mixed conditions ($F(1,10) = 14.66$, $p = 0.003$, partial $\eta^2 = 0.594$). Adolescent and adult response data for the thermal condition are depicted in Figure 16. The between-subjects factor of age did not show a significant difference between the adults and adolescents ($F(1,41) = 0.846$, $p = 0.363$) in the analysis of variance.

Similarity between thermal and tactile parametric response. A conjunction analysis was preformed to determine if any regions had a significant parametric response to both thermal and tactile stimulation. The parameters for this comparison were $t^2(144) > 3.15$, $p < 0.001$, 8 voxel extent threshold. From this analysis several regions of lateral frontal,

superior parietal, and insular cortex were active across modalities (Table 5 and Figure 17). Bilateral areas of anterior insula (Figure 18a, b), intraparietal sulcus (Figure 18c, d), right lateral prefrontal cortex (Figure 18e), and anterior cingulate (Figure 18f) were shown to have a similar parametric response to stimulus distance. Activity in these areas increased as the stimulus distance decreased. There were no areas in the conjunction analysis that demonstrated a positive relationship between increased stimulus distance and increased regional activity.

Differences between thermal and tactile parametric response. A directional *t*-contrast was used to test for regions activating parametrically to one modality over the other. The parameters for this comparison were $t(144) > 3.15$, $p < 0.001$, 8 voxel extent threshold. An array of significant clusters across frontal and temporal areas was found to have a thermal parametric response greater than that found in the tactile condition (Table 6 and Figure 19). Bilateral areas of anterior insula (Figure 20a, b), orbitofrontal cortex (Figure 20c), right mid insula (Figure 20d) were shown to increase activity as thermal stimulus distance was reduced. Areas of dorsolateral prefrontal cortex (Figure 20e) and anterior cingulate (Figure 20f) showed a similar pattern of activity. Significant clusters having a tactile parametric response superior to that found in the thermal condition were found in somatosensory and superior parietal cortex (Table 6 and Figure 19). Bilateral regions of secondary (Figure 20g, h) and primary (Figure 20i, j) somatosensory cortex were shown to increase activity as the tactile stimulus distance was reduced. Additional regions within the right intraparietal sulcus (Figure 20k) were also found.

Differences between multimodal and unimodal parametric responses. A directional *t*-contrast was used to test for regions in the mixed condition with a parametric response greater than that found in either the thermal or tactile conditions. The parameters for this comparison were $t(216) > 3.13$, $p < 0.001$, 8 voxel extent threshold. Most significant clusters

for this comparison were found in lateral frontal and superior parietal areas (Table 7 and Figure 21). Bilateral regions of orbital prefrontal cortex (Figure 22a, b), lateral prefrontal (Figure 22c, d), dorsolateral prefrontal (Figure 22e, f), intraparietal cortex (Figure 22g, h), and anterior cingulate (Figure 22i) were found to have a parametric response greater than that found in either the thermal or tactile conditions. There were no areas of greater thermal or tactile response relative to the mixed condition.

Differences in thermal parametric response between adults and adolescents. A directional *t*-contrast was used to test for regions showing differences in activity to the thermal task across development. The parameters for this comparison were $t(128) > 3.15$, $p < 0.001$, 8 voxel extent threshold. Several clusters were found to have a thermal response greater in the adolescent group relative to the adult group. Most of these areas were found along the precentral gyrus, postcentral gyrus, and the insula (Table 8 and Figure 23). Regions of the right mid insula (Figure 24a), left central operculum (Figure 24b, c), right primary somatosensory cortex (Figure 24d), right supplementary motor area (Figure 24e), and right secondary somatosensory cortex (Figure 24f) were found to have greater activity in the adolescent group. There were no clusters having a greater response in the adult group.

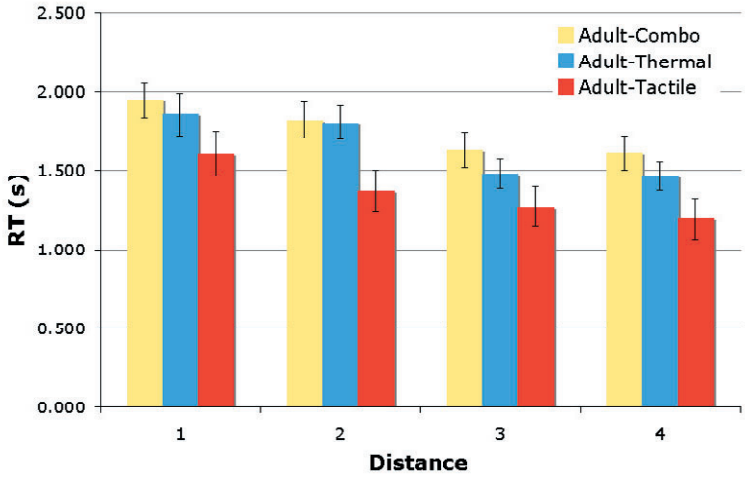

Figure 15. Plots of behavioral performance across modalities. Response data for the adult group only. A significant linear effect of decreasing reaction time with increasing stimulus distance was found across all conditions ($p < 0.001$).

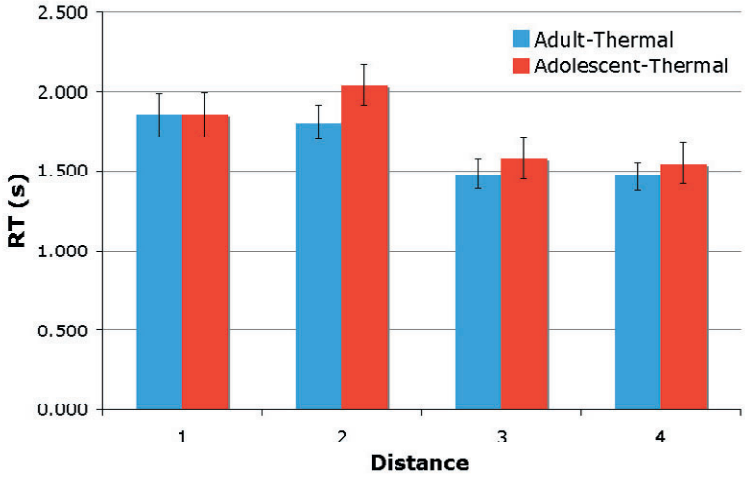

Figure 16. Response data showing thermal reaction time for the adult and adolescent groups. The two groups did not significantly differ across values of stimulus distance ($p = 0.363$).

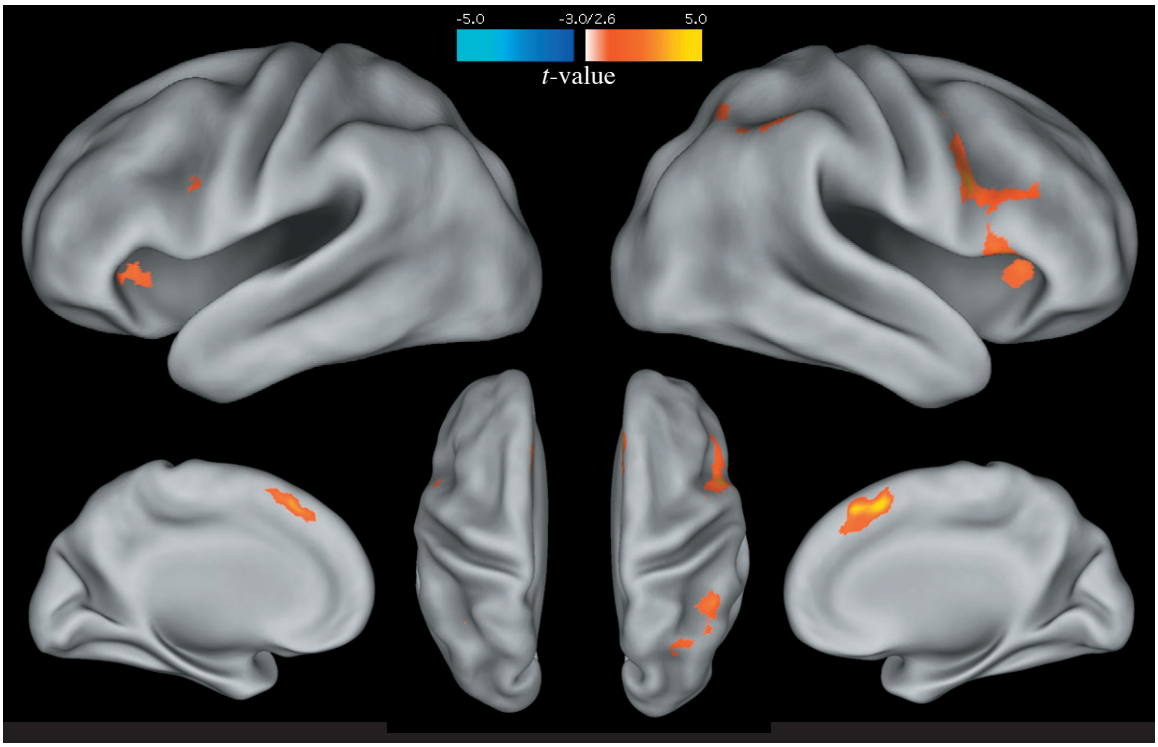

Figure 17. Regions of similar linear increases in activity between the thermal and tactile magnitude conditions. The parameters for this comparison were $t^2(144) > 3.15$, $p < 0.001$, 8 voxel extent threshold. From this analysis several regions of lateral frontal, superior parietal, and insular cortex we active across modalities.

Table 5
Regions showing activity to both thermal and tactile magnitude conditions

Region Name	HEM	BA	Area Notes	MNI Coordinates x	y	z	*z*-value	*p*(uncorr)	*p*(FDR)
Frontal									
Inferior Frontal Gyrus	R	10	Frontal Pole	48	42	-6	3.50	< 0.0001	0.053
Inferior Frontal Gyrus	R	45	Broca's Area	48	21	3	4.17	< 0.0001	0.013
Inferior Frontal Gyrus	R	44	Broca's Area	51	12	24	4.41	< 0.0001	0.007
Paracingulate Gyrus	Both	8		3	27	48	5.21	< 0.0001	0.003
Temporal									
Insula	L	13	Anterior Insula	-30	24	3	3.80	< 0.0001	0.029
Insula	R	13	Anterior Insula	33	21	3	3.57	< 0.0001	0.050
Parietal									
Intraparietal Sulcus	L	hIP1		-30	-51	36	3.33	< 0.0001	0.067
Intraparietal Sulcus	R	hIP1		30	-54	39	3.93	< 0.0001	0.021
Intraparietal Sulcus	R	hIP1		45	-45	42	3.70	< 0.0001	0.037
Superior Parietal Lobule	R	7		33	-60	54	3.34	< 0.0001	0.067

Table lists significant areas of activation ($p < 0.001$, extent threshold 6 voxels).
HEM = hemisphere in which cluster was located; BA = approximate Brodmann area of cluster;
p(uncorr) = uncorrected cluster probability; *p*(FDR) = cluster probability under false discovery rate

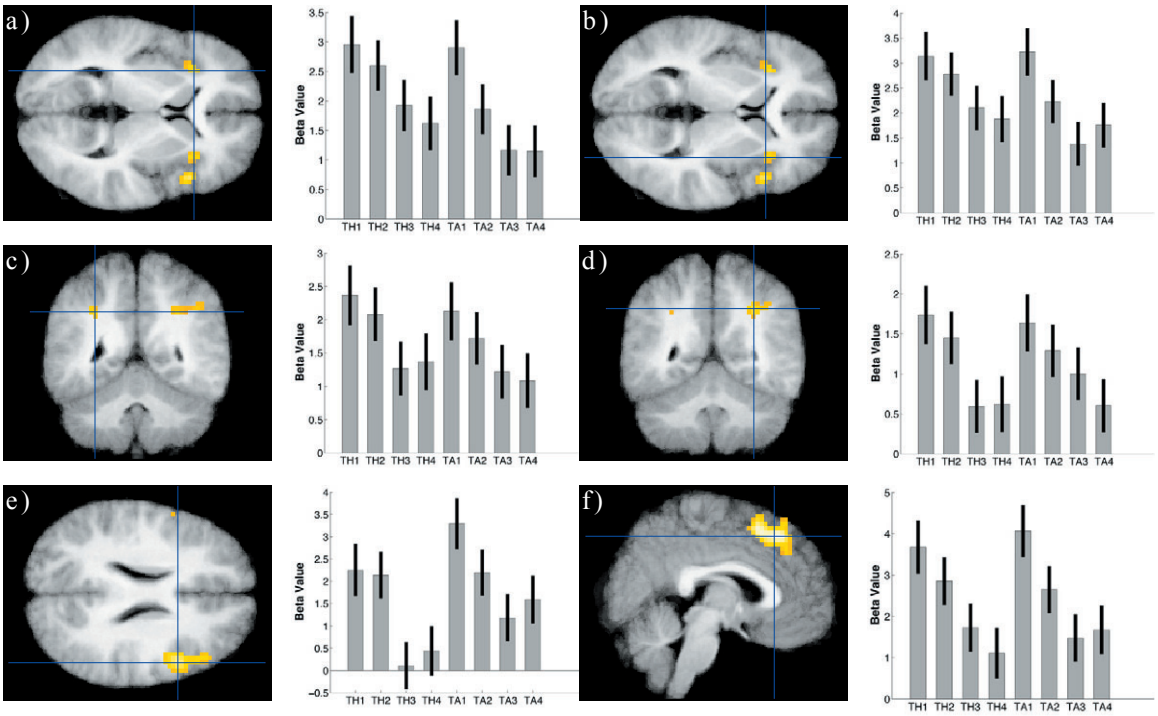

Figure 18. Parameter graphs of regions with a linear response to both thermal and tactile stimulation. Bars represent levels of thermal stimulation (TH1-TH4) and levels of tactile stimulation (TA1-TA4). Bilateral areas of anterior insula (a,b), intraparietal sulcus (c,d), right lateral prefrontal cortex (e), and anterior cingulate (f) were shown to have a similar parametric response to stimulus distance.

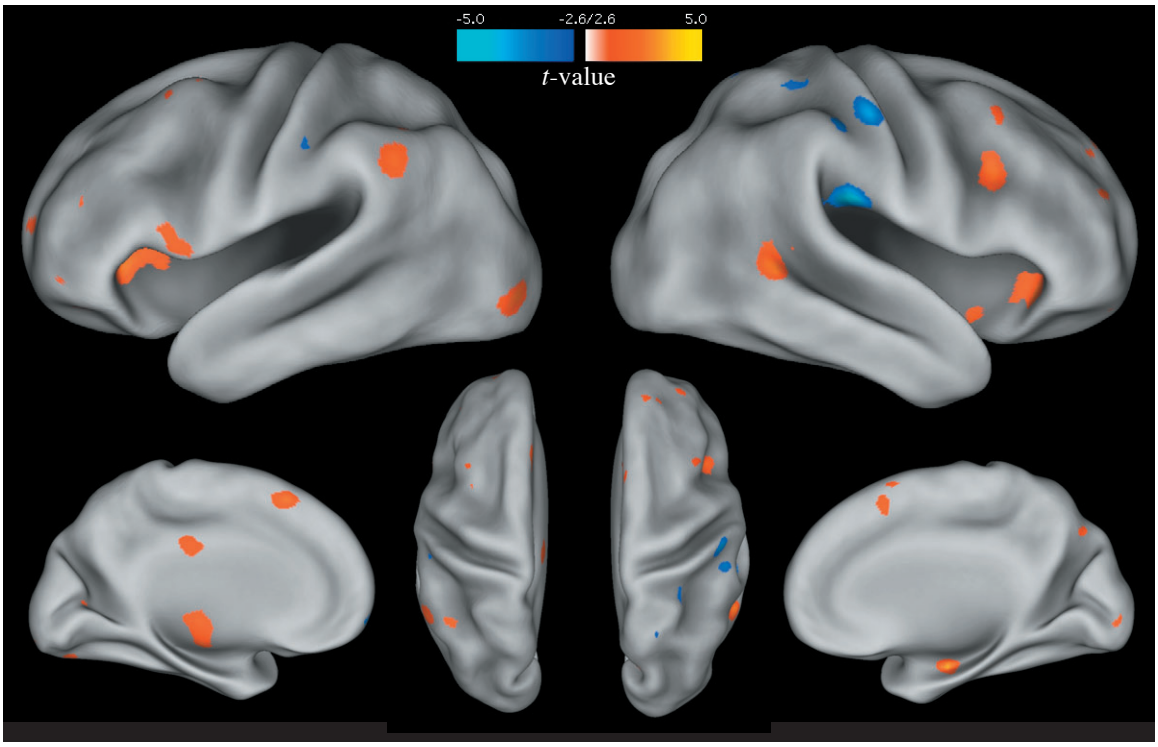

Figure 19. Areas of preferential increase in activity by modality. Areas with preferential activity to the thermal condition are depicted in red and areas with preferential activity to the tactile condition are depicted in blue. The parameters for this comparison were $t(144) > 3.15$, $p < 0.001$, 8 voxel extent threshold. An array of significant clusters across frontal and temporal areas was found to have a greater thermal parametric response. Significant clusters having a greater tactile parametric response were found in somatosensory and superior parietal cortex.

Table 6
Regions showing a linear effect of one modality relative to the other

Anatomical Location	HEM	BA	Area Notes	MNI Coordinates x	y	z	*z*-value	*p*(uncorr)	*p*(FDR)
Thermal Condition									
Frontal									
Inferior Frontal Gyrus	L	11	Orbital Frontal	-33	42	-9	4.3	< 0.0001	0.094
Superior Frontal Gyrus	L	10	Frontal Pole	-27	66	9	3.55	0.0003	0.145
Middle Frontal Gyrus	L	46	Lateral Frontal	-45	39	18	3.39	0.0005	0.155
Middle Frontal Gyrus	R	9	Lateral Frontal	33	54	24	3.41	0.0004	0.153
Inferior Frontal Gyrus	R	9	Lateral Frontal	39	15	27	3.84	< 0.0001	0.131
Cingulate Gyrus	L	23	Posterior Cingulate	-3	-24	30	3.25	0.0007	0.158
Middle Frontal Gyrus	L	9	Lateral Frontal	-48	24	33	3.36	0.0005	0.155
Superior Frontal Gyrus	Mid	8	Dorsal Cingulate	0	24	54	3.88	< 0.0001	0.131
Middle Frontal Gyrus	L	6	Lateral Frontal	-39	15	54	3.59	0.0002	0.145
Middle Frontal Gyrus	R	6	Lateral Frontal	45	21	51	4.27	< 0.0001	0.131
Temporal									
Insular Cortex	R	13	Mid Insula	36	9	-9	3.65	0.0002	0.144
Insular Cortex	R	13	Anterior Insula	33	27	-6	3.83	< 0.0001	0.132
Middle Temporal Gyrus	R	21		60	-45	6	4.94	< 0.0001	0.044
Insular Cortex	L	13	Anterior Insula	-27	27	3	4.05	< 0.0001	0.130
Insular Cortex	L	13	Mid Insula	-30	3	18	3.91	< 0.0001	0.132
Parietal									
Supramarginal Gyrus	L	40		-54	-51	36	3.59	0.0002	0.145
Occipital									
Fusiform Gyrus	L	37	Inferior Temporal	-30	-78	-18	3.38	0.0005	0.155
Lateral Occipital Cortex	L	18		-36	-87	-3	3.8	0.0001	0.132
Intracalcarine Cortex	L	17	Primary Visual / V1	-21	-72	9	3.85	< 0.0001	0.132
Subcortical									
Hippocampus	R			30	-12	-18	4.41	< 0.0001	0.094
Caudate	R			15	9	9	3.48	0.0003	0.150
Cerebellum									
Inferior Cerebellum (CrI)	R			44	-62	-41	4.44	< 0.0001	0.094
Tactile Condition									
Parietal									
Postcentral Gyrus	L	OP1	Secondary Somatosensory	-51	-21	24	3.33	0.0005	0.316
Postcentral Gyrus	R	OP1	Secondary Somatosensory	54	-24	21	4.24	< 0.0001	0.187
Postcentral Gyrus	L	2	Primary Somatosensory	-51	-24	39	3.64	0.0002	0.282
Postcentral Gyrus	L	3a	Primary Somatosensory	-39	-27	39	3.71	0.0001	0.277
Postcentral Gyrus	R	2	Primary Somatosensory	54	-21	48	4.61	< 0.0001	0.117
Intraparietal Sulcus	R	hIP1		42	-45	57	3.74	0.0001	0.261
Intraparietal Sulcus	R	hIP1		30	-66	51	3.51	0.0003	0.300

Table lists significant areas of activation ($p < 0.001$, extent threshold 6 voxels).
HEM = hemisphere in which cluster was located; BA = approximate Brodmann area of cluster;
p(uncorr) = uncorrected cluster probability; *p*(FDR) = cluster probability under false discovery rate

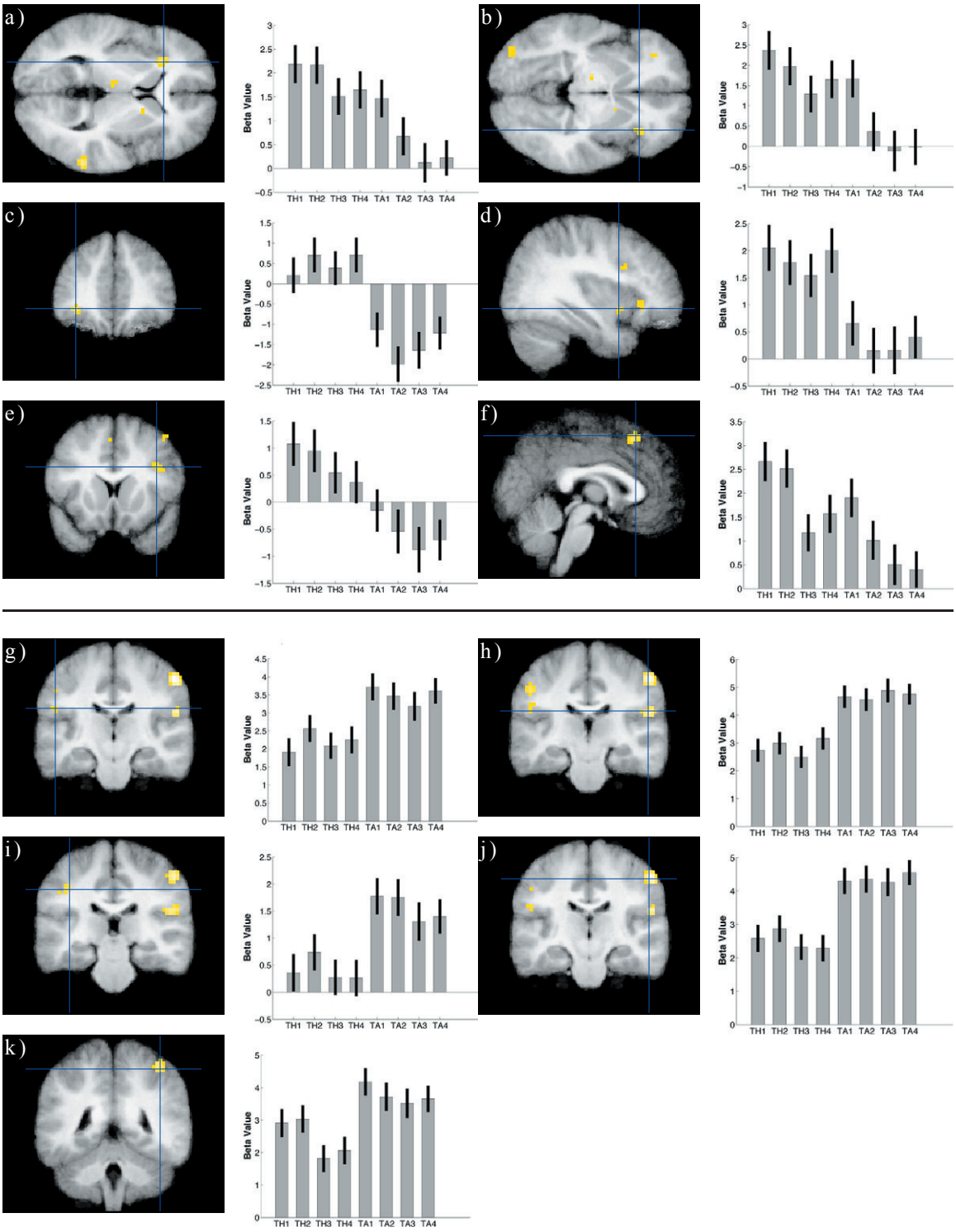

Figure 20. Parameter graphs of regions with a linear response to both thermal and tactile stimulation. Bars represent levels of thermal stimulation (TH1-TH4) and levels of tactile stimulation (TA1-TA4). Bilateral areas of anterior insula (a,b), orbitofrontal cortex (c), right mid insula (d) were shown to increase activity as thermal stimulus distance was reduced. Areas of dorsolateral prefrontal cortex (e) and anterior cingulate (f) showed a similar pattern of activity. For tactile stimuli bilateral regions of secondary (g,h) and primary (i,j) somatosensory cortex were shown to increase activity as the stimulus distance was reduced. Additional regions within the right intraparietal sulcus (k) we also found.

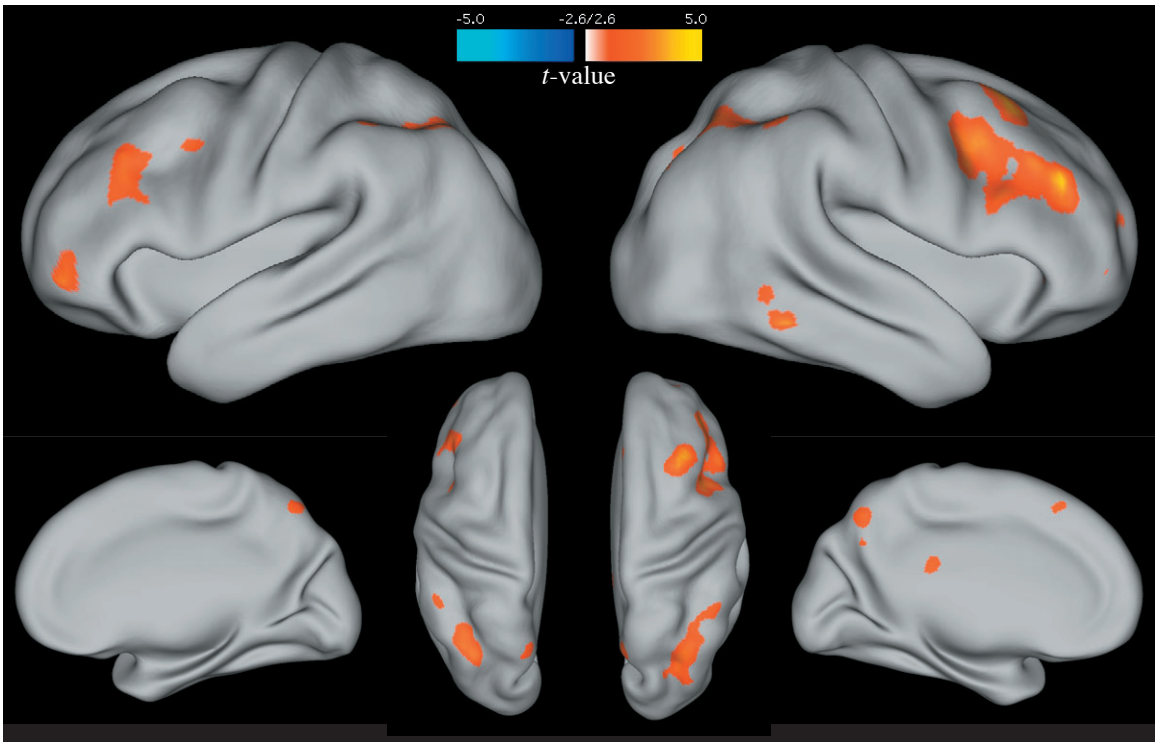

Figure 21. Areas showing differences in activity for the mixed modality condition. Relative increases over thermal and tactile are depicted in red. Relative decreases from thermal and tactile are depicted in blue. The parameters for this comparison were $t(216) > 3.13$, $p < 0.001$, 8 voxel extent threshold. Most significant clusters for this comparison were found in lateral frontal and superior parietal areas.

Table 7
Regions showing a linear effect of the mixed condition in the thermotactile task

Anatomical Location	HEM	BA	Area Notes	MNI Coordinates x	y	z	*z*-value	*p*(uncorr)	*p*(FDR)
Frontal									
Inferior Frontal Gyrus	L	11	Orbital Frontal	-27	27	-12	3.71	0.0001	0.012
Inferior Frontal Gyrus	R	11	Orbital Frontal	24	27	-9	3.85	0.0001	0.010
Inferior Frontal Gyrus	L	47	Lateral Frontal	-42	48	-6	4.76	< 0.0001	0.003
Inferior Frontal Gyrus	R	45	Broca's Area	39	36	0	3.92	0.0001	0.009
Inferior Frontal Gyrus	R	46	Lateral Frontal	36	42	3	3.90	0.0001	0.009
Middle Frontal Gyrus	R	46	Lateral Frontal	45	36	24	5.02	< 0.0001	0.002
Middle Frontal Gyrus	L	9	Lateral Frontal	-54	21	36	5.52	< 0.0001	0.001
Middle Frontal Gyrus	R	9	Lateral Frontal	45	9	36	5.04	< 0.0001	0.002
Paracingulate Gyrus	Bilat	8	Dorsal Cingulate	0	24	51	4.45	< 0.0001	0.004
Temporal									
Inferior Temporal Gyrus	L	37		-57	-51	-18	3.69	0.0001	0.012
Inferior Temporal Gyrus	R	20		57	-42	-15	4.50	< 0.0001	0.004
Insular Cortex	L	13	Anterior Insula	-36	21	0	3.73	0.0001	0.012
Parietal									
Intraparietal Sulcus	L	hIP1		-39	-57	48	4.86	< 0.0001	0.002
Intraparietal Sulcus	R	hIP1		33	-66	48	4.14	< 0.0001	0.006
Precuneus	Bilat	31		3	-69	54	4.18	< 0.0001	0.006

Table lists significant areas of activation ($p < 0.001$, extent threshold 6 voxels).
HEM = hemisphere in which cluster was located; BA = approximate Brodmann area of cluster; *p*(uncorr) = uncorrected cluster probability; *p*(FDR) = cluster probability under false discovery rate

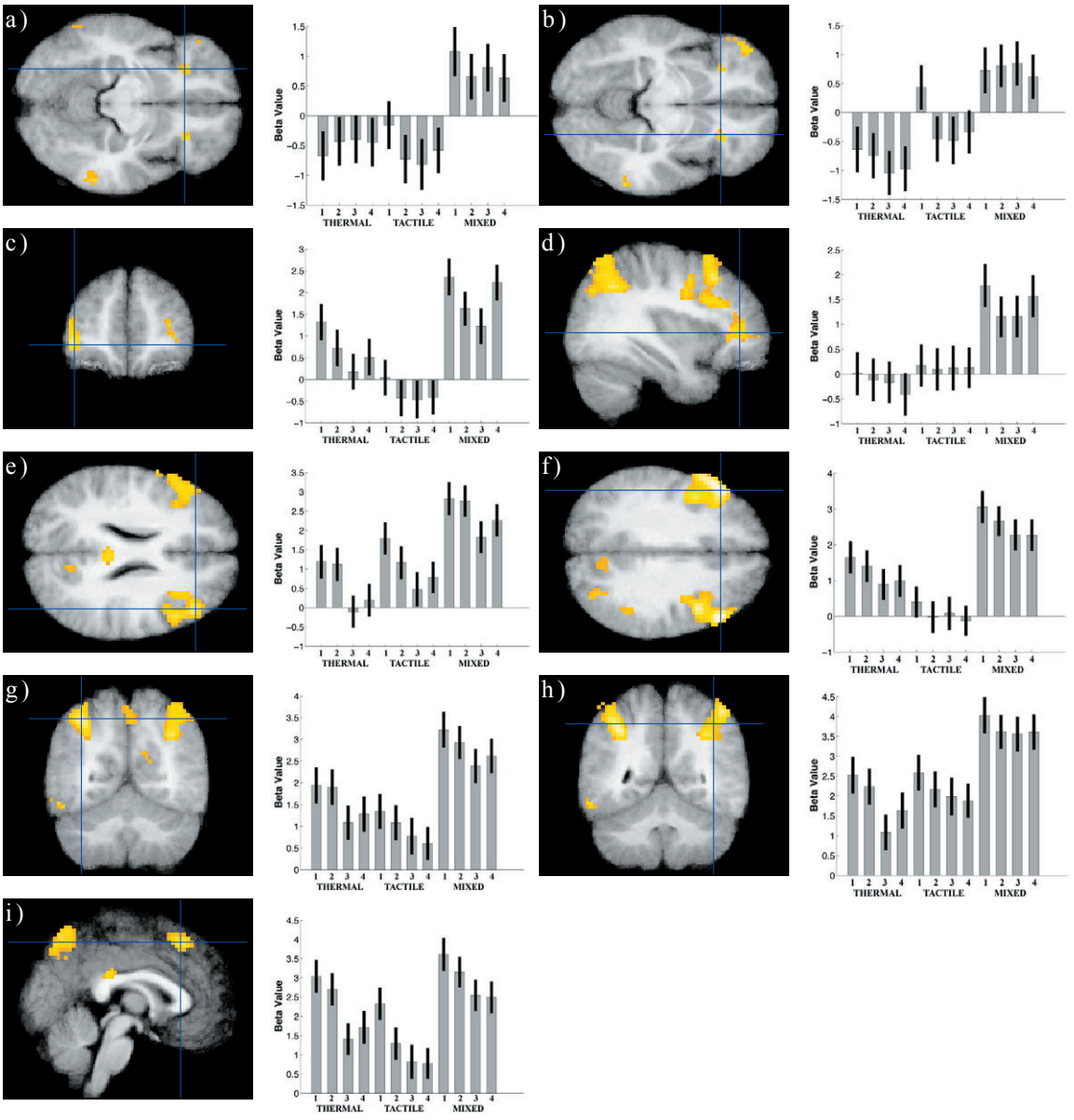

Figure 22. Parameter graphs of regions with a greater linear response to multimodal conditions. Bars represent levels of thermal stimulation (TH1-TH4), levels of tactile stimulation (TA1-TA4), and levels of multimodal stimulation (MX1-MX4). Bilateral regions of orbital prefrontal cortex (a,b), lateral prefrontal (c,d), dorsolateral prefrontal (e,f), intraparietal cortex (g,h), and anterior cingulate (i) were found to have a parametric response greater than that found in either the thermal or tactile conditions. There were no areas of greater thermal or tactile response relative to the mixed condition.

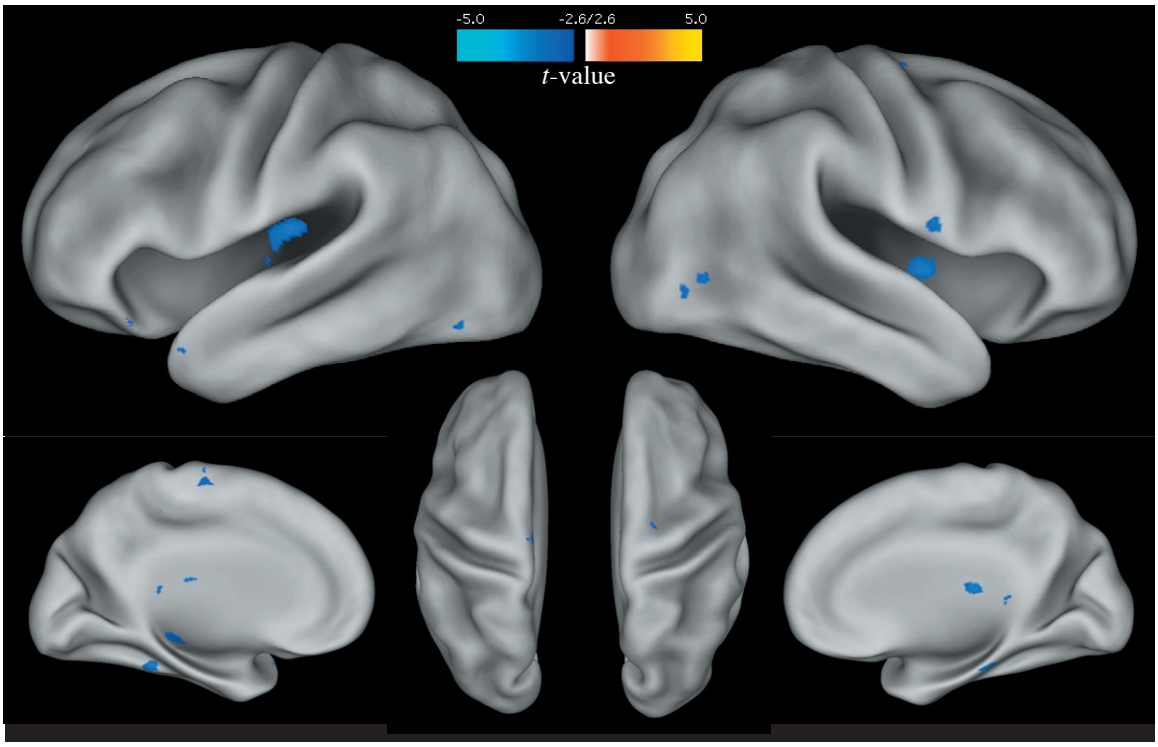

Figure 23. Developmental changes in activity within the thermal magnitude condition. Areas of increased response in the adult group are depicted in red and areas of increased response in the adolescents are depicted in blue. The parameters for this comparison were $t(128) > 3.15, p < 0.001$, 8 voxel extent threshold. Several clusters were found to have a thermal response greater in the adolescent group along the precentral gyrus, postcentral gyrus, and the insula. There were no clusters having a greater response in the adult group.

Table 8
Regions showing a main effect of age in the thermotactile task

Anatomical Location	HEM	BA	Area Notes	MNI Coordinates x	y	z	*z*-value	*p*(uncorr)	*p*(FDR)
Adolescents > Adults									
Frontal									
Precentral Gyrus	R	6	Premotor	45	-3	42	3.60	0.0002	0.206
Precentral Gyrus	L	6	Premotor	-33	12	39	3.20	0.0009	0.270
Precentral Gyrus	L	6	Premotor	18	-9	60	3.65	0.0002	0.200
Precentral Gyrus	L	6	Premotor	-9	-21	60	3.52	0.0003	0.230
Temporal									
Fusiform Gyrus	L	37	Inferior Temporal	-27	-36	-24	3.30	0.0006	0.252
Fusiform Gyrus	R	37	Inferior Temporal	24	-33	-27	3.65	0.0002	0.200
Fusiform Gyrus	L	37	Inferior Temporal	-36	-78	-12	4.12	< 0.0001	0.150
Insular Cortex	L	13	Anterior Insula	-39	21	-18	4.20	< 0.0001	0.150
Insular Cortex	R	13	Mid Insula	39	-3	3	3.47	0.0004	0.240
Insular Cortex	L	13	Anterior Insula	-33	21	18	4.61	< 0.0001	0.089
Insular Cortex	L	13	Posterior Insula	-30	-21	18	3.85	0.0001	0.185
Insular Cortex	L	13	Mid Insula	-36	6	21	3.34	0.0005	0.250
Parietal									
Central Parietal Operculum	R	OP4	Secondary Somatosensory	54	0	18	3.92	0.0001	0.169
Central Parietal Operculum	R	OP5	Secondary Somatosensory	42	-3	24	4.59	< 0.0001	0.089
Postcentral Gyrus	L	3a	Primary Somatosensory	-48	-6	21	3.45	0.0004	0.240
Postcentral Gyrus	R	3a	Primary Somatosensory	42	-3	24	4.59	< 0.0001	0.089
Subcortical									
Substantia Nigra	R			9	-12	-12	4.06	< 0.0001	0.150
Hippocampus	L			-18	-27	-6	3.68	0.0002	0.200
Pallidum (External)	L			-18	-3	-3	3.74	0.0001	0.197

Table lists significant areas of activation ($p < 0.001$, extent threshold 6 voxels).
HEM = hemisphere in which cluster was located; BA = approximate Brodmann area of cluster;
p(uncorr) = uncorrected cluster probability; *p*(FDR) = cluster probability under false discovery rate

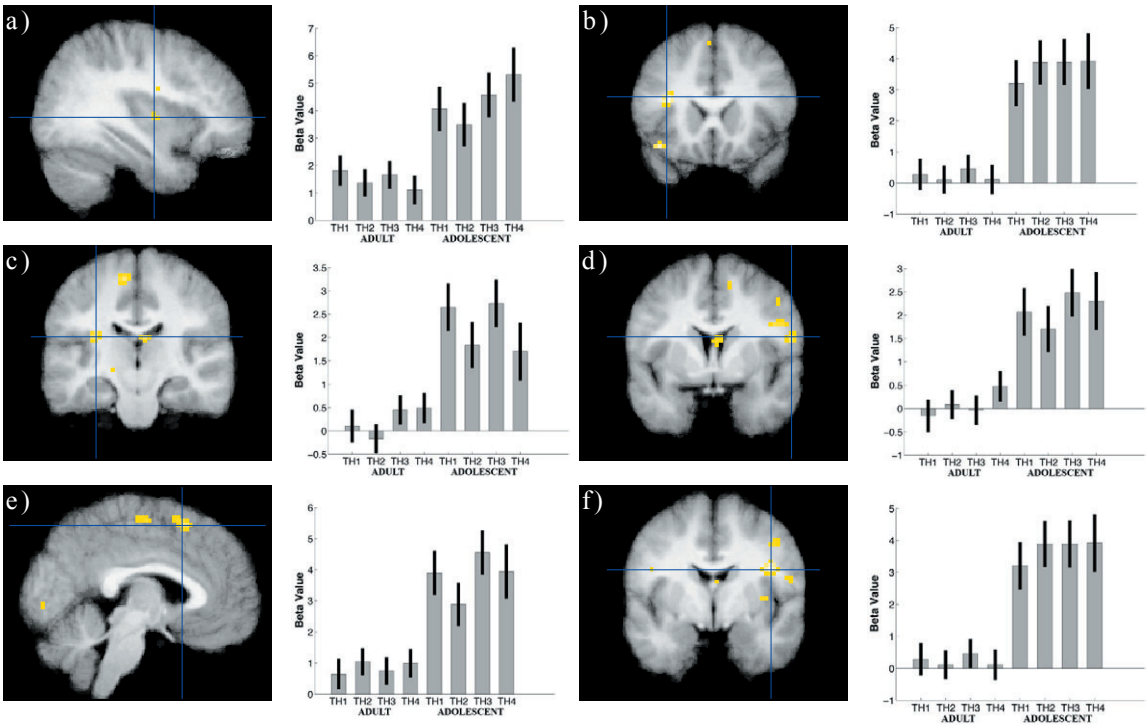

Figure 24. Parameter graphs of regions with a developmental difference in thermal stimulation. Bars represent levels of thermal stimulation for adults (AD1-AD4) and adolescents (ADO1-ADO4). Regions of the right mid insula (a), left central operculum (b,c), right primary somatosensory cortex (d), right supplementary motor area (e), and right secondary somatosensory cortex (f) were found to have greater activity in the adolescent group. There were no clusters having a greater response in the adult group.

Discussion

Effects of stimulus distance. From this experiment it is apparent that the higher-order construct of stimulus 'distance' can be used to test for cortical regions preferentially sensitive to a modality. It is important to note that areas found to be sensitive to one modality relative to the other were not modulated by overall stimulus intensity. For instance, a stimulus distance of two could easily have been a pairing of 1-3 or 3-5 between each hand. Instead the activity in those regions was modulated by overall information demand. At very large stimulus distances (4,5) the sensory discrimination is quite easy and requires very little information to complete. Conversely, when the stimulus distances were small (1,2) the discrimination is made more difficult and additional information regarding stimulus features is required. When thermal information demand was greatest areas of mid and anterior insula were more active. When tactile information demand was greatest activity in primary and secondary somatosensory cortex was increased.

These facts greatly expand our knowledge of modality-specific processing for thermal and tactile information. In the previous experiment these modalities were shown to have overlapping networks of regions that participate in unimodal information processing. This was discussed as evidence against the strong distinction between interoceptive and exteroceptive information in the cortex (Craig, 2002, 2003a). Still, as demand for stimulus features is increased these overlapping networks are shown to have preferred operating modalities at which they are most efficient. This may help to explain why certain areas of the anterior insula were active for both conditions while other neighboring areas showed modality-specific activity to thermal stimulation. The strong binary distinction between interoceptive and exteroceptive processing breaks down into a spectrum of involvement, with regions of the insula ideally processing some of each.

The multimodal results illustrate that the thermal and tactile distance results do not merely reflect difficulty, but rather information demand If the results of the unimodal conditions simply reflected decision difficulty then it would be expected that their activity

would be modulated in the mixed condition in the same way as it was during the unimodal conditions. Instead, it was found that areas of posterior parietal and lateral frontal association cortex had activity that parametrically varied by stimulus distance. From previous evidence this pattern of activity is likely to be a reflection of abstract multimodal processing (Banati, Goerres, Tjoa, Aggleton, & Grasby, 2000; Grefkes & Fink, 2005; Grefkes, Weiss, Zilles, & Fink, 2002; Romanski, 2007). It is meaningful that the frontal and parietal regions were not modulated in the thermal- and tactile-only conditions.

Developmental results. Developmental changes were seen as the reduction of activation foci in fronto-parietal operculum adjacent to the insula. The developmental changes most likely reflect inefficiency in adolescent insular cortex, requiring the secondary activation of adjacent regions. The lack of developmental change in the primary thermal regions identified in the adults is surprising. The original hypothesis was that the same regions shown to be preferentially involved in the thermal modality would have a different activity profile in the adolescents. The results instead point to an interoceptive system that is still immature and inefficient, relying on adjacent areas of cortex to 'pitch in' and assist with required information processing. Multiple areas of dorsal mid insula and adjacent central operculum were shown to have increased activity in the adolescent group relative to the adult group. In the adult group the signal change for these areas was zero, indicating that these were regions active only in the adolescent group. This means that regions that are not being used by the adults were being co-opted for the processing of thermal information in the adolescents.

The idea of immature brains utilizing a wider array of regions to complete a task is not new. The effect was identified many years ago during the early stages of developmental functional imaging (B. J. Casey et al., 1995). It is believed that these secondary activations reflect cortex that is immature, inefficient, and less specialized (B. J. Casey, Tottenham, Liston, & Durston, 2005; Johnson, 1997). Because a single cortical region cannot

completely process the information necessary for a given task the demands are instead farmed out to other areas that are either highly connected to the immature area or highly related to the processing of the task demands. While the behavioral performance of the adolescents was not significantly different from the adults it is clear that they used a different constellation of cortical regions to achieve this end. Luna et al. (2001) saw a similar pattern of equal behavior but different cortical activity in adolescents on an antisaccade task. They concluded that, while the adolescent groups may be equivalent in terms of their behavior, they were still developing in terms of the brain regions involved in completing the task, something they referred to as the 'emergence of collaborative function'.

One problem arose with regard to the thermotactile stimulus device and its compatibility with young adolescents. While the apparatus was validated across a wide range of adult hands the narrower hands of the young adolescents were not always large enough to routinely cover all tactile stimulation sites. Their hands would be positioned correctly when placed inside the scanner and the preceding passive task did not require the hands to move in any way. However, the current experiment required the participants to respond with a button press, requiring hand movement. A majority of the adolescent subjects missed several decisions because their hand was consistently out of place. As a result of this issue no developmental data was available for the tactile or mixed stimulus conditions.

Experiment Four

Rationale and hypothesis

It is a curious aspect of the brain's architecture that areas known to be involved in interoceptive information processing often play a role in executive control as well. Regions of the anterior insula and dorsal anterior cingulate have such a role. They receive abstract interoceptive information from primary sensory areas and have a role in higher-order executive networks (Dosenbach et al., 2007; Dosenbach et al., 2006). Why is this so? One hallmark of Damasio's Somatic Marker Hypothesis (Antonio R. Damasio, 1994) is the idea that a fast emotional bias signal that can quickly alter the dynamics of decision-making and executive control. Damasio argues that the Somatic Marker is the instantiation of the bias signal and originates from areas involved in internal state perception and integration. This theory is expanded upon the work of James [1890] and Nauta (1971), who both advocated a role of body state in decision-making and the generation of emotional states. According to Damasio's theory the right anterior insula and ventromedial prefrontal cortex are both critical areas for the generation and use of the emotional bias signal. Experiment 4 examines this by requiring the integration of interoceptive and exteroceptive information to accomplish higher-order cognitive control.

One area of particular interest for this study is the anterior cingulate. While there are many theories of cingulate function there is little consensus about the information processing that occurs in its many subregions. Cingulate activity has been demonstrated in tasks ranging from selective attention (Peterson et al., 1999) to induced sadness (George et al., 1995). Meta-analyses have been able to tease apart some of this uncertainty by grouping similar results across studies. One such analysis found that dorsal anterior cingulate showed activity for tasks that were generally cognitive while subgenual anterior cingulate was shown to be in involved in tasks that were more emotional in nature (Bush, Luu, & Posner, 2000). This dorsal area of the cingulate is the same region that shows increased activity during top-down autonomic control (Critchley, Tang et al., 2005) and

is known to receive visceral afferents from the thalamus (Craig, 2002). Because of its established function and connectivity, it is hypothesized that the dorsal cingulate will be critical to accomplishing cognitive control through interoceptive cues.

The hypothesis for this experiment is that executive processes used for sensory attention will show significantly different activity between interoception and exteroception. This hypothesis is based on other studies using cues for go/no-go decisions (Bekker, Kenemans, & Verbaten, 2005; B. Casey et al., 1997; Herrmann, Plichta, Ehlis, & Fallgatter, 2005) and existing knowledge of internal/external state representations in prefrontal cortex (Hurliman, Nagode, & Pardo, 2005; Simons, Davis, Gilbert, Frith, & Burgess, 2006). It is believed that areas of the dorsal anterior cingulate, bilateral anterior insula, and ventromedial prefrontal cortex will all show increased activity any time executive control must be engaged when using a thermal stimulus as a cue. The developmental hypothesis for this experiment is that younger subjects will be less able to consider interoceptive information for use in cognitive control. The reaction times will be higher for younger subjects and accuracy scores will be lower. Regions of interest will include bilateral anterior insula, anterior cingulate, and ventromedial prefrontal cortex.

Methods

Participants. Nineteen healthy right-handed adults (13 female, 6 male, mean age = 28.1, age range = 22.3 to 39.3 years) recruited from the local community and fifteen healthy right-handed adolescents (10 female, 5 male, mean age = 11.9 years, age range = 9.4 to 13.8 years) recruited from local schools participated in experiment four. One male adolescent subject was excluded from further analysis due to excessive head movement (1mm/TR) in their fMRI data. All subjects completed an informed consent procedure approved by the Committee for the Protection of Human Subjects at Dartmouth College and were compensated for their time.

Experimental design**.** The experiment is set up as an event-related go/no-go task with two sensory modality cues: thermal and visual. The participants completed two sessions of the task with 99 total trials per session. Of the 99 trials there were 69 'GO' events and 30 'NOGO' events assembled in 30 stimulus trains of 0 to 4 GO events preceding each NOGO event. This design closely matches the experimental setup of Durston et al. (2003). The number of preceding GO events was 3-back counterbalanced across the experiment. Within a stimulus train each event lasted 500ms and had 2500ms of rest between each event. Stimulus trains were separated by a blank period lasting between 3.5s and 5.5s. Large blocks of rest lasting 15s were placed at the beginning, first quarter, half, final quarter, and end of the task. The presentation order of thermal and visual sessions was counterbalanced across subjects. Reaction time and accuracy of go/no-go responses were recorded as dependent measures. Functional magnetic resonance imaging data was collected throughout the whole experiment. Total scan time was approximately 20 minutes.

Apparatus. Experiment 5 utilized the thermotactile stimulation apparatus described in appendix B. Briefly, the apparatus allowed for the parametric application of thermal and tactile stimuli to the palms of each hand.

Experimental procedure and task detail. Upon arrival the participant was first asked to go through a thermal calibration procedure. This was done to ensure that stimulation would encompass the entire dynamic range of perception without experiencing discomfort or pain. A stepwise progression of increasing temperature proceeded until the subject reported excessive heat. The calibration value was then the last level of thermal application without discomfort.

The participants were told that they would be completing a task called 'Go/NoGo' where they had to use either thermal or visual information to decide whether to press a

button. For the visual condition they were instructed to press a button any time they saw a large green square presented and to not press the button any time they saw a large red square presented. For the thermal condition the participants were instructed to press a button any time they felt a warm temperature and to not press the button any time they felt a cool temperature.

Before being placed in the scanner the participants received task instructions and completed a practice task consisting of four presentations of both thermal and visual stimuli. For the practice task the participant was asked if they could clearly discern the stimuli on each hand and what the correct response to each trial would have been. If an individual reported difficulty perceiving the thermal modality the apparatus calibration parameters were adjusted to ensure consistent stimulus perception.

Analysis of performance. Reaction time data was transformed using a reciprocal [1/x] calculation to satisfy assumptions of data normality in the linear analysis. Reaction time data was analyzed using a one-way multivariate analysis of variance (MANOVA) with age group [adults, adolescents] as a between-subjects factor. Mean reaction time data from the visual and thermal GO conditions were input as separate dependent variables in the analysis.

Preprocessing of imaging data. Data were preprocessed using the methods detailed in appendix A. Preparation of the data involved global artifact detection, realignment of the functional images, coregistration to the high-resolution anatomical image, normalization to the ICBM-152 atlas space, and smoothing using a Gaussian kernel of 8mm.

Functional MRI statistical analysis. A two-level mixed-effects methodology was used to analyze the functional imaging data. The first level consisted of a multiple regression analysis estimated using ordinary least squares (OLS) in SPM2 (Statistical Parametric

Mapping, www.fil.ion.ucl.ac.uk/spm/). Predictors were created using an impulse function based the stimulus onset times convolved with a canonical hemodynamic response function. Four predictors of interest were generated according to modality and task condition: thermal-GO, thermal-NOGO, visual-GO, and visual-NOGO. Only trials containing with appropriate GO and NOGO responses were be included. Incorrect trials for all conditions were modeled as a separate regressor of no interest. Other nuisance predictors were also created to account for low-frequency noise and subject head movement.

For each participant a set of four volumes was generated corresponding to the voxelwise beta estimates of each condition. These images were input into a multiple regression at the second level for final hypothesis testing. The second level was estimated using restricted maximum likelihood (ReML) to account for dependencies and unequal variance among the levels of each repeated measure. Additional details regarding statistical analysis of the fMRI data can be found in appendix A.

Contrasts of interest were generated at the second level to test a priori hypotheses. One contrast was made to test for differences between the visual GO and NOGO conditions. Another contrast was setup to examine similarities between the adults and adolescents in the visual condition. A third contrast was created to examine regions more responsive to thermal stimulation in the GO and NOGO conditions. A fourth contrast was created to examine differences between the adolescents and adults in the thermal NOGO > visual NOGO comparison.

An additional design matrix was created for each subject to test for regions whose activity is correlated with performance. These design matrices were similar to the ones described above but added an extra parametric predictor containing transformed and z-scored reaction time information. This enabled the creation of contrasts testing for performance-related activity. A contrast was created to test for differences between the thermal and visual modalities. A second contrast was created to test for differences between adults and adolescents in the thermal condition.

Region of interest analysis. Additional regions of interest were added to the whole-brain analysis based on the *a priori* hypothesis that bilateral areas of anterior insula would be involved in the thermal GO/NOGO task. These regions of left and right anterior insula were created from the significant regions of left dorsal anterior insula and right central anterior insula in the experiment three contrast of modality differences. These regions were only applied to the two performance-related contrasts and were evaluated at the reduced significance level of p = 0.05, Bonferroni-corrected to a value of $p = 0.025$.

Results

Analysis of response behavior in the GO condition. Response data for thermal and visual GO conditions is depicted by age group in Figure 25. A between-subjects multivariate analysis yielded a significant effect of age group across thermal and visual modalities ($F(2,26) = 5.09$, Wilks' Lambda = 0.719, $p = 0.014$, partial $\eta^2 = 0.281$). Follow-on univariate analyses indicated a significant effect of age group for the thermal modality ($F(1,27) = 7.82$, $p = 0.009$, partial $\eta^2 = 0.225$) and the visual modality ($F(1,27) = 6.41$, $p = 0.017$, partial $\eta^2 = 0.192$) individually.

Results from the visual GO/NOGO task. A directional *t*-contrast was used to test for regions with increased activity in the visual GO condition relative to the visual NOGO condition. The parameters for this comparison were $t(120) > 3.16$, $p < 0.001$, 8 voxel extent threshold. An array of significant clusters was found across cortical areas involved in visual processing and motor control (Table 9 and Figure 26). Significant regions included secondary somatosensory cortex (Figure 27c, d), bilateral ventral premotor cortex (Figure 27e, f), and bilateral primary visual cortex (Figure 27g). Subcortically, areas of the left striatum and left thalamus also showed increased activity in the visual GO condition. There were no regions of increased activity in the visual NOGO condition relative to the visual

GO condition.

Similarities between adults and adolescents on the visual GO/NOGO task. A conjunction analysis was preformed to determine which regions the adults and adolescents share during performance of the visual GO/NOGO task. The parameters for this comparison were $t^2(120) > 3.16$, $p < 0.001$, 8 voxel extent threshold. The results of this analysis closely mirrored the adult results (Table 10 and Figure 28). Significant regions included left primary motor cortex (Figure 29a), left supplementary motor cortex (Figure 29b), bilateral secondary somatosensory cortex (Figure 29c, d), bilateral ventral premotor cortex (Figure 29e, f), and bilateral primary visual cortex (Figure 29g). Subcortically, areas of the left striatum and left thalamus also showed increased activity in the visual GO condition.

Similarities between thermal GO and thermal NOGO relative to visual conditions. A conjunction analysis was preformed to determine if any regions had a significant response in the thermal GO relative to visual GO contrast and in the thermal NOGO relative to visual NOGO contrast. This was done to find regions responsive to thermal information integration regardless of the end behavior. The parameters for this comparison were $t^2(72) > 3.21$, $p < 0.001$, 8 voxel extent threshold. Generally, results were quite similar to those found in the contrasts described above (Table 11 and Figure 30). Bilateral areas of the mid insula (Figure 31a, b), secondary somatosensory cortex (Figure 31c, d), lateral frontal cortex (Figure 31e, f), superior parietal cortex (Figure 31g, h) and right central operculum (Figure 31i) showed greater activity to the thermal modality relative to the visual modality in both GO and NOGO conditions. Since there were no significant clusters in the visual NOGO condition relative to the thermal NOGO condition there were no significant clusters showing a superior response for the visual modality relative to the thermal modality across both GO and NOGO conditions.

Areas with activity related to response time, by modality. A directional *t*-contrast was used to test for regions that predicted reaction time preferentially for one modality relative to the other. This involved creating regressors of interest for each participant based on the response times for GO responses. The parameters for this comparison were $t(56) > 3.24$, $p < 0.001$, 8 voxel extent threshold. Areas related to thermal reaction time were found in the insula, medial prefrontal cortex, and lateral temporal cortex (Table 12 and Figure 32). Clusters observed in left lateral temporal cortex (Figure 33a), right anterior insula (Figure 33b), left caudate (Figure 33c), right inferior parietal lobule (Figure 33d), and bilateral dorsal medial prefrontal cortex (Figure 33e, f) demonstrated greater thermal predictive value. Only the a priori region of left anterior insula was found to be significant ($p = 0.011$), with the region of right anterior insula trending toward significance ($p = 0.037$). Several regions preferentially related to visual reaction time were also found. These areas were located in occipital and lateral temporal cortex (Table 12 and Figure 32). Clusters observed in bilateral medial occipital cortex (Figure 33g, h), bilateral cuneal cortex (Figure 33i), and left mid insula (Figure 33j) demonstrated greater visual predictive value.

Developmental differences in the thermal NOGO > visual NOGO contrast. A directional *t*-contrast was used to test for developmental differences in regions having a greater response to the thermal NOGO condition relative to the visual NOGO condition. This involved creating the thermal NOGO > visual NOGO contrast individually for each subject and then completing a two-sample *t*-test at the second level. The parameters for this comparison were $t(30) > 3.39$, $p < 0.001$, 8 voxel extent threshold. Adolescents were found to have greater activity in areas of lateral frontal cortex, lateral temporal cortex, medial occipital cortex, and in the brainstem (Table 13 and Figure 34). Adolescents showed greater values in left Broca's area (Figure 35a), lateral occipital cortex (Figure 35b), bilateral substantia nigra (Figure 35c, d), and posterior cingulate (Figure 35e). There were no regions with greater values in the adult group.

Developmental differences in regions correlated with thermal response time. A directional *t*-contrast was used to test for regions that predicted thermal GO reaction time preferentially for one age group relative to the other. This involved creating regressors of interest for each participant based on the response times for thermal GO responses. The parameters for this comparison were $t(56) > 3.24$, $p < 0.001$, 8 voxel extent threshold. The adult group had greater predictive activity in areas of lateral temporal cortex, medial prefrontal cortex, and lateral frontal cortex (Table 14 and Figure 36). Adults had greater predictive activity in left superior temporal gyrus (Figure 37a, b), right anterior insula (Figure 37c), right substantia nigra (Figure 37d), right caudate (Figure 37e), and right dorsal medial prefrontal cortex (Figure 37f). Other clusters were observed in left lateral frontal pole, left parahippocampal gyrus, and left lateral occipital cortex. The a priori region of left anterior insula was found to be significant ($p = 0.020$) as was the region of right anterior insula ($p = 0.024$). The adolescent group had greater predictive activity relative to adults in areas of lateral frontal and parietal cortex (Table 14 and Figure 36). The adolescent group had greater predictive activity in left central operculum (Figure 37g) and parietal operculum (Figure 37h). Other regions included lateral frontal pole and left medial occipital cortex.

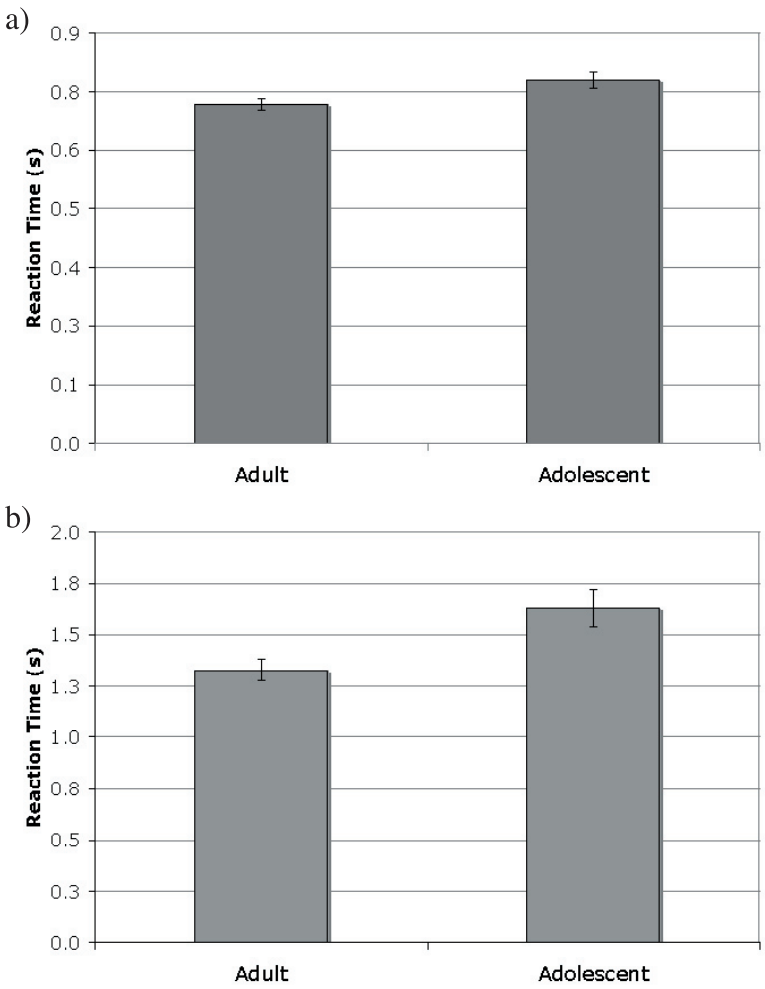

Figure 25. Plots of behavioral performance during GO responses. a) Adult and adolescent responses within the visual condition. The groups were significantly different (p = 0.017), with the adolescents taking longer to respond compared to the adults. b) Adult and adolescent responses within the thermal condition. The groups were significantly different (p = 0.009), with the adolescents taking longer to respond compared to the adults.

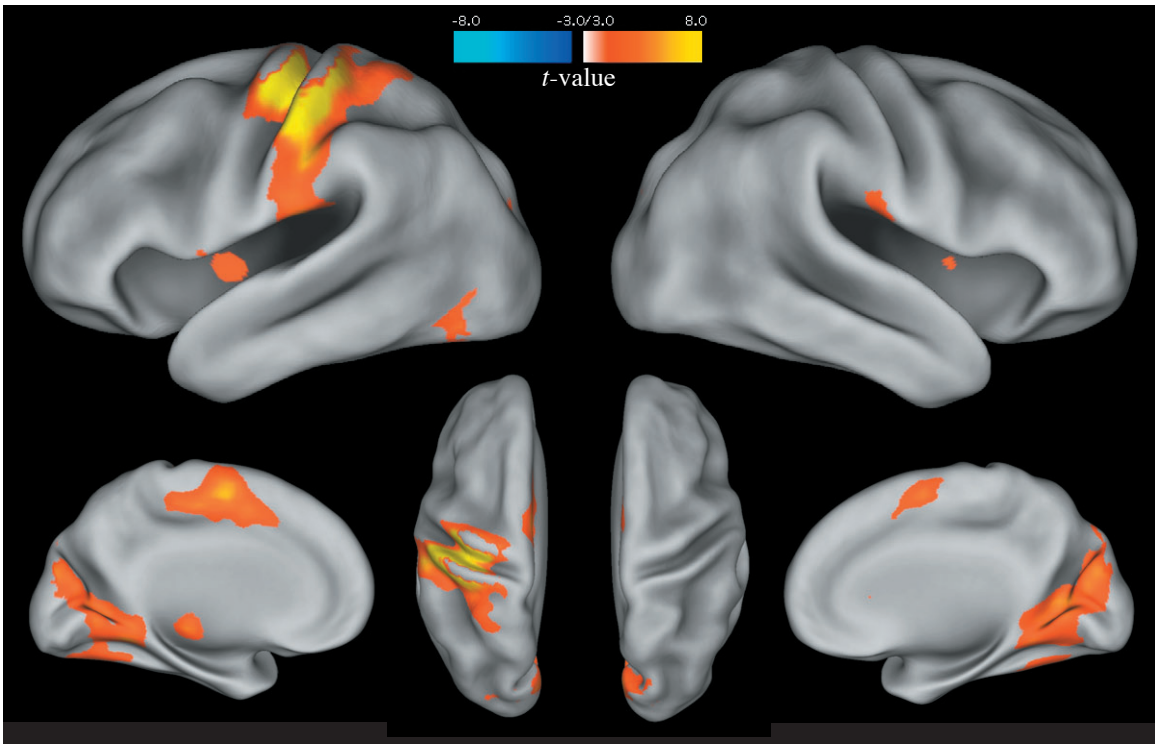

Figure 26. Areas of increased activity in the visual GO condition relative to the visual NOGO condition. The parameters for this comparison were $t(120) > 3.16$, $p < 0.001$, 8 voxel extent threshold. An array of significant clusters was found across cortical areas involved in visual processing and motor control.

Table 9
Regions showing increased activity in the visual GO > visual NOGO contrast

Region Name	HEM	BA	Area Notes	MNI Coordinates x	y	z	*z*-value	*p*(uncorr)	*p*(FDR)
Frontal									
Postcentral Gyrus	L	4a	Primary Motor	-39	-27	60	8.04	< 0.001	< 0.001
Medial Frontal Gyrus	Bilat	6	Supplementary Motor	0	0	54	5.08	< 0.001	< 0.001
Temporal									
Insula	L	13	Mid Insula	-36	-6	3	3.39	< 0.001	0.007
Parietal									
Central Operculum	L	13		-45	0	9	3.62	< 0.001	0.004
Central Operculum	R	13		48	3	9	3.42	< 0.001	0.007
Parietal Operculum	L	OP1	Secondary Somatosensory	-54	-24	18	4.31	< 0.001	0.001
Parietal Operculum	R	OP1	Secondary Somatosensory	63	-12	18	3.60	< 0.001	0.004
Occipital									
Fusiform Gyrus	L	19		-39	-72	-12	4.23	< 0.001	0.001
Intracalcarine Cortex	L	17	Primary Visual / V1	-15	-69	6	4.24	< 0.001	0.001
Intracalcarine Cortex	R	17	Primary Visual / V1	18	-60	9	4.71	< 0.001	< 0.001
Cuneus	R	18	Visual Cortex / V2	3	-81	24	4.50	< 0.001	< 0.001
Subcortical									
Thalamus	L			-12	-21	0	4.40	< 0.001	< 0.001
Cerebellum									
Posterior Lobe	R			6	-69	-39	3.52	< 0.001	0.005
Anterior Lobe	R			12	-51	-15	5.85	< 0.001	< 0.001
Anterior Lobe	L			-18	-48	-9	4.62	< 0.001	< 0.001

Table lists significant areas of activation ($p < 0.001$, extent threshold 6 voxels).
HEM = hemisphere in which cluster was located; BA = approximate Brodmann area of cluster;
p(uncorr) = uncorrected cluster probability; *p*(FDR) = cluster probability under false discovery rate

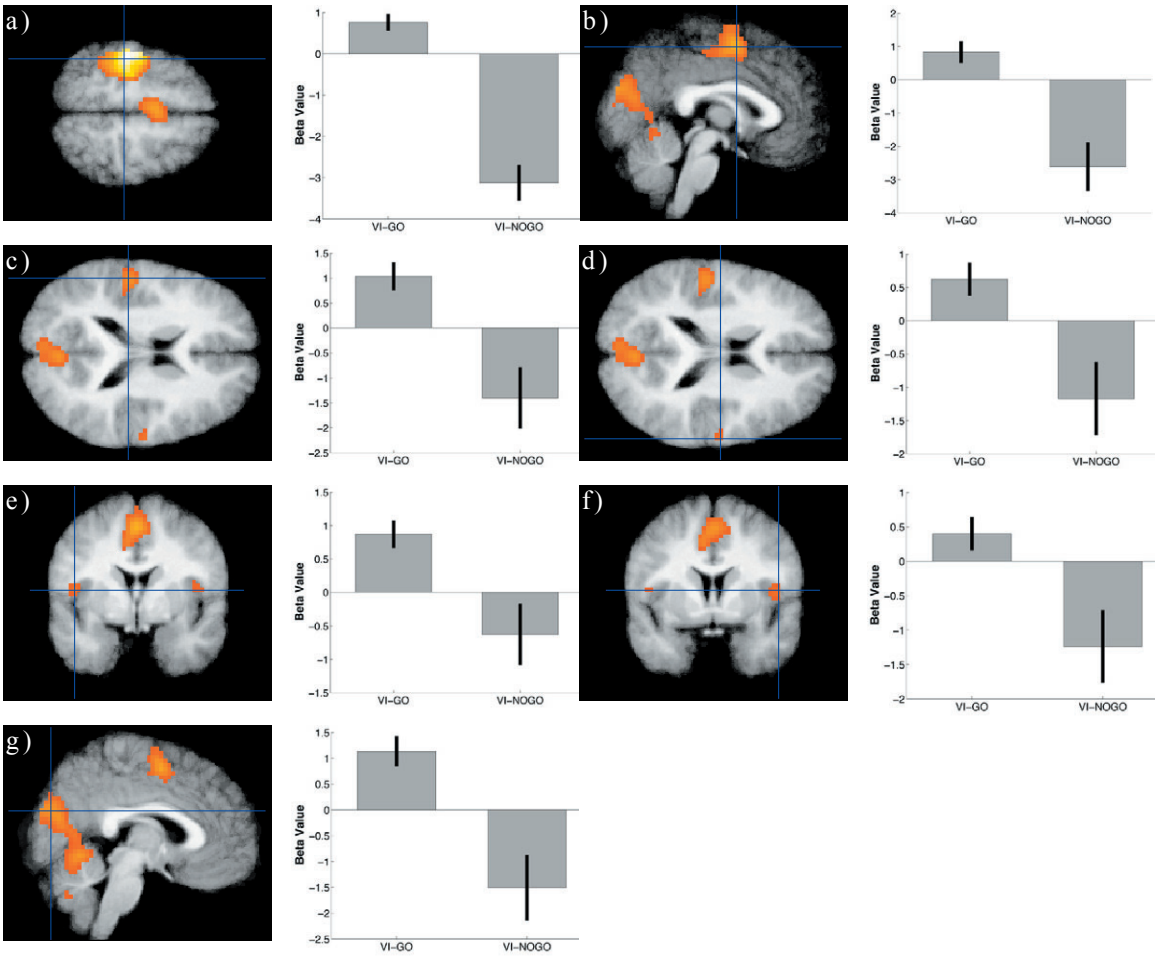

Figure 27. Parameter graphs of the visual GO > visual NOGO contrast. From left to right bars represent activity in the visual GO and visual NOGO conditions. Significant regions included left primary motor cortex (a), left supplementary motor cortex (b), bilateral secondary somatosensory cortex (c,d), bilateral ventral premotor cortex (e,f), and bilateral primary visual cortex (g).

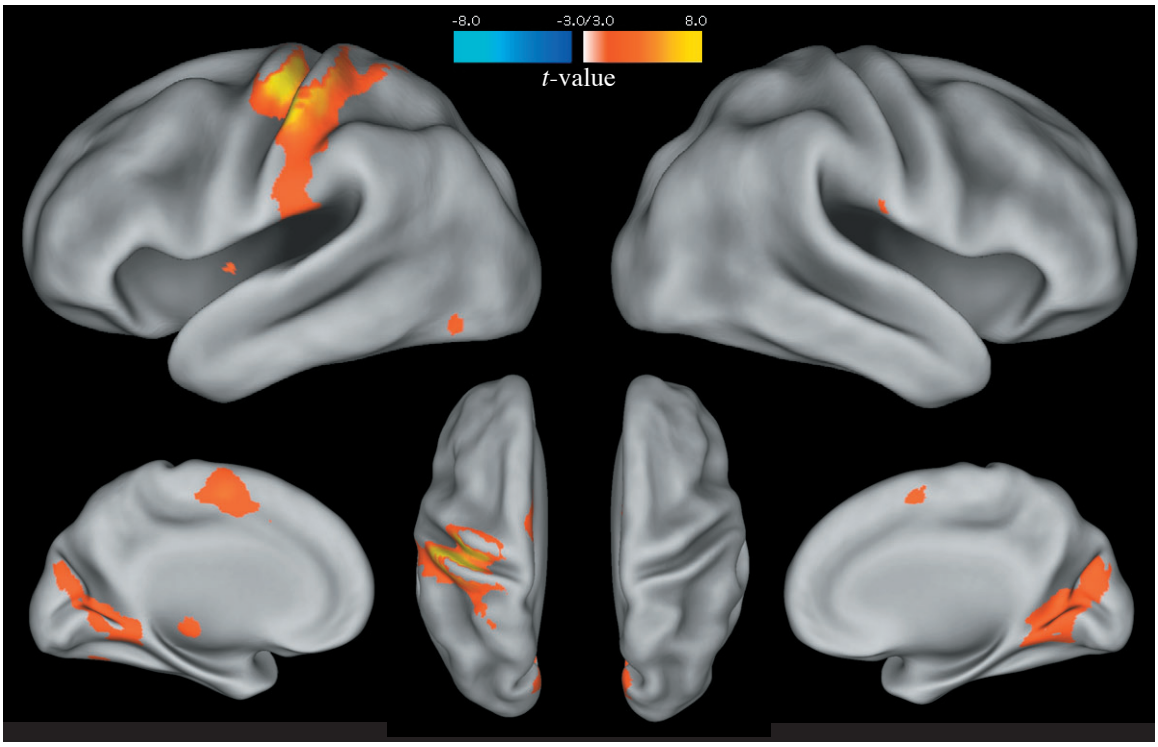

Figure 28. Areas showing a similar response in visual conditions between adolescents and adults. This figure represents a conjunction analysis between visual GO > visual NOGO for the adolescent and adult groups. The parameters for this comparison were $t^2(120) > 3.16, p < 0.001$, 8 voxel extent threshold. The results of this analysis closely mirrored the adult results.

Table 12

Regions showing increased activity in the visual GO > visual NOGO contrast for the adolescent and adult group.

Region Name	HEM	BA	Area Notes	MNI Coordinates x	y	z	*z*-value	*p*(uncorr)	*p*(FDR)
Frontal									
Postcentral Gyrus	L	4a	Primary Motor	-39	-24	60	8.04	< 0.001	< 0.001
Medial Frontal Gyrus	Bilat	6	Supplementary Motor	0	0	54	5.08	< 0.001	< 0.001
Temporal									
Insula	L	13	Mid Insula	-36	-6	3	3.39	< 0.001	0.008
Parietal									
Central Operculum	L	13		-45	0	9	3.62	< 0.001	0.004
Central Operculum	R	13		42	3	6	3.19	0.001	0.013
Parietal Operculum	L	OP1	Secondary Somatosensory	-54	-24	18	4.31	< 0.001	0.001
Parietal Operculum	R	OP1	Secondary Somatosensory	63	-12	21	3.58	< 0.001	0.005
Occipital									
Fusiform Gyrus	L	19		-39	-72	-12	4.23	< 0.001	0.001
Intracalcarine Cortex	L	17	Primary Visual / V1	-21	-60	3	4.28	< 0.001	0.001
Intracalcarine Cortex	R	17	Primary Visual / V1	18	-60	9	4.71	< 0.001	< 0.001
Cuneus	R	18	Visual Cortex / V2	3	-81	24	4.49	< 0.001	< 0.001
Subcortical									
Thalamus	L			-12	-21	0	4.44	< 0.001	< 0.001
Cerebellum									
Posterior Lobe	R			6	-69	-39	3.52	< 0.001	0.006
Anterior Lobe	R			12	-51	-15	5.85	< 0.001	< 0.001
Anterior Lobe	L			-30	-63	-18	3.61	< 0.001	0.005

Table lists significant areas of activation ($p < 0.001$, extent threshold 6 voxels).
HEM = hemisphere in which cluster was located; BA = approximate Brodmann area of cluster;
p(uncorr) = uncorrected cluster probability; *p*(FDR) = cluster probability under false discovery rate

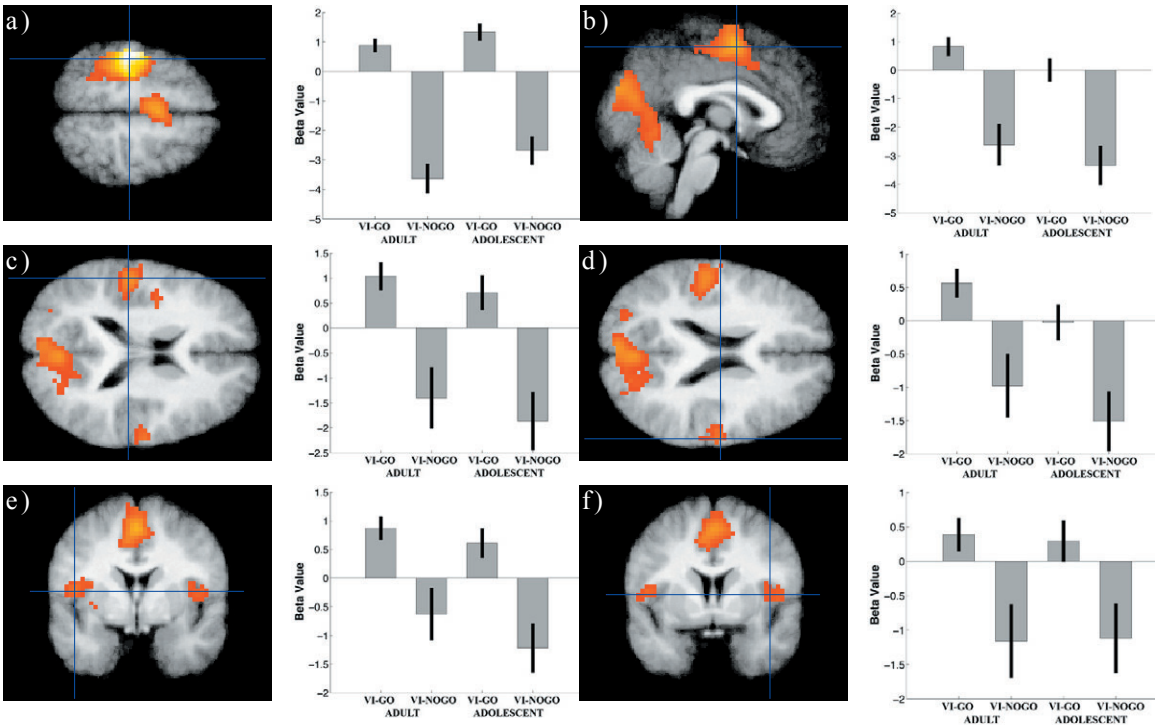

Figure 29. Parameter graphs of the visual GO > visual NOGO conjunction for adults and adolescents. From left to right bars represent adult visual GO and visual NOGO conditions and adolescent visual GO and visual NOGO conditions. Significant regions included left primary motor cortex (a), left supplementary motor cortex (b), bilateral secondary somatosensory cortex (c,d), bilateral ventral premotor cortex (e,f), and bilateral primary visual cortex (g).

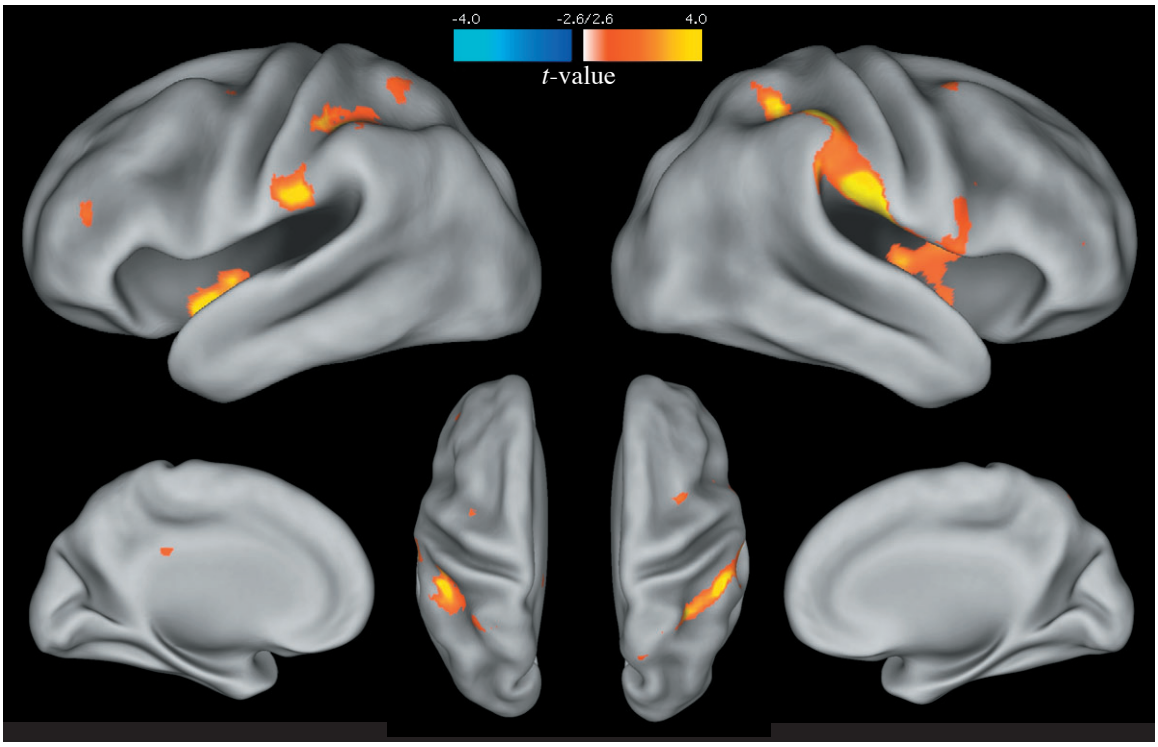

Figure 30. Regions with a preferential response to thermal conditions. This contrast is a conjunction analysis of the thermal GO > visual GO contrast and the thermal NOGO > visual NOGO contrast. The parameters for this comparison were $t^2(72) > 3.21$, $p < 0.001$, 8 voxel extent threshold. Bilateral areas of the mid insula, secondary somatosensory cortex, and right central operculum showed superior activity to the thermal modality relative to the visual modality in both GO and NOGO conditions.

Table 10
Regions showing increased activity in the thermal > visual GO contrast and thermal > visual NOGO contrasts

Region Name	HEM	BA	Area Notes	MNI Coordinates x	y	z	*z*-value	*p*(uncorr)	*p*(FDR)
Frontal									
Inferior Frontal Gyrus	R	10	Frontal Pole	39	36	9	3.13	0.001	0.068
Middle Frontal Gyrus	L	10	Frontal Pole	-42	39	15	3.51	< 0.001	0.039
Inferior Frontal Gyrus	R	44	Broca's Area	60	12	21	3.32	< 0.001	0.050
Middle Frontal Gyrus	R	6		36	3	57	3.34	< 0.001	0.050
Temporal									
Insula	L	13	Ventral Mid Insula	-39	3	-9	4.31	< 0.001	0.009
Insula	R	13	Ventral Mid Insula	39	0	-12	3.35	< 0.001	0.050
Insula	R	13	Mid Insula	42	-9	6	3.93	< 0.001	0.021
Insula	R	13	Dorsal Mid Insula	51	-12	12	3.29	0.001	0.053
Parietal									
Postcentral Gyrus	L	OP4	Secondary Somatosensory	-63	-21	27	4.71	< 0.001	0.006
Postcentral Gyrus	R	OP4	Secondary Somatosensory	63	-18	24	4.89	< 0.001	0.006
Intraparietal Sulcus	L	hIP2		-42	-48	54	4.33	< 0.001	0.009
Intraparietal Sulcus	R	hIP2		42	-48	54	3.79	< 0.001	0.027
Cerebellum									
Superior Cerebellum	L			-21	-63	-27	3.04	0.001	0.078

Table lists significant areas of activation ($p < 0.001$, extent threshold 6 voxels).
HEM = hemisphere in which cluster was located; BA = approximate Brodmann area of cluster;
p(uncorr) = uncorrected cluster probability; *p*(FDR) = cluster probability under false discovery rate

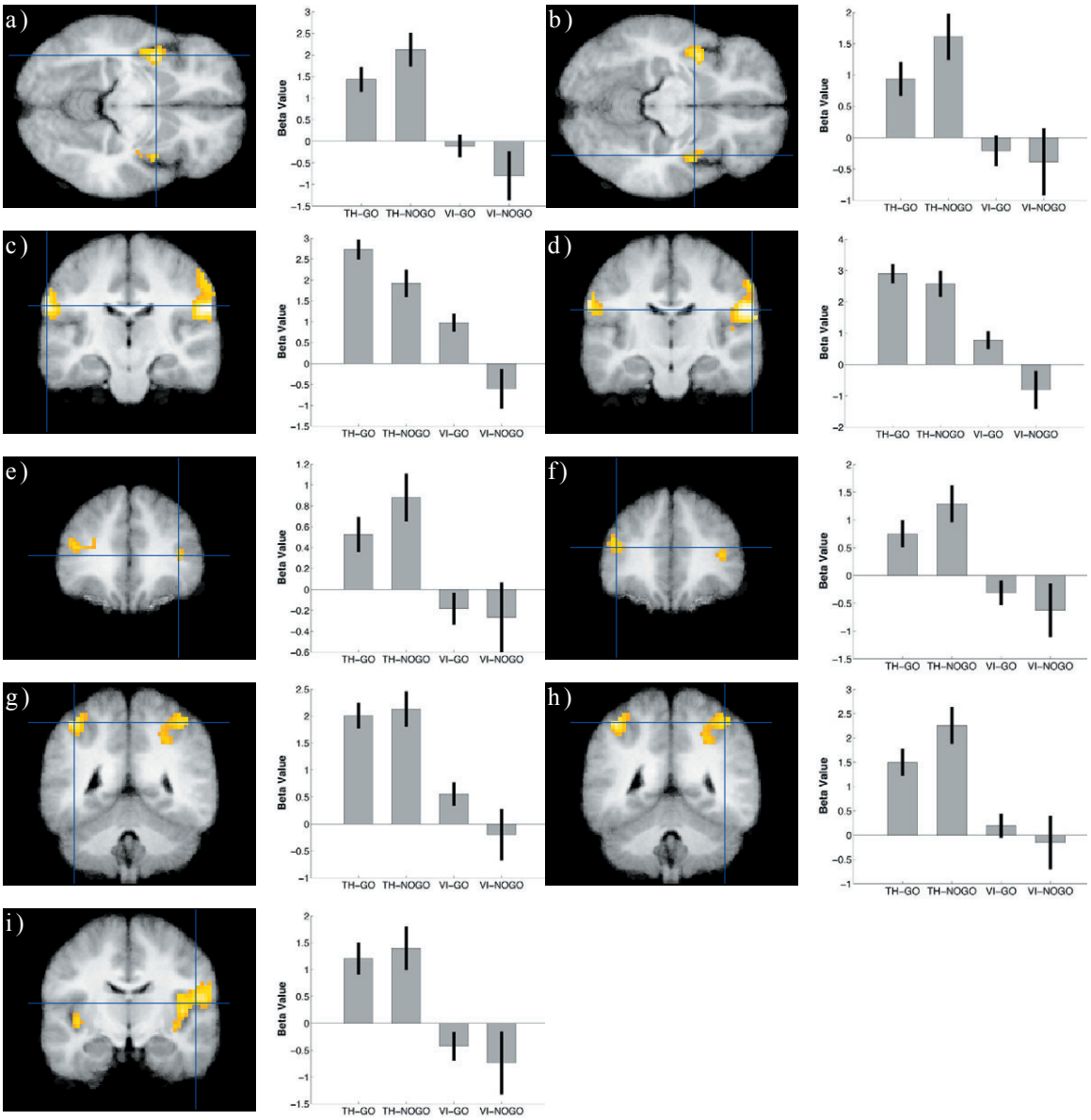

Figure 31. Parameter graphs showing regions with a significant thermal response. From left to right bars represent thermal-GO, thermal-NOGO, visual-GO, and visual-NOGO conditions. Bilateral areas of the mid insula (a,b), secondary somatosensory cortex (c,d), lateral frontal cortex (e,f), superior parietal cortex (g,h) and right central operculum (i) showed greater activity to the thermal modality relative to the visual modality in both GO and NOGO conditions.

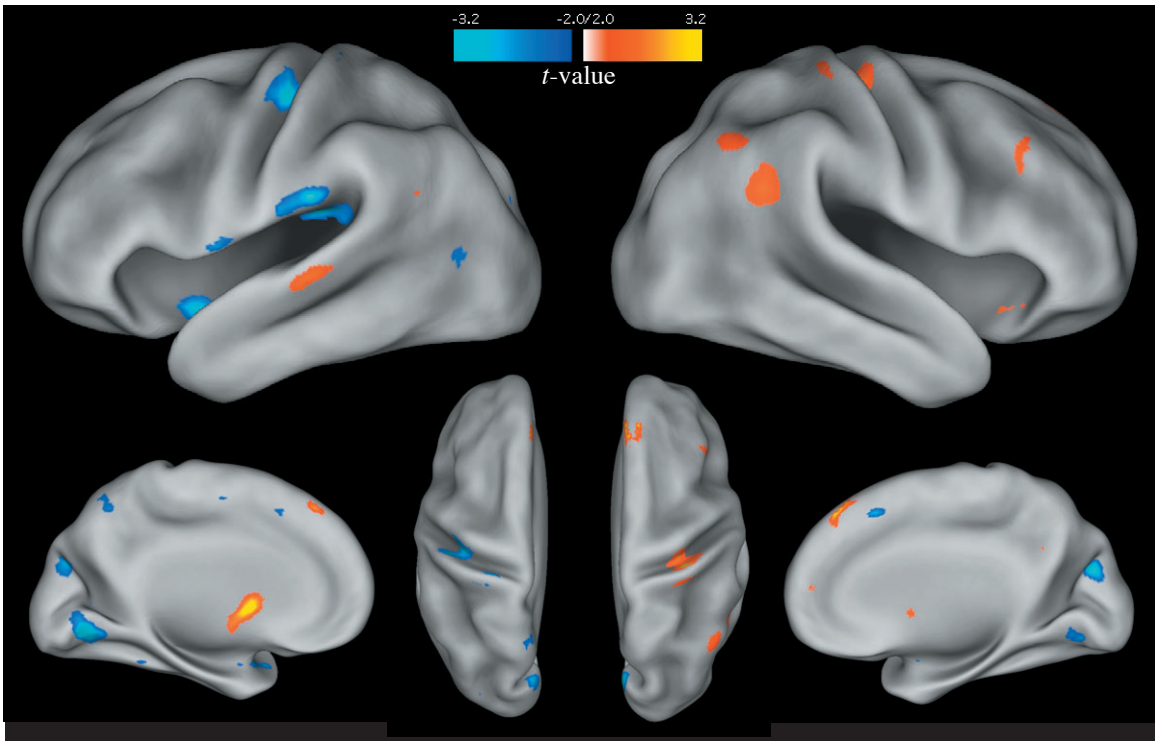

Figure 32. Areas predicting reaction time. Areas in red are regions that show predictive activity to thermal relative to visual GO and areas in blue are regions that show predictive activity to visual relative to thermal GO. The parameters for this comparison were $t(56) > 3.24, p < 0.001$, 8 voxel extent threshold. Areas related to thermal reaction time were found in the insula, medial prefrontal cortex, and lateral temporal cortex. Regions preferentially related to visual reaction time were found in occipital and lateral temporal cortex.

Table 11
Regions with activity predicting reaction time by modality.

Region Name	HEM	BA	Area Notes	MNI Coordinates x	y	z	*z*-value	*p*(uncorr)	*p*(FDR)
Thermal RT > Visual RT									
Frontal									
Superior Forntal Gyrus	L	8	Medial Prefrontal	-6	39	48	2.92	0.002	0.934
Superior Forntal Gyrus	R	8	Medial Prefrontal	9	45	48	3.64	< 0.001	0.934
Precentral Gyrus	R	6	Premotor	36	-24	60	2.84	0.002	0.934
Temporal									
Superior Temporal Gyrus	L	42		-60	-30	0	2.63	0.004	0.934
Insula	R	13	Anterior Insula	39	30	0	2.81	0.002	0.934
Parietal									
Inferior Parietal Lobule	R	40		51	-60	45	3.13	0.001	0.934
Subcortical									
Caudate	L			-6	6	3	3.37	< 0.001	0.934
Cerebellum									
Anterior Lobe	L			-18	-33	-27	2.82	0.002	0.934
Anterior Lobe	L			-15	-51	-24	2.79	0.003	0.934
Anterior Lobe	L			-6	-45	-18	2.73	0.003	0.934
Visual RT > Thermal RT									
Frontal									
Precentral Gyrus	L	4p	Primary Motor	-36	-21	51	3.04	0.001	0.983
Temporal									
Insula	L	13	Mid Insula	-42	6	-9	3.66	< 0.001	0.983
Parietal									
Supramarginal Gyrus	L	40		-63	-27	21	3.53	< 0.001	0.983
Parietal Operculum	L	OP1		-39	-30	21	2.85	0.002	0.983
Occipital									
Lingual Gyrus	L	18		-18	-66	-6	3.27	0.001	0.983
Lingual Gyrus	R	18		9	-66	-6	3.17	0.001	0.983
Cuneus	R	18		6	-75	27	3.26	0.001	0.983

Table lists significant areas of activation ($p < 0.005$, extent threshold 6 voxels).
HEM = hemisphere in which cluster was located; BA = approximate Brodmann area of cluster; *p*(uncorr) = uncorrected cluster probability; *p*(FDR) = cluster probability under false discovery rate

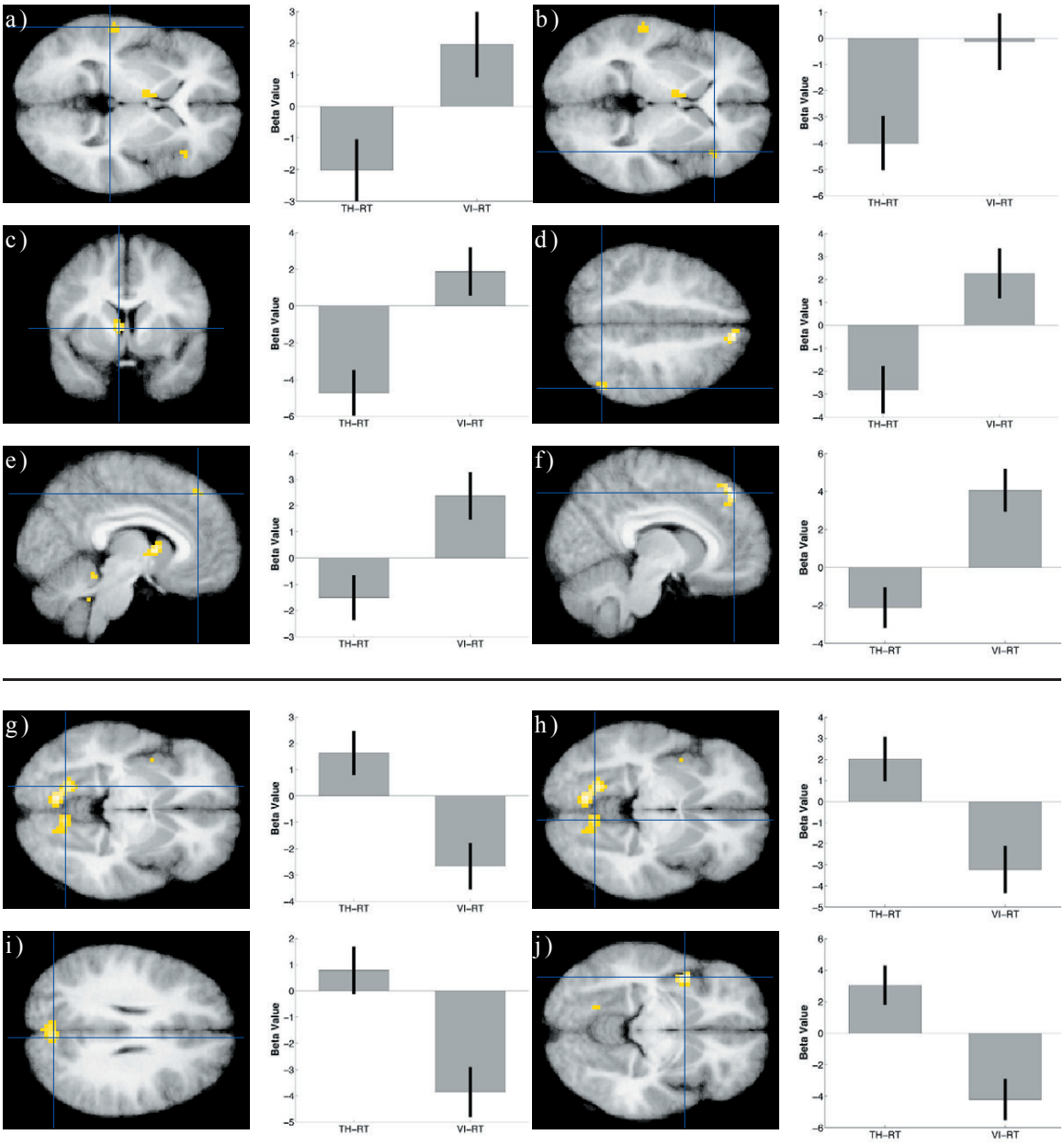

Figure 33. Parameter graphs of reaction time prediction by condition. Left bars represent predictive values for the thermal-GO condition and right bars represent predictive values for the visual-GO condition. Negative values indicate grater predictive value due to the reciprocal transform performed on the data. In the thermal condition left lateral temporal cortex (a), right anterior insula (b), left caudate (c), right inferior parietal lobule (d), and bilateral dorsal medial prefrontal cortex (e,f) demonstrated greater predictive value. In the visual condition bilateral medial occipital cortex (g,h), bilateral cuneal cortex (i), and left mid insula (j) demonstrated greater predictive value.

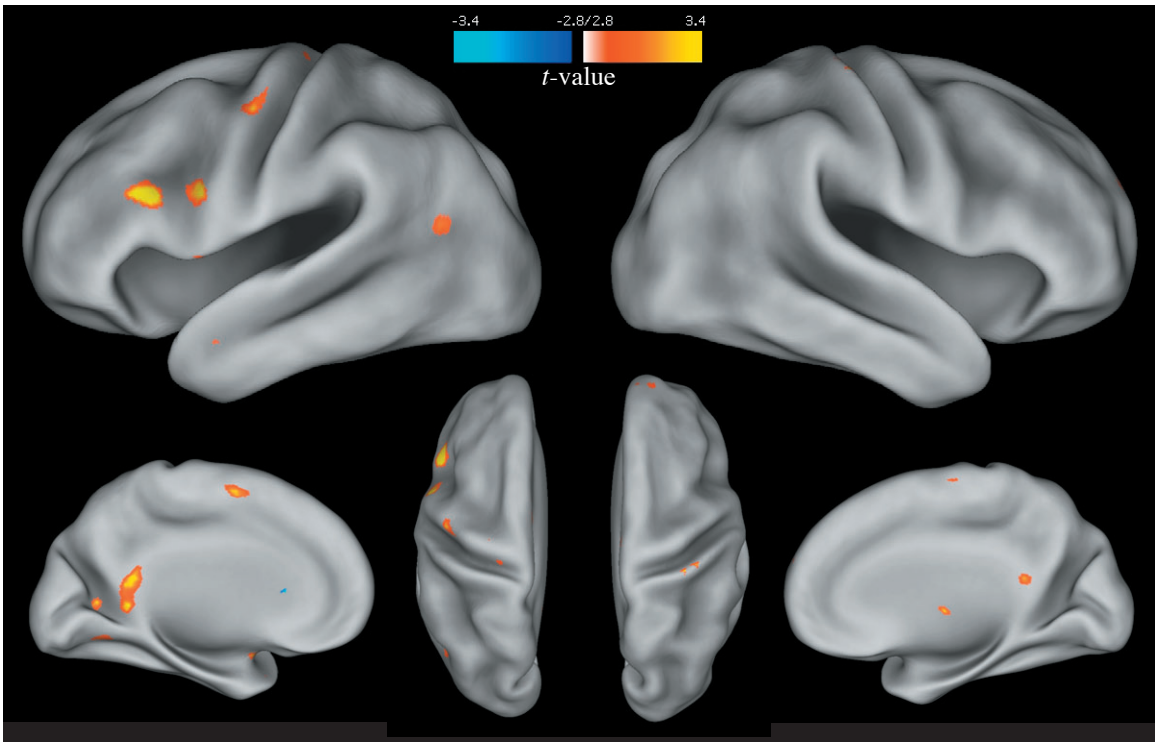

Figure 34. Areas showing a developmental change in the thermal NOGO condition relative to the visual NOGO condition. Areas in red are regions of increased adolescent activity. There were no areas of increased adult activity. The parameters for this comparison were $t(30) > 3.39$, $p < 0.001$, 8 voxel extent threshold. Adolescents were found to have greater activity in areas of lateral frontal cortex, lateral temporal cortex, medial occipital cortex, and in the brainstem.

Table 13
Regions showing developmental changes in the Thermal NOGO > Visual NOGO contrast

Region Name	HEM	BA	Area Notes	MNI Coordinates x	y	z	*z*-value	*p*(uncorr)	*p*(FDR)
Adolescents > Adults									
Frontal									
Inferior Frontal Gyrus	L	44	Broca's Area	-42	21	21	3.62	< 0.001	0.360
Inferior Frontal Gyrus	L	44	Broca's Area	-54	9	24	3.71	< 0.001	0.360
Occipital									
Lateral Occipital Cortex	L	21		-39	-57	12	3.63	< 0.001	0.360
Cingulate Gyrus	Bilat	30	Posterior Cingulate	0	-48	18	3.39	< 0.001	0.360
Subcortical									
Brainstem	L		Substantia Nigra	-6	-21	-18	4.20	< 0.001	0.360
Brainstem	R		Substantia Nigra	9	-21	-21	3.89	< 0.001	0.360

Table lists significant areas of activation ($p < 0.001$, extent threshold 6 voxels).
HEM = hemisphere in which cluster was located; BA = approximate Brodmann area of cluster;
p(uncorr) = uncorrected cluster probability; *p*(FDR) = cluster probability under false discovery rate

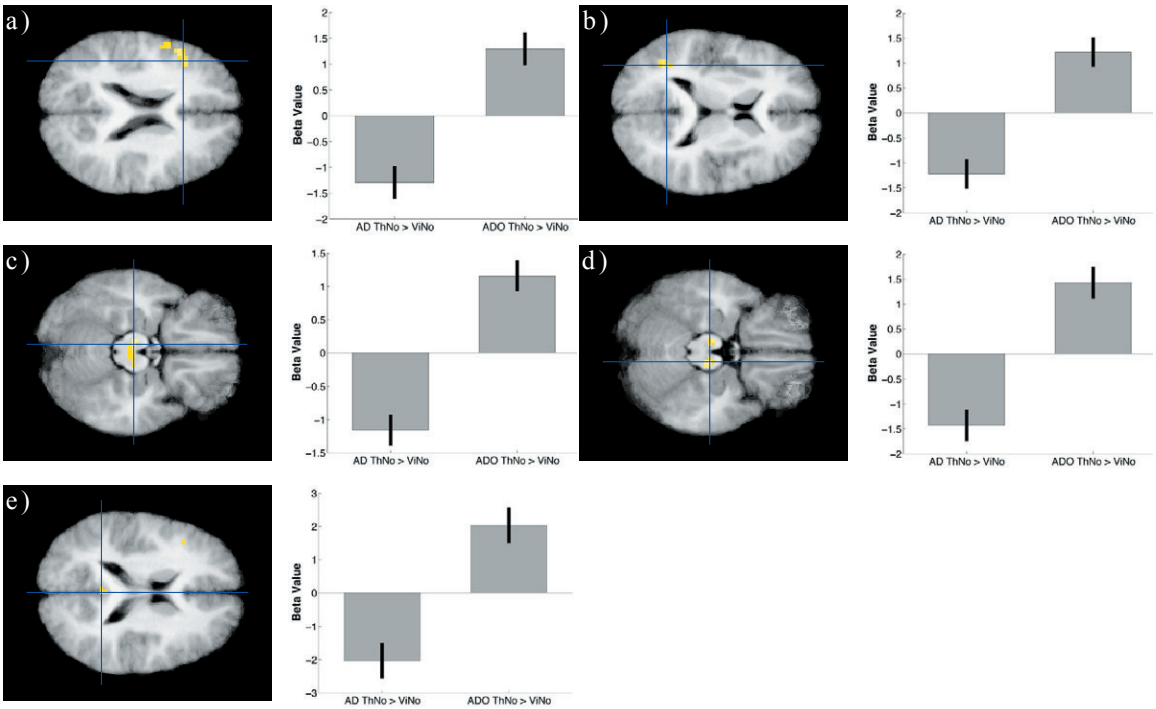

Figure 35. Parameter graphs of developmental differences in the Thermal NOGO > Visual NOGO contrast. Left bars represent adult contrast values and right bars represent adolescent contrast values. Negative values indicate grater predictive value due to the reciprocal transform performed on the data. Adolescents showed greater values in left Broca's area (a), lateral occipital cortex (b), bilateral substantia nigra (c,d), and posterior cingulate (e). There were no regions with greater values in the adult group.

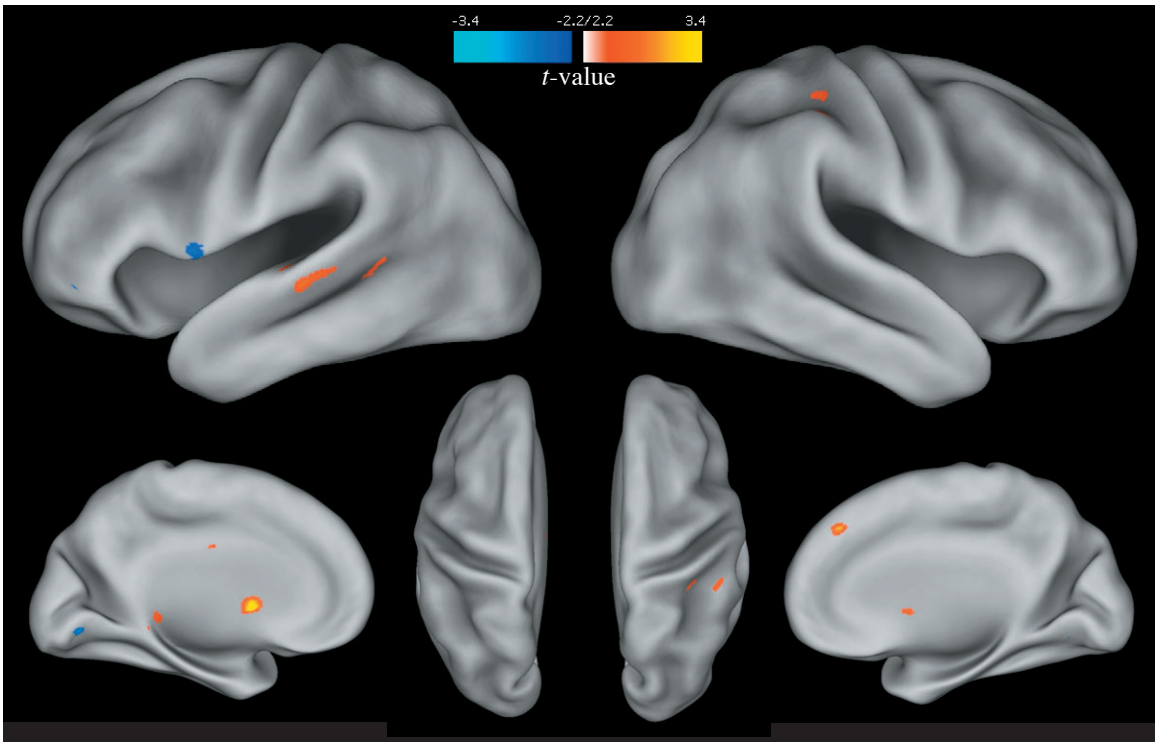

Figure 36. Areas showing a developmental change in thermal reaction time prediction. Areas in red are more predictive for adults and areas in blue are more predictive for adolescents. The parameters for this comparison were $t(56) > 3.24$, $p < 0.001$, 8 voxel extent threshold. The adult group had greater predictive activity in areas of lateral temporal cortex, medial prefrontal cortex, and lateral frontal cortex. The adolescent group had greater predictive activity in areas of lateral frontal and parietal cortex.

Table 14
Regions showing a developmental change in relation to reaction time

Region Name	HEM	BA	Area Notes	MNI Coordinates x	y	z	*z*-value	*p*(uncorr)	*p*(FDR)
Adults > Adolescents									
Frontal									
Frontal Operculum	R	13	Anterior Insula / Operculum	39	27	3	2.76	0.003	0.736
Inferior Frontal Gyrus	L	10	Frontal Pole	-30	36	6	2.66	0.004	0.736
Medial Frontal Gyrus	R	8	Medial Prefrontal	9	42	39	3.07	0.001	0.736
Paracingulate Gyrus	R	6	Premotor	3	21	45	2.81	0.002	0.736
Temporal									
Parahippocampal Gyrus	L			-9	-36	0	3	0.001	0.736
Superior Temporal Gyrus	L	22		-57	-21	0	3.16	0.001	0.736
Superior Temporal Gyrus	L	22		-42	-33	0	4.01	< 0.001	0.736
Middle Temporal Gyrus	L	21		-51	-48	-3	3.16	0.001	0.736
Occipital									
Lateral Occipital Cortex	L	37		-39	-63	0	2.82	0.002	0.736
				-24	-72	9	2.84	0.002	0.736
Subcortical									
Brainstem	R		Substantia Nigra	12	-24	-18	2.89	0.002	0.736
Caudate	L			-6	6	3	3.58	< 0.001	0.713
Cerebellum									
Anterior Lobe				-30	-57	-27	3.16	0.001	0.736
Anterior Lobe				-6	-45	-12	3.17	0.001	0.736
Adolescents > Adults									
Frontal									
Inferior Forntal Gyrus	R	10	Frontal Pole	33	45	-3	2.58	0.005	0.999
Central Operculum	L	13		-51	6	3	2.59	0.005	0.999
Parietal									
Parietal Operculum	L	13	Posterior Insula	-33	-42	21	3.31	< 0.001	0.999
Occipital									
Lingual Gyrus	L	17	Primary Visual / V1	-6	-75	-6	2.69	0.003	0.999

Table lists significant areas of activation ($p < 0.005$, extent threshold 6 voxels).
HEM = hemisphere in which cluster was located; BA = approximate Brodmann area of cluster;
p(uncorr) = uncorrected cluster probability; *p*(FDR) = cluster probability under false discovery rate

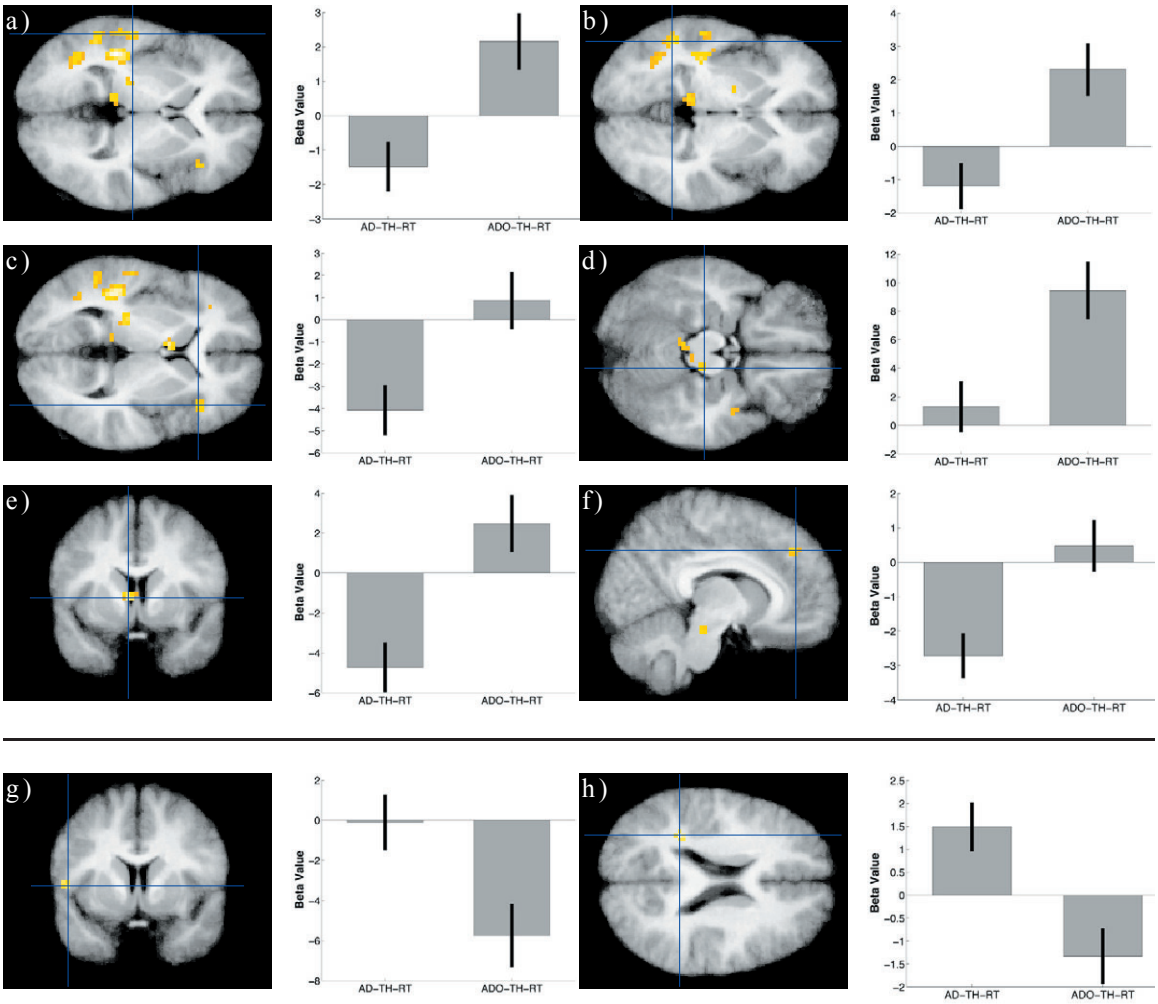

Figure 37. Parameter graphs of developmental differences in thermal reaction time prediction. Left bars represent predictive values for the adult group and right bars represent predictive values for the adolescent group. Negative values indicate grater predictive value due to the reciprocal transform performed on the data. Adults had greater predictive activity in left superior temporal gyrus (a,b), right anterior insula (c), right substantia nigra (d), right caudate (e), and right dorsal medial prefrontal cortex (f). The adolescent group had greater predictive activity in left central operculum (g) and parietal operculum (h).

Discussion

An important distinction in this experiment is the difference between regions that show task-related activity and regions that show performance-related activity. When comparing thermal GO/NOGO conditions to visual GO/NOGO conditions the observed pattern of activity is quite similar to the results of experiment two, the passive experience task. Areas of posterior and mid insula were observed, as were areas of primary and secondary somatosensory cortex. This is taken to be task-related activity that occurs with each thermal GO or NOGO response and likely reflects sensory activation necessary for thermal stimulus processing. However, these regions had no relation to observed variability in reaction time. Instead, hypothesized areas of bilateral anterior insula and dorsal medial prefrontal cortex were found to be performance-related in the thermal condition relative to the visual condition. This result builds on the findings of experiment three to further suggest that the anterior insula plays a critical role in integrating thermal information and making it available for higher-order decision making and executive control.

The developmental results also dissociate between maturation in task-related regions and maturation in performance-related regions. Changes in task-related activity were found to consist of increased regional efficiency over time. This was observed in the current experiment as fewer active regions in the adult group during the thermal NOGO condition. This finding is generally similar to that of Tamm, Menon, and Reiss (2002) and supports the idea of more focal, reduced activity in adults (Durston et al., 2006). A separate set of developmental differences was observed in terms of performance-related activity. In this case it seems that the adults were better able to modulate task-relevant areas by difficulty of the decision. During thermal GO trials adults had more predictive activity in areas of right anterior insula/operculum and dorsal medial prefrontal cortex relative to the adolescents. These were the same areas found to preferentially track thermal response time relative to visual response time in the adult group. Activity in these regions may help account for the observed developmental difference in response time, as the adolescents took, on average,

300ms longer to respond.

In the developmental literature one hypothesized effect of maturation is task-related regions changing their response profile to become more performance-related in adulthood (Luna & Sweeney, 2004; Luna et al., 2001). An example of this effect in the current data is the activity of the substantia nigra. In the adolescent group the substantia nigra showed bilateral task-related activity relative to the adults. However, in the adult group this region was lateralized to the right hemisphere and more active during trials with faster reaction time. While this difference is intriguing, it is uncertain what function the substantia nigra is contributing to information processing in the current task. It is known to have a role in both novelty processing (Bunzeck & Duzel, 2006) and the initiation of motor responses (Boecker, Jankowski, Ditter, & Scheef, 2008). Still, the identification of a developmental difference in a major dopaminergic center is consistent with current theories regarding the development of the novelty/reward system. Galvan et al. (2006) showed that activity in the nucleus accumbens was higher in adolescents relative to children and adult when performing a reward-learning task. A similar pattern of exaggerated accumbens response has been shown by Ernst et al. (2005) and May et al. (2004). While the current study did not shown accumbens activity, it does add evidence to the case for developmental differences in the dopaminergic system.

It is important to note that the findings from the visual GO/NOGO task do not completely mirror those from previous studies. While the GO > NOGO contrast was very similar to previous tasks, the null results of the NOGO > GO condition are aberrant. This is especially odd given that the experimental deign for this task was based closely on the parameters detailed in Durston et al. (2003), who found that several frontal and subcortical regions that were more active in the NOGO condition. There were also far fewer errors made by participants in the current study, eliminating the possibility of investigating error trials set apart from general NOGO trials. This brings up the question of why the current results are different from those of Durston et al., even though the experimental designs are

so similar. Two likely candidates are the difficulty of the task and habituation to stimuli.

While Durston et al. used complex visual characters from the cartoon series Pokémon, our experiment used large squares of red or green color as stimuli. Given the less complex nature of the stimulus and the strong association between color and action (green = go, red = stop) it may be that little additional response inhibition was necessary to complete this task. Another difference found in our study is the overall experiment length. While Durston et al. used several runs lasting 4 minutes, the current experiment used a single long run of 8 minutes. Some participants reported being somewhat bored when finished with the visual GO/NOGO task. Because the task was so easy and the run length was extended it may be that subtler effects were diminished in the data. However, these effects were not recovered when analyzing only the first half of the functional run. Finally, the aberration is not thought to be caused by group effects, as the adolescent results were shown to be virtually identical to the pattern of activity seen in the adults. This was shown by the conjunction analysis combining data from the two groups. In the end it is uncertain why the results of the visual GO/NOGO experiment are aberrant from previous results.

Experiment Five

Rationale and hypothesis

A peculiar aspect of human cognition is the capacity to engage in stimulus-independent thought. This ability enables the individual to consider information outside the spatial and temporal scope of the current environment and is a key part of many advanced cognitive functions (Buckner & Carroll, 2007). It is the state of stimulus-independent thought that gives rise to mental imagery, which is the ability to vividly experience a stimulus that isn't within the current context (Kosslyn, Ganis, & Thompson, 2001). Even while undergoing functional neuroimaging, assailed by loud noise and claustrophobic conditions, individuals are able to use their minds eye to imagine what a trumpet sounds like, or what jumbo jet looks like. The same is true of internal state sensations. If you are cued by the word 'freezing' you are undoubtedly able to conjure the feeling of being cold from past experiences. How is this past recollection and subsequent interoceptive feeling accomplished within the brain?

The previous experiments of this thesis have investigated interoception using a bottom-up, stimulus driven model. By creating thermal changes in the hand of a participant or directing them to attend to cardiovascular internal sensations it was hypothesized that changes in the activity of interoceptive cortex would occur. However, none of these experiments have investigated interoception from a purely top-down, stimulus-independent perspective. Previous work has highlighted the role of early cortical areas in the top-down imagery of visual scenes (Kosslyn et al., 2001; Kosslyn, Thompson, Kim, & Alpert, 1995), music (Kleber, Birbaumer, Veit, Trevorrow, & Lotze, 2007; Kraemer, Macrae, Green, & Kelley, 2005), action (Decety & Grezes, 2006; Jeannerod & Decety, 1995), and touch (Yoo, Freeman, McCarthy, & Jolesz, 2003). Could these findings hold true for internal state sensations as well? If so, what regions act as the bridge between sensory and association areas of cortex?

Experiment five uses an interoceptive imagery task to investigate whether bringing sensations of internal state to mind require the use of interoceptive cortex. A similar task

involving imagery of everyday actions was used as a control. The hypothesis for this experiment is that interoceptive imagery will require the use of the right anterior insula and bilateral mid insula, but not areas of posterior insula. It is thought that the areas of mid insula will be critical for the representation of internal state sensations while the right anterior insula will be critical for the top-down drive of the interoceptive system.

Methods

Participants. Nineteen healthy right-handed adults (13 female, 6 male, mean age = 28.1, age range = 22.3 to 39.3 years) recruited from the local community and fifteen healthy right-handed adolescents (10 female, 5 male, mean age = 11.9 years, age range = 9.4 to 13.8 years) recruited from local schools participated in experiment five. One male adolescent subject was excluded from further analysis due to excessive head movement (1mm/TR) in their fMRI data. All subjects completed an informed consent procedure approved by the Committee for the Protection of Human Subjects at Dartmouth College and were compensated for their time.

Experimental design**.** The experiment was set up as a 2x2 factorial design with principal factors of visualization modality [internal state imagery and imagery of everyday actions] and age [adolescent and adult]. Each subject completed two fMRI runs consisting of six blocks of each condition. Blocks were counterbalanced across the run to avoid order effects. Each block lasted 15 seconds with 12.5 seconds of rest following each block. Within each block the subject was presented with a cue to alert them to the visualization condition and then three words from either the internal or action visualization condition were displayed. Total scan time for this task was 7 minutes.

Experimental procedure and task detail. Each participant was instructed to visualize, as clearly as possible, either the everyday action or internal state event described by the text

on the screen. Before scanning commenced the participant was walked through a series of practice phrases to ensure that they clearly understood what to do in both the internal state imagery condition and the action imagery condition. For each phrase that was presented they were encouraged to make the experience as 'real and vivid' as possible. If the phrase was for an everyday action they were instructed to visualize themselves doing the action from a first-person perspective. Examples of such actions were 'brushing your teeth' and 'stapling pages together'. If the phrase was for an internal state sensation they were encouraged to literally 'feel' their body in that state. Examples of internal state sensations were 'freezing cold' and 'upset stomach'. During scanning no explicit response, such as a button press, was required. Participants were asked about their subjective alertness and visualization performance after scanning was complete.

Preprocessing of imaging data. Data were preprocessed using the methods detailed in appendix A. Preparation of the data involved global artifact detection, realignment of the functional images, coregistration to the high-resolution anatomical image, normalization to the ICBM-152 atlas space, and smoothing using a Gaussian kernel of 8mm.

General linear model analysis of imaging data. A two-level mixed-effects methodology was used to analyze the functional imaging data. The first level consisted of a multiple regression analysis estimated using ordinary least squares (OLS) in SPM2 (Statistical Parametric Mapping, www.fil.ion.ucl.ac.uk/spm/). Predictors were created using a square wave based the block onset and length convolved with a canonical hemodynamic response function. Two predictors of interest were generated according to the imagery conditions: internal state imagery and action imagery. Other nuisance predictors were also created to account for low-frequency noise and subject head movement.

For each participant a set of two volumes was generated corresponding to the voxelwise beta estimates of each imagery condition. These images were input into a

multiple regression at the second level for final hypothesis testing. The second level was estimated using restricted maximum likelihood (ReML) to account for dependencies and unequal variance among the levels of each repeated measure. Additional details regarding statistical analysis of the fMRI data can be found in appendix A.

Contrasts of interest were generated at the second level to test a priori hypotheses. Contrasts were set up to test for similarities and differences between internal state and action imagery conditions. Two other contrasts were made to separately test for developmental differences in internal state and action imagery.

Region of interest analysis. Additional regions of interest were added to the whole-brain analysis based on the *a priori* hypothesis that bilateral areas of anterior insula would be involved in the internal state visualization condition. These regions of left and right anterior insula were created from the significant regions of left dorsal anterior insula and right central anterior insula in the experiment three contrast of modality differences. These regions were only applied to the internal > action contrast in the adults and the adult > adolescent internal visualization comparison. These regions were evaluated at the reduced significance level of $p = 0.05$, Bonferroni-corrected to a value of $p = 0.025$.

Results

Similarity between internal state and action imagery. A conjunction analysis was preformed to determine if any regions responded strongly to both internal state and action imagery conditions. The parameters for this comparison were $t^2(36) > 3.33$, $p < 0.001$, 8 voxel extent threshold. From this analysis a wide array of regions across all four lobes of the brain were found to be significant (Table 15 and Figure 38). Bilateral areas of inferior temporal cortex (Figure 39a, b), polar visual cortex (Figure 39c, d), frontal operculum/ anterior insula (Figure 39e, f), lateral frontal cortex (Figure 39g, h), premotor cortex (Figure 39i, j), and anterior cingulate (Figure 39k) were shown to be active within both imagery

modalities.

Differences between internal state and action imagery. A directional t-contrast was used to test for regions activating preferentially to one imagery modality over the other. The parameters for this comparison were $t(36) > 3.33$, $p < 0.001$, 8 voxel extent threshold. Several regions were shown to have increased activity in the internal state imagery condition relative to the action imagery condition. These areas were found primarily in areas of the insula and adjacent frontal cortex (Table 16 and Figure 40). In the internal visualization condition multiple significant voxel clusters were found along the right anterior, mid, and posterior insula (Figure 41a-d). Additional regions were found along the central operculum (Figure 41e) and anterior cingulate (Figure 41f). Only the a priori region of right anterior insula was found to be significant ($p < 0.001$). The region of right anterior insula not significant even at the reduced significance level of $p = 0.05$. Multiple regions were found to have increased activity in the action imagery condition relative to the internal state imagery condition. These areas were found in regions of lateral frontal, superior parietal, and visual cortex (Table 16 and Figure 40). In the action visualization condition significant clusters of left premotor cortex (Figure 41g), left primary somatosensory cortex (Figure 41h), left intraparietal sulcus (Figure 41i), and bilateral visual cortex (Figure 41j) were found.

Developmental changes in internal state imagery. A directional *t*-contrast was used to test for regions showing developmental differences in activity within the internal state imagery condition. The parameters for this comparison were $t(60) > 3.23$, $p < 0.001$, 8 voxel extent threshold. Adults were found to have increased activity relative to the adolescents in areas of frontal cortex and central operculum (Table 17 and Figure 42). Bilateral areas of the dorsal insula / parietal operculum (Figure 43a, b), dorsolateral prefrontal cortex (Figure 43c, d), and anterior cingulate (Figure 43e) were all shown to have increased activity in the

adult group. The adolescents had increased activity in areas of inferior temporal cortex, parietal operculum, and frontal cortex (Table 17 and Figure 42). Significant clusters in the left posterior insula (Figure 43f), left secondary somatosensory cortex (Figure 43g), bilateral inferior temporal cortex (Figure 43h), bilateral visual cortex (Figure 43i), and bilateral superior parietal lobule (Figure 43j, k) were shown to have increased activity in the adolescent group.

Developmental changes in action imagery. A directional t-contrast was used to test for regions showing developmental differences in activity within the action imagery condition. The parameters for this comparison were $t(60) > 3.23$, $p < 0.001$, 8 voxel extent threshold. Adults were found to have increased activity relative to the adolescents in areas of frontal and superior parietal cortex (Table 18 and Figure 44). Bilateral regions of the frontal pole (Figure 45a, b) lateral frontal cortex (Figure 45c, d), dorsal premotor cortex (Figure 45e, f), and left central operculum (Figure 45g) we all shown to be more active in the adult group. Only one area of left frontal operculum / insula was found to be more active in the adolescent group (Table 18 and Figure 45h).

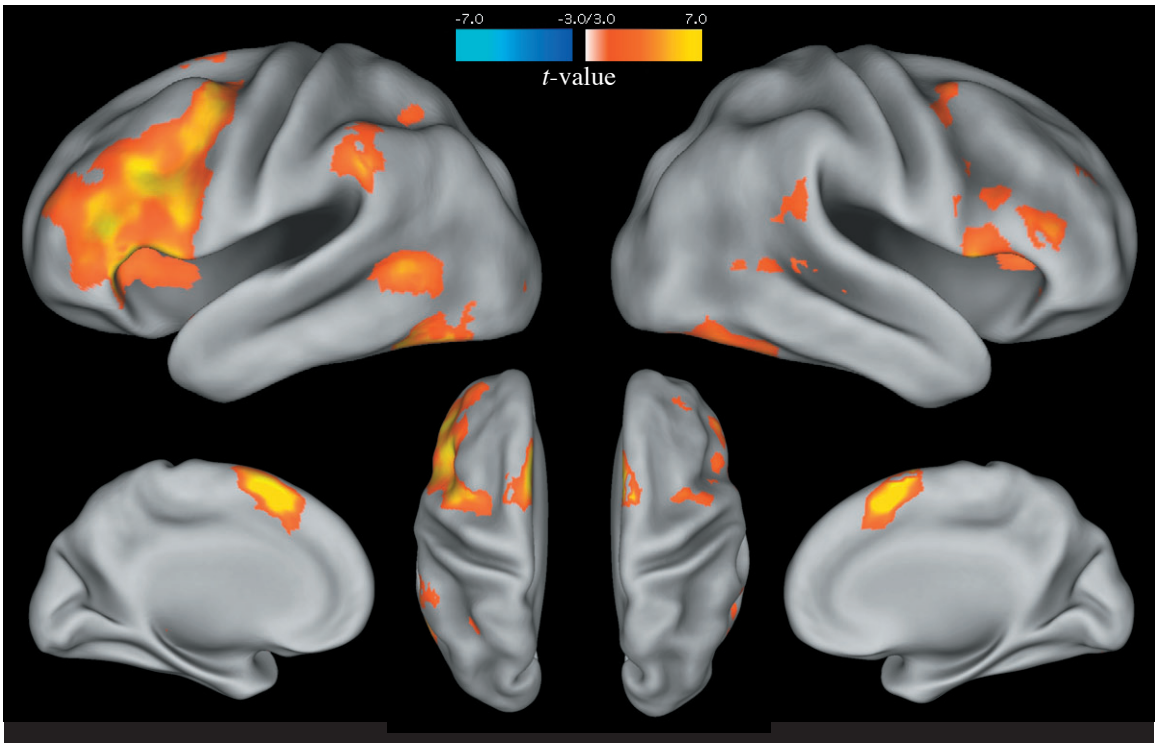

Figure 38. Regions showing a similar level of increased activity during the internal state visualization and action visualization conditions. The parameters for this comparison were $t^2(36) > 3.33, p < 0.001$, 8 voxel extent threshold. From this analysis a wide array of regions across all four lobes of the brain were found to be significant.

Table 15
Regions showing similar activity during internal state and action visualization

Region Name	HEM	BA	Area Notes	MNI Coordinates x	y	z	*z*-value	*p*(uncorr)	*p*(FDR)
Frontal									
Frontal Operculum Cortex	L	13		-42	24	0	6.25	< 0.0001	< 0.001
Frontal Operculum Cortex	R	13		45	27	3	4.93	0.0002	< 0.001
Inferior Frontal Gyrus	L	46		-48	33	12	6.04	0.0003	< 0.001
Middle Frontal Gyrus	R	46		-42	24	27	5.9	0.0004	< 0.001
Middle Frontal Gyrus	L	10	Frontal Pole	-33	45	18	4.49	0.0005	< 0.001
Middle Frontal Gyrus	R	9		33	42	27	3.74	< 0.0001	0.001
Inferior Frontal Gyrus	L	9		-51	18	27	5.59	< 0.0001	< 0.001
Inferior Frontal Gyrus	R	45	Broca's Area	51	21	27	4.36	< 0.0001	< 0.001
Precentral Gyrus	L	6	Premotor	-39	0	45	5.14	< 0.0001	< 0.001
Precentral Gyrus	R	6	Premotor	51	6	45	3.72	< 0.0001	0.001
Superior Frontal Gyrus	Both	6	Supplementary Motor	3	15	54	6.41	< 0.0001	< 0.001
Temporal									
Inferior Temporal Gyrus	L	37		-45	-48	-21	6.56	< 0.0001	< 0.001
Inferior Temporal Gyrus	R	37		39	-42	-24	5.64	< 0.0001	< 0.001
Middle Temporal Gyrus	L	21		-54	-54	3	5.43	< 0.0001	< 0.001
Superior Temporal Gyrus	R	21		53	-33	0	3.47	< 0.0001	0.003
Parietal									
Supramarginal Gyrus	L	40		-60	-39	36	4.77	< 0.0001	< 0.001
Intraparietal Sulcus	L	hIP1		-30	-51	42	3.67	< 0.0001	0.002
Occipital									
Occipital Pole	L	18	Visual Cortex / V2	-21	-96	-9	6.35	< 0.0001	< 0.001
Occipital Pole	R	18	Visual Cortex / V3	24	-93	-6	7.3	< 0.0001	< 0.001
Subcortical									
Hippocampus	L			-27	-30	0	3.91	< 0.0001	0.001
Hippocampus	R			30	-21	-3	4.02	< 0.0001	0.001
Pallidum	L			-21	-3	3	4.52	< 0.0001	< 0.001
Putamen	R			18	12	6	4.79	< 0.0001	< 0.001
Cerebellum									
Superior Cerebellum	L			-39	-57	-24	6.07	< 0.0001	< 0.001
Superior Cerebellum	R			39	-54	-30	6.21	< 0.0001	< 0.001

Table lists significant areas of activation ($p < 0.001$, extent threshold 6 voxels).
HEM = hemisphere in which cluster was located; BA = approximate Brodmann area of cluster;
p(uncorr) = uncorrected cluster probability; *p*(FDR) = cluster probability under false discovery rate

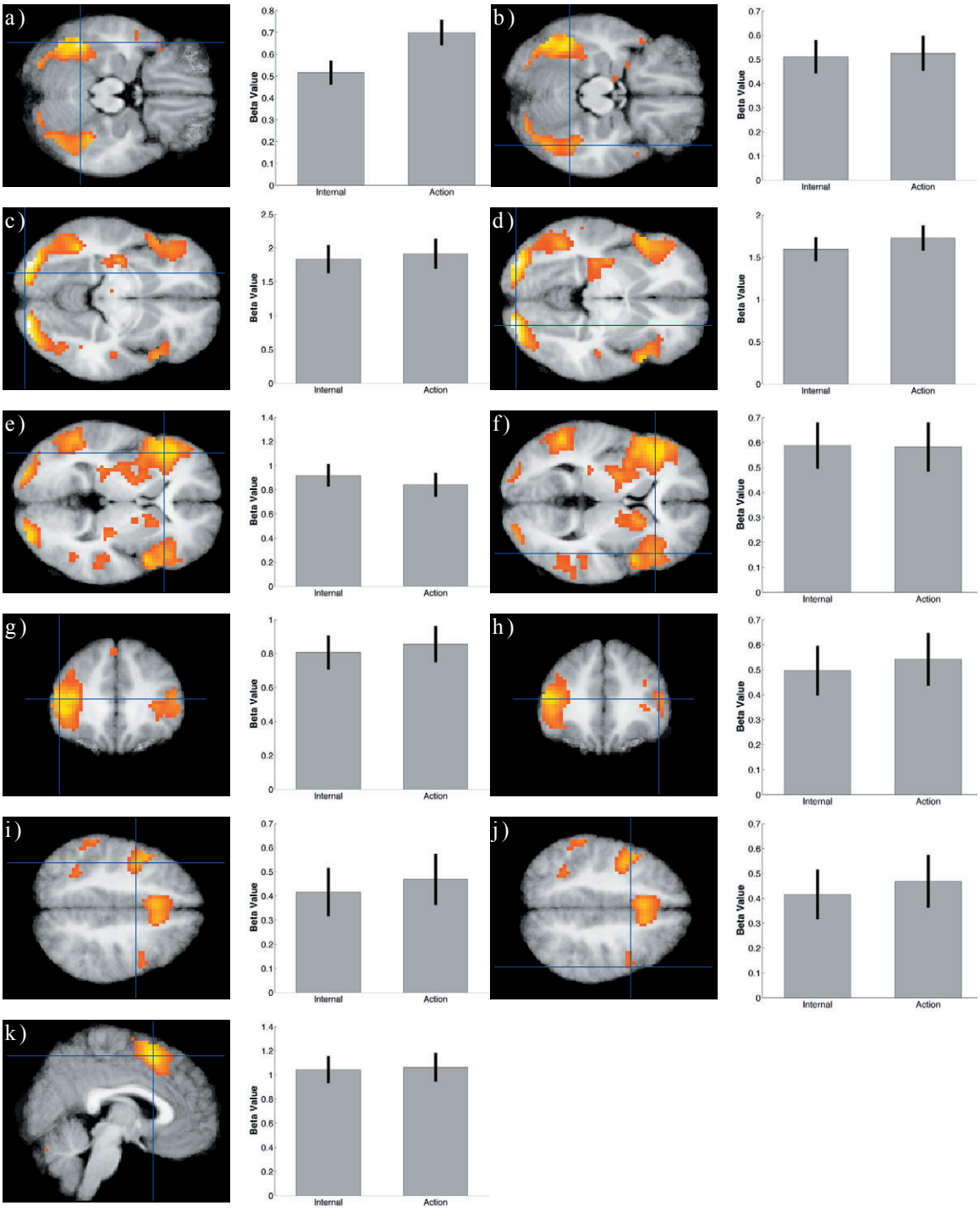

Figure 39. Parameter graphs of the internal/action conjunction analysis. Left bars represent activity to internal state visualization and right bars represent activity to action visualization. Bilateral areas of inferior temporal cortex (a,b), polar visual cortex (c,d), frontal operculum/anterior insula (e,f), lateral frontal cortex (g,h), premotor cortex (i,j), and anterior cingulate (k) were shown to be active within both imagery modalities.

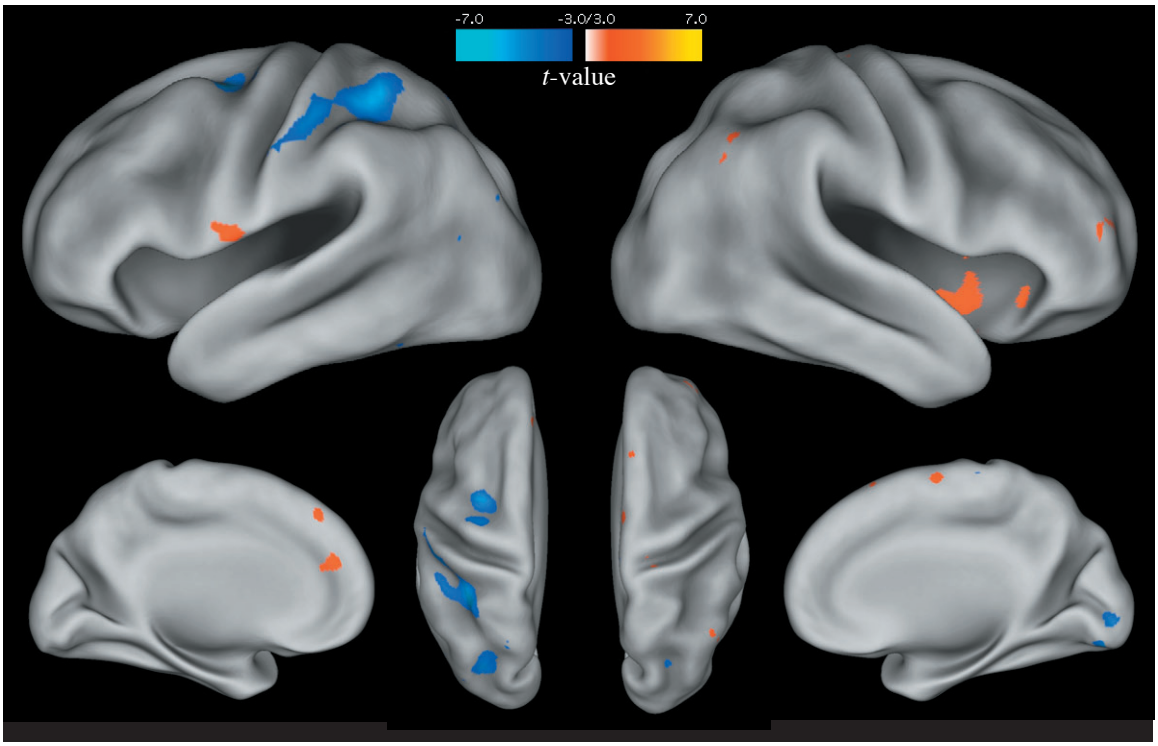

Figure 40. Regions showing preferential activity to the internal state visualization condition (red) or the action visualization condition (blue). The parameters for this comparison were $t(36) > 3.33$, $p < 0.001$, 8 voxel extent threshold. Regions shown to have increased activity in the internal state imagery condition were found primarily in areas of the insula and adjacent frontal cortex. These areas were found in regions of lateral frontal, superior parietal, and visual cortex.

Table 16
Regions showing preferential activity to the internal visualization or action visualization condition

Region Name	HEM	BA	Area Notes	MNI Coordinates x	y	z	*z*-value	*p*(uncorr)	*p*(FDR)
Internal > Action									
Frontal									
Paracingulate Gyrus	Bilat	9	Anterior Cingulate	9	51	12	3.41	< 0.001	0.152
Central Operculum	L	OP4	Frontal Operculum	-57	-3	9	3.47	< 0.001	0.152
Superior Frontal Gyrus	L	8		-3	39	42	3.52	< 0.001	0.152
Temporal									
Insula	R	13	Anterior Insula	30	24	-3	3.43	< 0.001	0.152
Insula	R	13	Mid Insula	36	6	-9	4.09	< 0.001	0.148
Insula	R	13	Posterior Insula	39	-18	-3	4.25	< 0.001	0.148
Insula	R	13	Dorsal Mid Insula	36	6	12	3.37	< 0.001	0.153
Parietal									
Inferior Parietal Lobule	R	40		51	-60	45	3.06	< 0.001	0.171
Subcortical									
Substantia Nigra	Bilat			0	-15	-18	3.11	< 0.001	0.171
Amygdala	R			18	-3	-9	3.49	< 0.001	0.152
Action > Internal									
Frontal									
Middle Frontal Gyrus	L	6		-27	-3	54	4.22	< 0.001	0.036
Temporal									
Fusiform Cortex	L	37		-39	-51	-18	4.176	< 0.001	0.036
Middle Frontal Gyrus	L	21		-60	-54	3	3.26	< 0.001	0.066
Parietal									
Postcentral Gyrus	L	2	Primary Somatosensory	-57	-21	42	3.106	< 0.001	0.083
Postcentral Gyrus	L	2	Primary Somatosensory	-42	-30	48	4.24	< 0.001	0.036
Intraparietal Sulcus	L	19		-30	-72	36	3.77	< 0.001	0.044
Occipital									
Fusiform Gyrus	R	18	Visual Cortex / V2	15	-84	-9	4.42	< 0.001	0.036
Fusiform Gyrus	R	18	Visual Cortex / V2	15	-90	-3	4.42	< 0.001	0.036

Table lists significant areas of activation ($p < 0.001$, extent threshold 6 voxels).
HEM = hemisphere in which cluster was located; BA = approximate Brodmann area of cluster;
p(uncorr) = uncorrected cluster probability; *p*(FDR) = cluster probability under false discovery rate

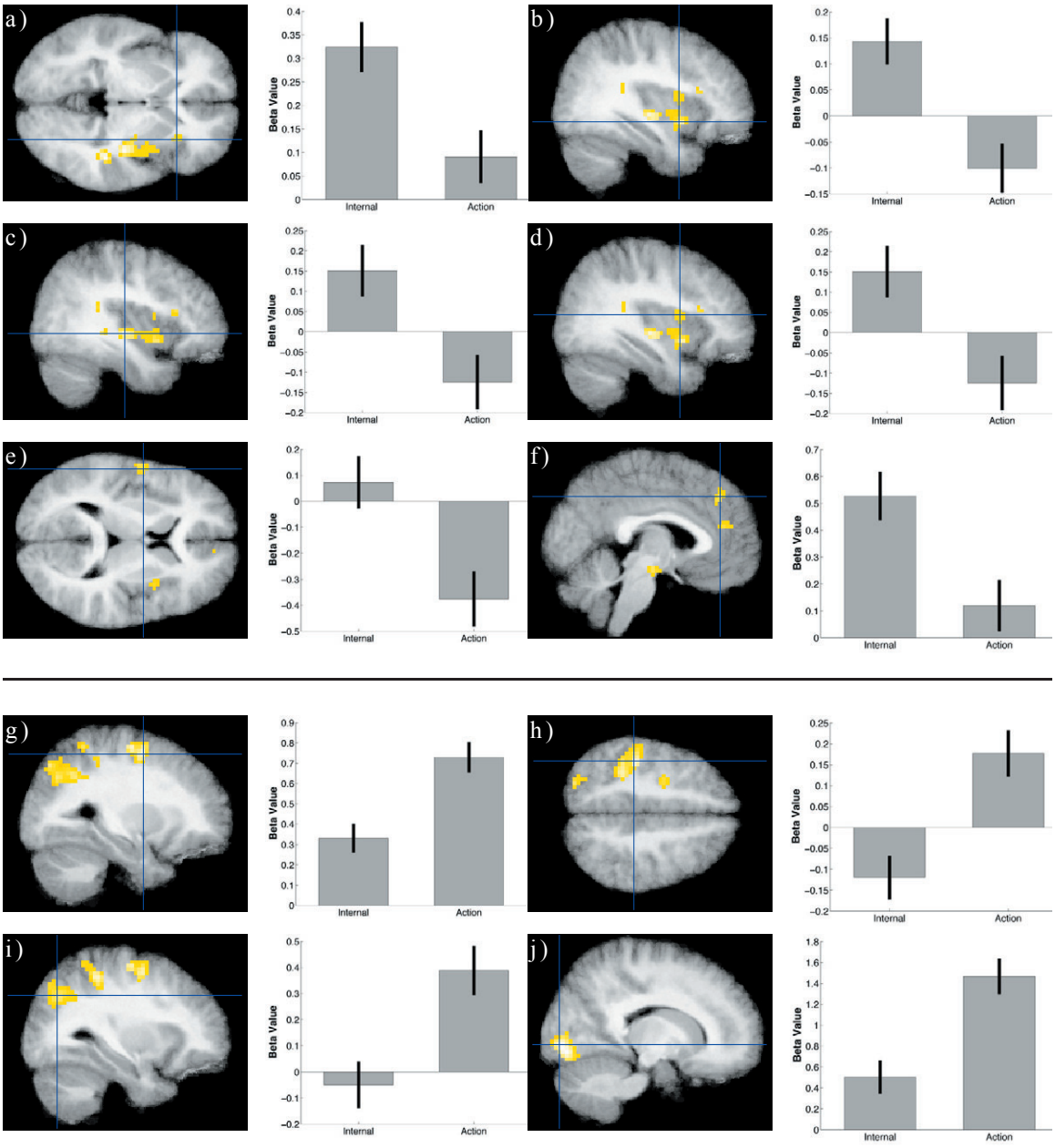

Figure 41. Parameter graphs of internal state and action visualization differences. Left bars represent activity to internal state visualization and right bars represent activity to action visualization. In the internal visualization condition multiple significant voxel clusters were found along the right anterior, mid, and posterior insula (a-d). Additional regions were found along the central operculum (e) and anterior cingulate (f). In the action visualization condition significant clusters of left premotor cortex (g), left primary somatosensory cortex (h), left intraparietal sulcus (i), and bilateral visual cortex (j) were found.

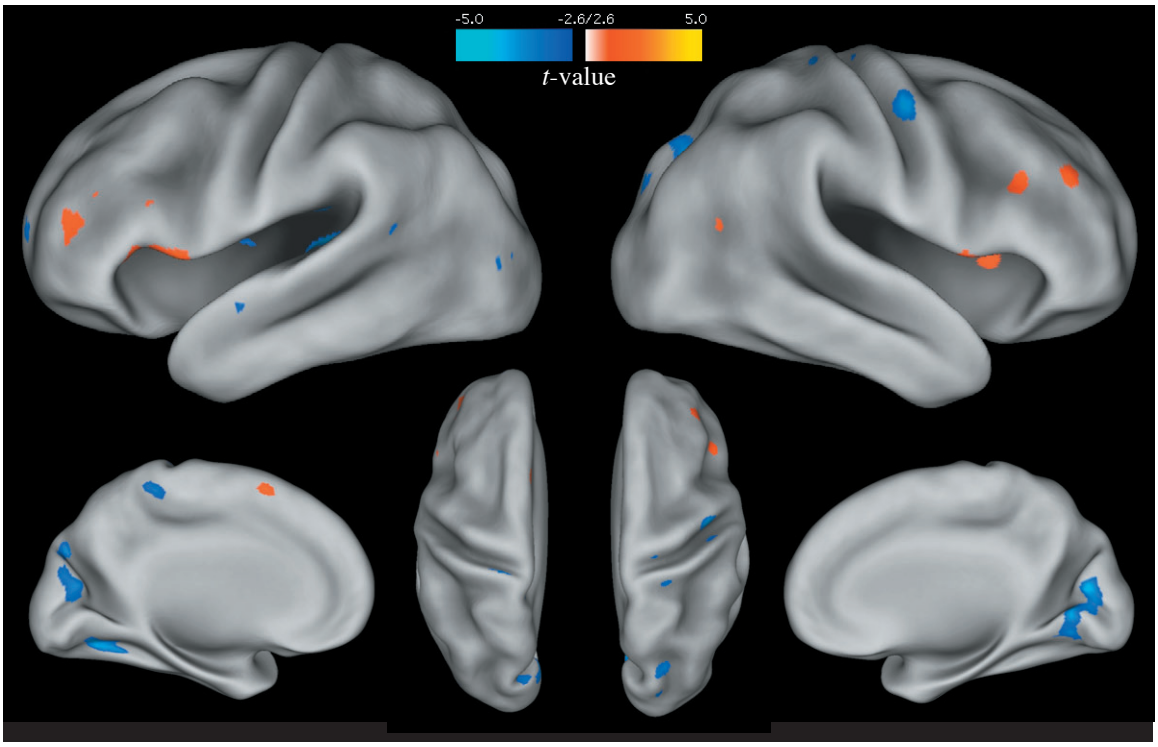

Figure 42. Regions demonstrating a developmental difference in the internal state visualization condition. Regions with greater activity in the adult group are depicted in red and regions with greater activity in the adolescent group are depicted in blue. The parameters for this comparison were $t(60) > 3.23$, $p < 0.001$, 8 voxel extent threshold. Adults were found to have increased activity in areas of frontal cortex and central operculum. Adolescents had increased activity in areas of inferior temporal cortex, parietal operculum, and lateral frontal cortex.

Table 17
Regions showing differences in activity across development within the internal state visualization condition

Region Name	HEM	BA	Area Notes	MNI Coordinates x	y	z	z-value	p(uncorr)	p(FDR)
Adults > Adolescents									
Frontal									
Inferior Frontal Gyrus	L	45	Broca's Area	-45	39	12	3.05	< 0.001	0.544
Inferior Frontal Gyrus	R	44	Broca's Area	45	15	24	3.44	< 0.001	0.544
Middle Frontal Gyrus	R	9	Lateral Frontal	36	39	27	3.27	< 0.001	0.544
Middle Frontal Gyrus	R	9	Lateral Frontal	18	57	27	3.34	< 0.001	0.544
Paracingulate Gyrus	Bilat	6	Dorsal Cingulate	0	12	54	3.35	< 0.001	0.544
Temporal									
Insula / Central Operculum	L	13	Dorsal Mid Insula	-51	12	0	3.76	< 0.001	0.544
Insula / Central Operculum	R	13	Dorsal Mid Insula	48	6	0	3.20	< 0.001	0.544
Insula / Central Operculum	R	13	Dorsal Mid Insula	36	3	24	3.54	< 0.001	0.544
Adolescents > Adults									
Frontal									
Superior Frontal Gyrus	L	10	Frontal Pole	-18	60	9	3.85	< 0.001	0.167
Precentral Gyrus	R	6	Premotor	48	-9	48	3.69	< 0.001	0.167
Precentral Gyrus	L	4a	Primary Motor	-9	-39	60	3.25	< 0.001	0.196
Temporal									
Insula	L	13	Posterior Insula	-36	-30	12	3.99	< 0.001	0.167
Parietal									
Parietal Operculum	L	OP1	Secondary Somatosensory	-42	-30	27	4.21	< 0.001	0.167
Occipital									
Fusiform Gyrus	L	37		-27	-63	-6	3.76	< 0.001	0.167
Lingual Gyrus	R	18	Visual Cortex / V2	9	-66	6	3.93	< 0.001	0.167
Intracalcarine Cortex	Bilat	18	Visual Cortex / V3	6	-75	15	3.92	< 0.001	0.167
Cuneus	L	18		-18	-75	30	3.57	< 0.001	0.167
Lateral Occipital Cortex	R	19		24	-69	39	3.78	< 0.001	0.167

Table lists significant areas of activation ($p < 0.001$, extent threshold 6 voxels).
HEM = hemisphere in which cluster was located; BA = approximate Brodmann area of cluster;
p(uncorr) = uncorrected cluster probability; p(FDR) = cluster probability under false discovery rate

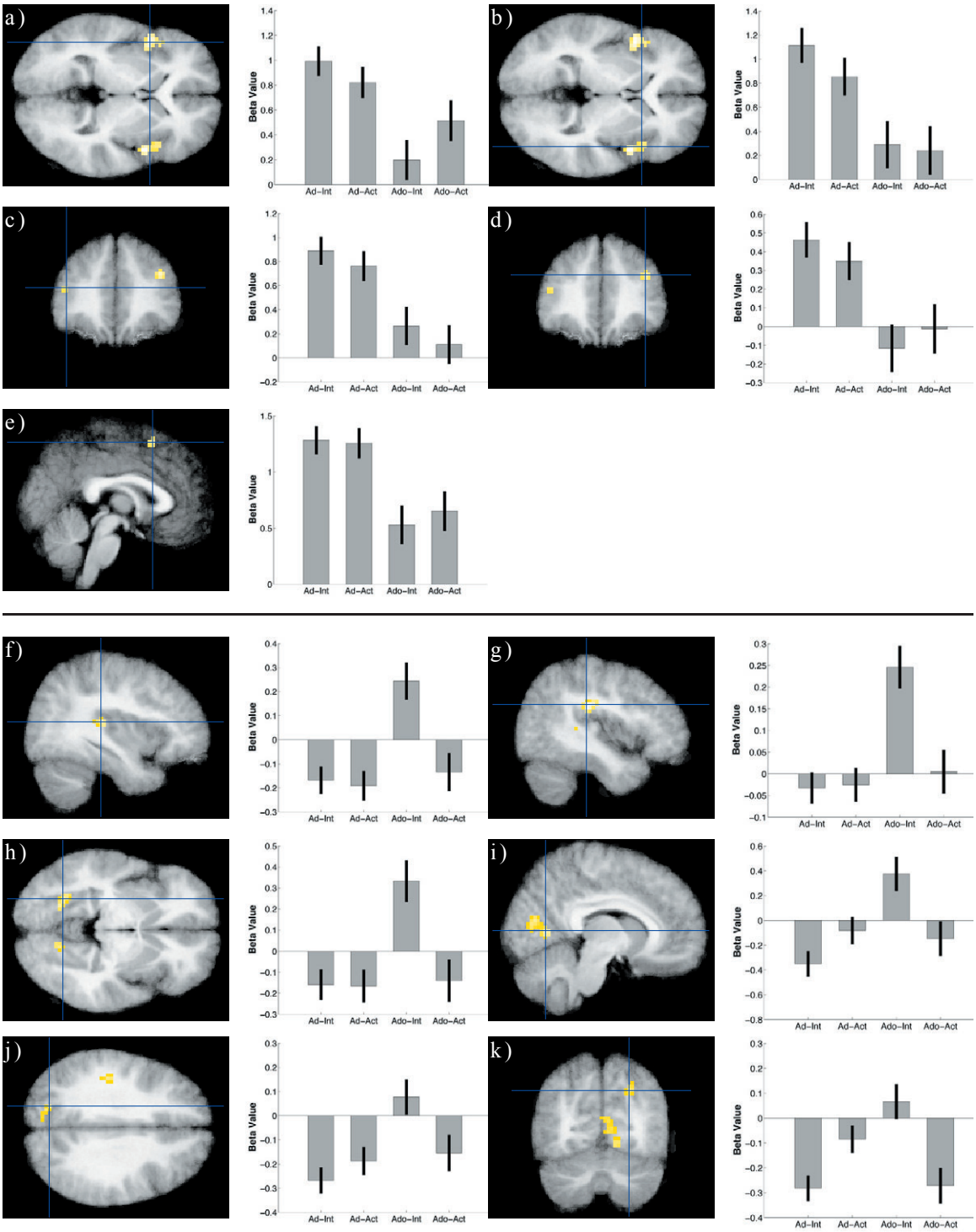

Figure 43. Parameter graphs of developmental differences in internal state visualization. From left to right bars represent adult-internal, adult-action, adolescent-internal, and adolescent-action conditions. Bilateral areas of the dorsal insula / parietal operculum (a, b), dorsolateral prefrontal cortex (c, d), and anterior cingulate (e) were all shown to have increased activity in the adult group. Significant clusters in the left posterior insula (f), left secondary somatosensory cortex (g), bilateral inferior temporal cortex (h), bilateral visual cortex (i), and bilateral superior parietal lobule (j, k) were shown to have increased activity in the adolescent group.

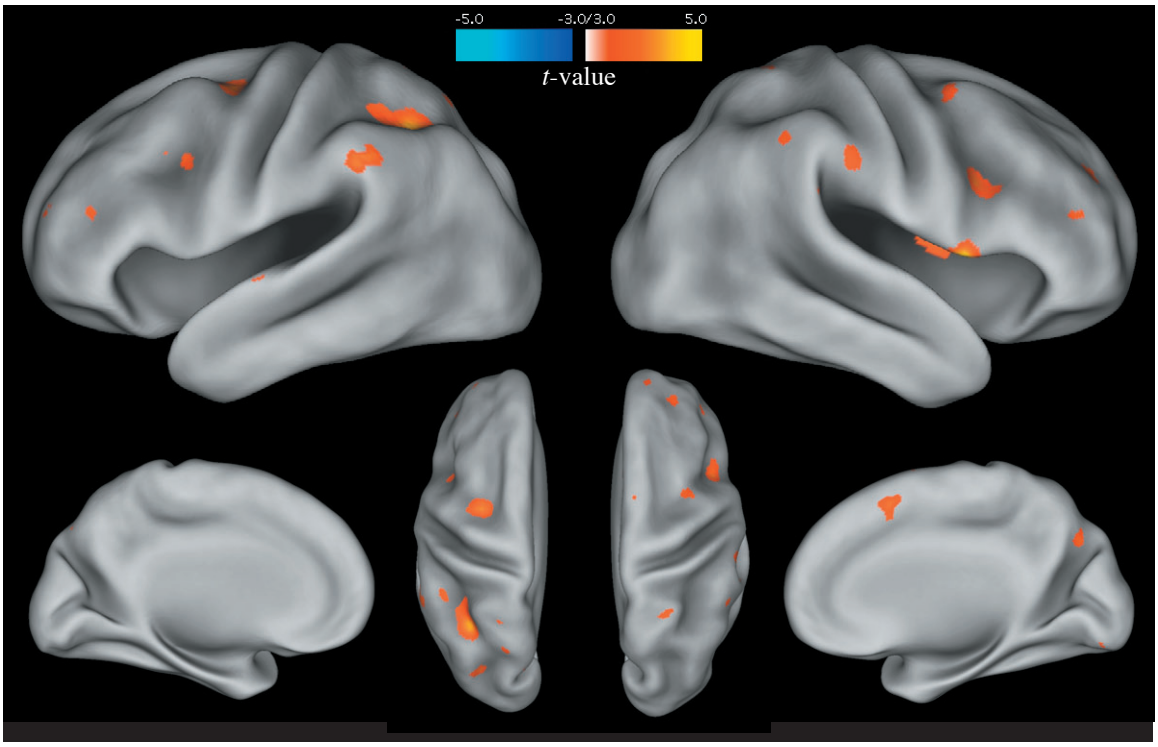

Figure 44. Regions demonstrating a developmental difference in the action visualization condition. Regions with superior activity in the adult group are depicted in red and regions with superior activity in the adolescent group are depicted in blue. The parameters for this comparison were $t(60) > 3.23$, $p < 0.001$, 8 voxel extent threshold. Adults were found to have increased activity in areas of frontal and superior parietal cortex. One area of left frontal operculum / insula was found to be more active in the adolescent group.

Table 18

Regions showing a developmental change between adults and adolescents within the action visualization conditi

Region Name	HEM	BA	Area Notes	MNI Coordinates x	y	z	*z*-value	*p*(uncorr)	*p*(FDR)
Adult > Adolescent									
Frontal									
Middle Frontal Gyrus	L	45	Broca's Area	-48	36	18	3.28	0.001	0.071
Middle Frontal Gyrus	L	10	Frontal Pole	-33	51	15	3.04	0.001	0.088
Middle Frontal Gyrus	R	10	Frontal Pole	30	42	27	3.53	< 0.001	0.053
Inferior Frontal Gyrus	R	44	Broca's Area	45	12	24	3.88	< 0.001	0.037
Middle Frontal Gyrus	L	44	Broca's Area	-42	9	33	3.35	< 0.001	0.064
Middle Frontal Gyrus	L	6	Premotor	-27	-6	51	3.91	< 0.001	0.037
Middle Frontal Gyrus	R	6	Premotor	39	3	57	3.58	< 0.001	0.049
Paracingulate Gyrus	Bilat	6		3	12	51	3.89	< 0.001	0.037
Temporal									
Insula / Central Operculum	R	13	Dorsal Mid Insula	54	9	0	4.45	< 0.001	0.033
Parietal									
Parietal Operculum	R	OP1	Secondary Somatosensory	63	-24	27	3.50	< 0.001	0.054
Intraparietal Sulcus	L	hIP1		-30	-75	36	4.00	< 0.001	0.034
Intraparietal Sulcus	R	hIP1		-12	69	36	3.69	< 0.001	0.043
Supramarginal Gyrus	L	40		-57	-42	39	4.105	< 0.001	0.033
Superior Parietal Lobule	L	7		-27	-54	39	4.50	< 0.001	0.033
Angular Gyrus	R	40		51	-42	42	3.29	< 0.001	0.070
Subcortical									
Putamen	R			24	-9	6	3.63	< 0.001	0.047
Adolescent > Adult									
Temporal									
Insula	L	13	Anterior Insula	-33	36	0	3.62	< 0.001	1.000

Table lists significant areas of activation ($p < 0.001$, extent threshold 6 voxels).
HEM = hemisphere in which cluster was located; BA = approximate Brodmann area of cluster;
p(uncorr) = uncorrected cluster probability; *p*(FDR) = cluster probability under false discovery rate

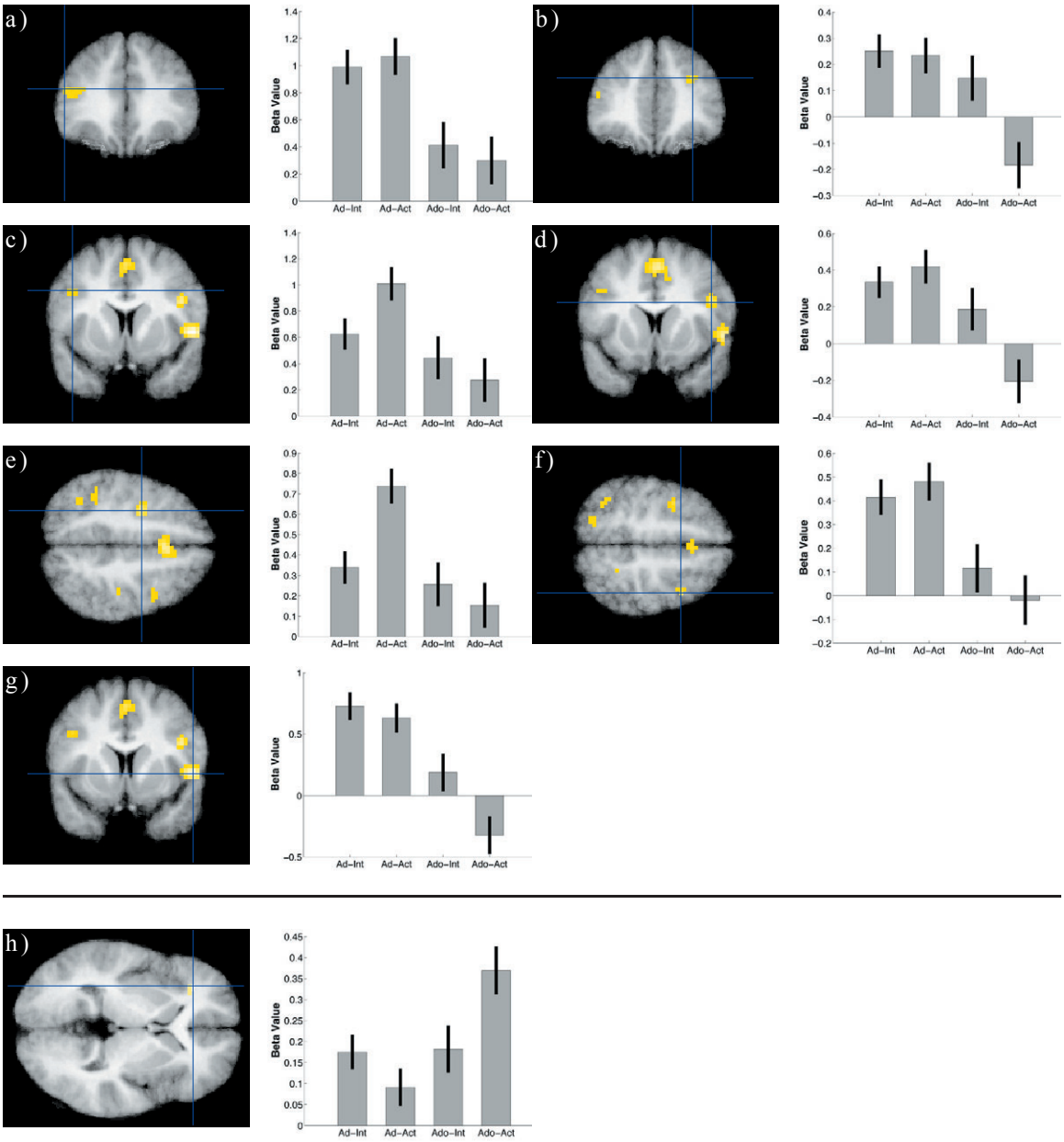

Figure 45. Parameter graphs of developmental differences in action visualization. From left to right bars represent adult-internal, adult-action, adolescent-internal, and adolescent-action conditions. Bilateral regions of the frontal pole (a, b), lateral frontal cortex (c, d), dorsal premotor cortex (e, f), and left central operculum (g) we all shown to be more active in the adult group. Only one area of left frontal operculum / insula was found to be more active in the adolescent group (h).

Discussion

Imagery results. A similar pattern of activity was observed across the brain for both visualization conditions, showing that both internal state and action imagery were conducted in a consistent manner. Still, differences were seen in modality-specific areas that give rise to the unique qualities of each visualization condition. For the internal state imagery condition this meant activity in areas of bilateral mid and right anterior insula. For the action imagery condition this meant activity in left premotor, somatosensory, and parietal cortex. This echoes the results from previous visualization experiments, which demonstrated that cortical areas involved in processing information of a particular modality are also utilized in the mental visualization of that modality (Farah, 1984; Kosslyn et al., 2001).

One current debate regarding mental imagery is the degree to which primary sensory areas are employed in creating the visualization. A number of studies support the finding of primary visual cortex (V1, BA 17) being involved in visual imagery (Kosslyn, Thompson, Costantini-Ferrando, Alpert, & Spiegel, 2000; Kosslyn et al., 1995) . Similar results have also been shown regarding primary motor cortex (M1, BA 4) activity during motor visualization (Decety & Grezes, 2006; Ganis, Keenan, Kosslyn, & Pascual-Leone, 2000). Conversely, studies of auditory imagery have not observed activity in primary auditory cortex (A1, BA 41,42) during auditory imagery (Kraemer et al., 2005; Zatorre & Halpern, 2005). The results of the current study support previous evidence showing primary motor cortex involvement in motor visualization. They also extend our knowledge by showing that posterior insula, an area hypothesized to be primary interoceptive cortex, did not show involvement in the internal state imagery condition. Instead, areas of anterior and mid insula were shown to be active. Since these areas are not the targets of cortical afferents conveying internal state information (Craig & Dostrovsky, 2001) it can be argued that internal state visualization does not require primary interoceptive cortical regions.

Developmental results. Very little work has been done on the development of mental imagery from childhood to adolescence and into adulthood. Most of the developmental research to date has been focused on aspects of mental rotation. One important result from this previous research is that by the age of six children are already quite adept at mental imagery (Estes, 1998; Kosslyn, Margolis, Barrett, Goldknopf, & Daly, 1990; Marmor, 1975). This means that the adolescents certainly have the capacity to engage in visualization. Still, the ability of individuals to perform mental imagery operations continues to increase across development. Early adolescents have demonstrated better performance on mental rotation tasks than children (Waber, Carlson, & Mann, 1982). Also, studies have indicated that children suffer greater performance deficits relative to adults when completing a mental rotation task under cognitive load (Funk, Brugger, & Wilkening, 2005). It has also been shown that when engaging in mental rotation adults are able to recruit additional areas of parietal association cortex relative to adolescents (Kucian et al., 2007).

In terms of developmental change important differences were observed between adults and adolescents in the internal state visualization condition. The adults showed greater activity in areas of lateral frontal, mid insular, and central opercular cortex while adolescents showed greater activity in regions of medial occipital, inferior occipital, and primary motor cortex. This pattern of results may be due a number of developmental effects. One potential interpretation is that the adolescents were unable to sufficiently recruit areas of association cortex and instead relied on more mature areas of motor and visual cortex to compensate. This follows from the Kucian et al. (2007) results, which showed children had a greater response in visual areas while adults had a greater response in parietal association cortex.

Another possibility is that the adolescents were using a different visualization strategy relative to the adults. While the adults were focusing on the 'feeling' of the internal state sensation the adolescents may have been focused on the visual and motor correlates of that condition. For example, while the adults could feel the sensation of being cold the

adolescents may have been focusing on what it looks like when you are cold. Post-scan interviews with the adolescents indicated that they believed they were completing the task as outlined. Still, without an explicit response to rely on it is impossible to know the task was being accomplished in the same manner across groups.

General Discussion.

Interoception

To paraphrase Winston Churchill, the brain is a riddle inside a mystery wrapped in an enigma. The individual experiments of this thesis each uncovered a unique aspect of interoceptive information processing. Some results confirmed our scientific knowledge of interoceptive processes while others contained evidence against long-held assumptions of internal state information processing. From their summation comes the potential to better understand a broader view of the relationship between mind and body.

A number of articles have been written regarding the distinction between interoceptive and exteroceptive afferents (Craig, 2002). The lamina I spinothalamocortical pathway has been shown to uniquely convey signals of pain, temperature, itch, muscle burn, hunger, thirst, taste, and sensual touch (Craig, 1996). The distinctive processing of these modalities continues through areas of the brainstem and thalamus until finally arriving at cortical sites in the posterior insula (Oliver G. Cameron, 2002; Craig et al., 2000). This area is hypothesized to be a region of primary interoceptive cortex based on the distinctive nature of interoceptive afferents, the anatomical connections conveying this information to the posterior insula, and several functional neuroimaging studies indicating its involvement in the experience of interoceptive sensations (DelParigi, Chen, Salbe, Reiman, & Tataranni, 2005; Henderson, Gandevia, & Macefield, 2007; Kuhtz-Buschbeck et al., 2005; Mochizuki et al., 2007). Based on this evidence the posterior insula was thought to possess a dissociable representation of internal state. This formed the basis for the hypotheses of experiment two.

The problem inherent to discussions of cortical interoceptive representation is that many of the imaging studies have been poorly controlled. While a study may show that posterior insula has activity related to thermal intensity this result has not been contrasted against another modality. This is especially true of the modality most highly related to interoception: somatosensory stimulation. The structure of posterior insula is very similar

to granular areas of secondary somatosensory cortex (Augustine, 1996), and a number of studies have shown that the posterior insula is active during several forms of somatosensory stimulation (Dresel et al., 2008; Huang & Sereno, 2007; McGlone et al., 2002). The results of this thesis show that the hypothesized distinction between interoceptive and exteroceptive information processing completely breaks down once the information arrives at the cerebral cortex. In direct comparisons between thermal and tactile stimulation the areas of posterior insula were shown to be quite multimodal. As additional evidence of this fact most areas of the insula were more active during tactile conditions relative to thermal conditions.

Curiously, distinctions between interoceptive and exteroceptive information processing did appear in areas known to handle higher-order information processing. These results were not binary interoceptive-or-exteroceptive distinctions, but were seen as a preferential involvement in the processing of modality-specific stimulus features. This pattern was observed during tasks that varied the demand for interoceptive stimulus features and during tasks that required the use of interoceptive stimulus features for executive control. This result mirrors the findings of several other papers detailing the role of anterior insula in higher-order integration of interoceptive information (Critchley et al., 2001; Critchley et al., 2004; Symonds, Gordon, Bixby, & Mande, 2006). It also helps speak to the idea that the anterior insula has a role in initiating executive control. From previous work it appears that it is the anterior insula that acts as a type of switch to push the brain out of the default mode of processing (Dosenbach et al., 2007; Seeley et al., 2007). Because subregions of the anterior insula have preferential representation of interoceptive information this may provide evidence for Damasio's somatic marker: a way for internal state information to quickly bias decision making through unique influence on higher-order processing.

A unique finding of this thesis is the role of the dorsal mid insula with regard to interoceptive experience. When discussing the conscious awareness of internal state sensations most studies reference the right anterior insula as the locus of higher-order integration (Craig, 2003b; Critchley, 2005). What the results of this thesis indicate is that

there may be another important route to higher-order integration through the dorsal mid insula and central operculum. Recent evidence regarding the anatomical connectivity of this region has emerged since the experiments of this thesis first began. A paper by Saleem, Kondo, and Price (2008) describes a series of anatomical tracing studies designed to investigate the connectivity of prefrontal and temporal/insular/opercular cortex. One focus of their work was the relationship between orbitofrontal cortex and the insula and central operculum. Their results show that the bulk of connectivity between the two regions occurs between Brodmann areas 11 and 12 of orbital cortex and the mid insula. This is strong evidence against the original hypothesis of the anterior insula being the unique interoceptive conduit to orbital cortex and provides support to the idea that orbital cortex may posses a more rich array of interoceptive information than previously thought.

With regard to orbital prefrontal cortex, it is important to again note that the collection of data from this region was incomplete. A large area of ventromedial prefrontal cortex is absent from all experiment datasets due to the influence of susceptibility artifact in the high-field (3 Tesla) MR environment. This is a important limiting factor, as additional information processing could be occurring in this region that would go unnoticed in the current studies. This is especially notable given the strong connectivity between orbital areas and the mid insula (Saleem et al., 2008).

Development

The idea of linear developmental change from childhood to adulthood is a popular view of maturation. The serial-stage theories of Piaget (1954) and Kohlberg (1984) are intuitive and parsimonious in their description of developmental events. Still, a large amount of evidence suggests that they do not accurately reflect the underlying neurodevelopment taking place across the first twenty years of life. While straightforward marches to maturity may still be a valid model for early sensory and motor regions, in areas of higher-order association cortex the developmental trajectory is dramatically different. For example,

within regions involved in emotional integration adolescence actually represents a step backward in performance before taking two steps forward (McGivern et al., 2002). This is thought to reflect developmental processes that require not only maturity of individual regions of the brain, but also coordination of information processing across the entire cortex (Luna & Sweeney, 2004). The inclusion of adolescent participants throughout the thesis experiments capitalized on these effects to learn more about higher-order interoceptive development.

Interoceptive development was shown to closely follow overall cognitive development. Basic interoceptive processes, such as simple thermal detection, were mature before adolescence. From this data it is likely that primary interoceptive processing follows a developmental trajectory similar to that of primary somatosensory cortex, reaching adult levels of maturity during the first decade of life (Gogtay et al., 2004; Shumeiko, 1998). This stands in contrast to the developmental profiles of higher-order areas of interoceptive cortex, which showed activity differences between the adolescent and adult groups. Areas of mid insula, central operculum, and anterior insula all showed developmental changes in activity. Most often this was observed as the adolescent group recruiting a more diverse array of cortical regions to engage in task-related activity. Many of theses areas were uniquely active in the adolescent group, with no significant response in the adult group. Other results were observed which suggest that increases in performance-related activity could be observed across cortical regions in the adults. These results converge to show that interoceptive development is a process of moving from diffuse task-relevant regions of activity to a set of more focused and efficient set of regions more directly tied to task performance.

These results of processing differences within the insula are notable given the insula's hypothesized role in decision-making, risk perception, and consequence representation. One function of the insula is thought to be the representation of negative outcomes in decision-making (Berns et al., 2006; Paulus et al., 2005). While areas of orbital cortex

represent the positive outcomes of a decision based on their hedonic value (Bechara et al., 2000; Kringelbach, 2005), the insula can represent negative outcomes based on their negative emotional valence (Paulus et al., 2003). Given the immaturity of this system it has important implications for risk taking behavior in teens, especially given evidence showing overactive dopaminergic reward systems in adolescents (Galvan et al., 2006).

Future Work

There is still some data acquired during the completion of this thesis that has yet to be analyzed. As part of each fMRI scanning session a high-resolution [1 mm^3] T1 anatomical scan was acquired. In the future this data will enable associations to be made between the differences observed in function with differences in the composition of the underlying anatomy. This can be approached using methods such as voxel-based morphometry (Ashburner & Friston, 2000) or metrics of cortical thickness (Gogtay et al., 2004; Sowell et al., 2004). In conjunction with the T1 scan a set of diffusion-tensor imaging data [DTI] was also acquired in all subjects. The DTI data yields information regarding the Brownian motion of water within a 2 mm^3 voxel (Le Bihan, 2003). This data can be used to construct maps of fractional anisotropy, which can be taken as an index of regional white matter integrity (Mukherjee & McKinstry, 2006). The DTI data can also be used to perform reconstructions of probable white matter pathways (Mori & van Zijl, 2002; Ramnani, Behrens, Penny, & Matthews, 2004). This may be useful to help characterize individual differences in interoceptive ability rising from variability in white matter connectivity or to further investigate developmental differences between the adolescent and adult groups.

Future functional imaging studies should focus on interoceptive information processing differences between the anterior insula and the central operculum. The data from this thesis suggest that these areas are involved in extracting abstract features of interoceptive stimuli for use in higher-order processes. It may be that differences exist with regard to the type of sensory features that each is extracting. For example, it may

be that the anterior insula is extracting features relevant for executive control while the central operculum is extracting features useful for multimodal sensory integration. Further research is necessary to examine this hypothesis, as data from this work cannot speak conclusively on the topic.

Conclusion

In summary, the experiments of this thesis resulted in four main findings related to interoception and interoceptive development. The first point is that early sensory areas considered to be 'primary interoceptive cortex' are actually much more multimodal than previously believed. The second point is that a distinction between interoceptive and exteroceptive stimuli does exist at a higher, more abstract level of processing. The third point is that there are few developmental differences between adolescents and adults in terms of primary interoceptive sensory processing. Finally, the fourth point is that areas involved in higher-order interoceptive processing do show developmental differences between adults and adolescents. The window of time between the onset of adolescence and young adulthood contains some of the greatest changes the body experiences after infancy. We cannot continue to believe that brain regions supporting internal state do not change as well.

Appendix A

Neuroimaging Details

Anatomical neuroimaging. Participants were scanned in a 3T Philips Achieva whole body scanner with a SENSE 8-element phased-array headcoil for RF transmission and reception [Philips Medical Systems, Andover, MA]. Foam padding was placed in the head coil to limit subject head movement during image acquisition. T1-weighted three-dimensional magnetization-prepared rapid acquisition gradient echo [3D-MPRAGE] sagittal images were obtained. Scanning parameters were as follows: echo time [TE] = 4.6 ms, repetition time, [TR] = 9.8 ms, flip angle = 8 degrees, acquisition matrix = 256 x 256, 160 sagittal slices, and voxel size = 1 x 1 x 1 mm with no gap. Additionally, diffusion-tensor imaging [DTI] data was collected for each subject. Single-shot echo planar [SS-EPI] diffusion-sensitized images were acquired in 32 non-collinear gradient directions. Scanning parameters were as follows: echo time [TE] = 91 ms, repetition time [TR] = 9023 ms, b = 1000 s/mm^2, flip angle 90 degrees, acquisition matrix 128 x 128, 70 axial slices, 2 x 2 x 2 mm, no gap. Multiple excitations were utilized for the MPRAGE and DTI scans to increase the signal to noise ratio [SNR] of voxel signal intensities.

Functional neuroimaging. Four of the experiments in this project involved the acquisition of functional MRI data. Scanning parameters for the whole-brain T2* echo-planar imaging [EPI] sequence were as follows: 36 interleaved axial slices [4mm thick, 1mm gap], TR = 2500ms, TE = 30ms, flip angle = 90º, field of view 256 x 256. Four dummy RF shots were used during the first 10 seconds of scanning to ensure magnetization equilibrium. Visual stimuli were projected onto a ground glass screen located at the head of the magnet bore by an LCD projector [Epson America, Long Beach, CA]. A mirror directly above the head coil allowed the subject to observe the projected image. Thermal and tactile stimuli were presented using the device detailed in appendix B. Stimulus timing

was accomplished using the experiment-scripting program Psyscope (Macwhinney, Cohen, & Provost, 1997) and synchronized by a TTL voltage trigger from the scanner. Responses to stimuli were made with an in-house fiber-optic keypad and recorded using Psyscope.

Overall fMRI preprocessing. Raw imaging data was subjected to an artifact detection technique based on quantitative analysis of fMRI volume quality. The global signal level, standard deviation, overall motion, and volume-to-volume motion were all calculated using the ArtRepair software package (Mazaika, Whitfield, & Cooper, 2005 ; Mazaika, Whitfield-Gabrieli, & Reiss, 2007). Volumes containing more than 1mm/TR of movement were eliminated and replaced with the mean of volumes coming before and after the corrupted image. Volumes with a global signal level more than four standard deviations away from the global mean were also eliminated and replaced with the mean of surrounding volumes. Runs requiring the replacement of more than 5% of the acquired images were eliminated completely from subsequent analysis.

Image preprocessing was completed using the program SPM5 (Wellcome Department of Imaging Neuroscience, www.fil.ion.ucl.ac.uk/spm/, London, UK) with all available software updates installed. For experiments utilizing an event-related design the first preprocessing step was a slice-timing correction, which shifts the time-series data on each slice using sinc-interpolation (Gitelman, 1998). Images from all EPI scans were then spatially realigned to the first image using a least squares approach with a 6-parameter rigid body affine transformation (Friston et al., 1995). Realigned images were processed using the 'unwarp' function to reduce the influence of residual movement-related variance on BOLD signal intensity (Andersson, Hutton, Ashburner, Turner, & Friston, 2001). Images were normalized into a standard 3D stereotaxic space defined by the nonlinear International Consortium for Brain Mapping [ICBM]-152 atlas space (Ashburner & Friston, 1999; Ashburner, Neelin, Collins, Evans, & Friston, 1997; Mazziotta, Toga, Evans, Fox, & Lancaster, 1995). The normalization of the EPI images to the atlas template image was

completed using a combination of 12-parameter linear affine transformation and 3x2x3 nonlinear three-dimensional discrete cosine transform. A 7th degree B-spline was used as the interpolation method for creating normalized images. Finally, all images were smoothed with an 8mm full-width at half-maximum (FWHM) isotropic Gaussian kernel.

Overall fMRI statistical analysis. Each set of functional MRI data was analyzed using a two-level mixed effects methodology detailed within each results section. The first level was completed on each subject's data individually through a ordinary least-squares (OLS) estimation using the general linear model. For experiments with a block design hemodynamic responses was modeled by a boxcar convolved with a canonical hemodynamic response. For event-related designs the hemodynamic responses was modeled by an impulse response convolved with the canonical hemodynamic response and its temporal and dispersion derivatives. A high pass filter with a frequency cutoff of 128 seconds was used to remove linear, quadratic, and other forms of low frequency drift. Appropriate contrasts were created to compare conditions to rest and to compare condition against condition.

The resulting beta-value estimates from each subject were then entered into a second-level statistical test to examine areas of consistent activation across subjects and between groups. Unless otherwise noted, the alpha for these comparisons was $p < 0.05$, corrected with False Discovery Rate (Genovese, Lazar, & Nichols, 2002). To account for correlations among the levels of a factor in repeated measures designs covariance components were estimated with ReML (restricted maximum likelihood) hyperparameters. The ReML estimates were then used to whiten the data giving maximum likelihood (ML) or Gauss-Markov estimators.

Appendix B

Thermotactile Device Details

Thermotactile apparatus. The design of the Thermotactile system involved the use of four Peltier-effect thermoelectric devices for thermal stimulation and ten pneumatically driven wooden pegs for tactile stimulation. These elements were embedded within wood blocks designed to fit the contours of an average human hand (see Figure 46). Each hand block (one each left and right) contained two thermoelectric devices, five tactile stimulators, and one thumb button for responses.

For each wooden block the two thermoelectric devices were arranged together to yield a large 3" x 3.5" surface area where thermal changes could be felt along the length of the fingers. The thermoelectric devices used for this project were Tellurex Z-Max C1-1.4-127-1.14 modules (Tellurex Corp., Traverse City, MI). These devices were chosen specifically for the use of bismuth telluride in their construction. This material is diamagnetic, reducing the possibility of MR artifact generation due to movement. Low-pass filters were also fitted to the thermoelectric power supply lines to eliminate high-frequency electrical noise from entering the scanner suite.

When the thermoelectric devices are active all of the energy used to induce thermal changes is translated directly into heat. Thus, to provide 80 watts of thermal transfer a total of 200 watts of heat will need to be dissipated. To enable the event-related application of thermal stimulation each thermoelectric device required water-cooling. Small cooling blocks made entirely of copper (Thermaltake W3 Northbridge Water Block, Thermaltake Technology Inc., Los Angeles, CA) were attached to the backside of each thermoelectric device and then connected to a low-pressure water recirculation system. This method removed waste heat and kept the mean temperature of the device at a consistent value between each stimulus presentation.

Tactile feedback was accomplished through the use of wooden pegs embedded into

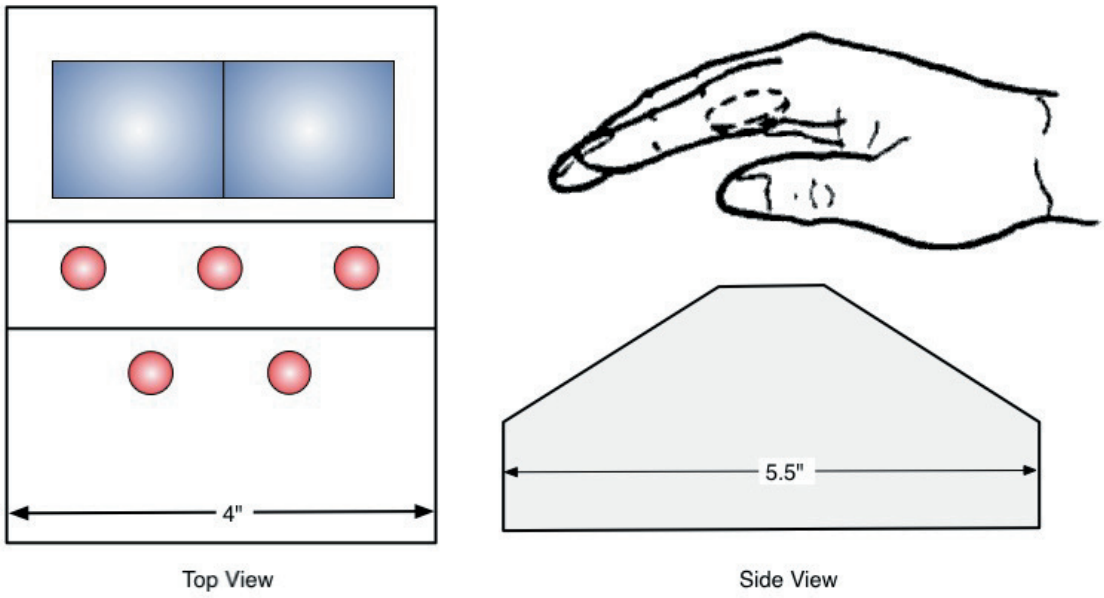

Figure 46. Schematic representation of the thermotactile device. The wooden blocks that the device is made of are angled to comfortably fit the contours of a relaxed human hand. There are five peg holes embedded in the top of the device to support tactile stimulation. On the finger side of the block are two thermoelectric devices to generate thermal stimulation

the surface of the wooden hand block. Each stimulator consisted of a polycarbonate tube silo with an air-driven wood dowel inside. In their normal position the pegs are recessed away from the top surface of the block. When activated the pegs are pushed up into contact with the palm of the subject using compressed air delivered from the control room. Pneumatic pressure was used to ensure that each peg was pressed up to the subject's hand with an equal amount of force, even if the height of the subject's hand varies across pegs. There were five available pegs per hand, with each peg able to be activated on an individual basis. The tubes were equidistant from each other and arrayed in such a way to allow tactile stimulation across the surface of the palm.

Thermal and tactile stimulus application was controlled through the use of a BASIC Stamp II microcontroller (Model BS2-IC; Parallax Inc., Rocklin, CA). This system enabled reliable millisecond timing for event-related stimulus application. Ten channels of the microcontroller were used to drive 2-way pneumatic valves for the tactile stimulators. Since each pneumatic valve was independently controlled the application of 0-5 pegs on each hand could be accomplished. Two channels of the device were used for the pulse-width modulated signaling of thermal level to a set of H-bridge motor controllers (Parallax Model HB-25, Rocklin, CA). This enabled 250 levels of increased temperature and 250 levels of decreased temperature for each hand independently. A benchtop thermal calibration of the device was undertaken to ensure equivalent temperature changes in each direction. Microcontroller and valve power was provided by a 28 volt, 2.4 amp DC power supply (Mean Well model PS-65-27, Mean Well USA, Fremont, CA). Thermoelectric device power was provided by a 15 volt, 20 amp DC power supply (Mean Well model SE-600-15, Mean Well USA, Fremont, CA).

Thermotactile device validation. Validation of the equipment included onset time measurement, thermal range quantification, and artifact testing within an MRI scanner suite. Using a computer-based data acquisition system (USB-6008, National Instruments Corp.,

Austin, TX) the mean onset time of thermal change at maximum power was determined to be 416ms with a total range of 362ms to 470ms for hot stimuli and 351ms with a total range of 290ms to 398ms for cold stimuli. The mean time for peg engagement was 192ms with a total range of 185ms to 220ms. Peg engagement time did not depend on air pressure levels within the testing range of 50-65psi.

Using the same data acquisition system the total thermal range of the thermoelectric devices was quantified. Within 750ms the device temperature could reach 130 degrees F at maximum and 25 degrees F at minimum. These parameters were used in the final device calibration to yield equivalent increases and decreases in temperature.

Finally, use of the system within the shielded MRI scanner suite did not generate quantifiable amounts of artifact when tested with a standard MR phantom. This was initially tested by way of standard RF spike testing conducted by a Philips engineer. Additional tests involving voxelwise variance and independent components analysis of MRI phantom data were also completed as a final verification. The only examination shown to cause MR signal artifact was the rapid (3 in/sec) movement of the device within the bore of the magnet. To guard against potential artifacts participants were instructed to limit motion of the device hand blocks during scanning.

Subject-specific calibration scheme. To eliminate individual variability in thermal and tactile sensitivity as a source of error each subject completed a calibration procedure before participation. For temperature calibration a series of thermal events was presented to the subject with increasing temperature. The instructions to the subject were to press the response button when the temperature became painfully hot. The calibration range was then the array of values between zero and the level of the last non-painful event. The tactile calibration was similar, with the adjustment of regulated air pressure to ensure that the subject could quickly perceive the tactile stimuli but that pegs were not accelerated too quickly into the surface of the palm.

Thermotactile threshold testing. Sixteen adult participants (10 females, 6 males) participated in testing of thermal and tactile device parameters. The first aspect of this testing was to determine the minimal thermal change necessary for perception. The starting temperature for all thermal deviation testing was the equilibrium value of the participant's hand as it rested on the device. Participants were asked to rest their hand on the device for 5 minutes before testing to allow thermal equilibrium to take place. For warm stimulation 88% of participants required less than 2º F to perceive a thermal change and 100% of participants could detect a 3º F thermal change. For cool stimulation 94% of participants required less than a 2º F negative change to perceive thermal change and 100% of participants could detect a 3º F negative change. These values are consistent with the results of Bartlett, Stewart, Tamblyn, and Abrahamowicz (1998) and with Golja, Tipton, and Mekjavic (2003) who both found that 100% of individuals could perceive a 2º C warm shift and a 1º C cool shift at a 32º C baseline.

The second part of threshold testing was to determine the minimal air pressure necessary to have a detectable tactile sensation. Air pressure was changed randomly through the use of a variable air pressure regulator controlled manually by the experimenter. The range of the regulator was 10-120psi. A minimum value of 15psi was necessary to engage the pegs due to pressure losses in the pneumatic line and energy required to raise the pegs out of the hand block silos. At this minimum air pressure value 81% of participants could reliably detect the pegs. At 20 psi of air pressure 100% of participants could reliably detect peg engagement. To ensure clear tactile detection a value of 40psi was used as a minimum value for all experiments.

References

Adleman, N. E., Menon, V., Blasey, C. M., White, C. D., Warsofsky, I. S., Glover, G. H., et al. (2002). A developmental fMRI study of the Stroop color-word task. *Neuroimage, 16*(1), 61-75.

Aleman, A. (2005). Feelings you can't imagine: towards a cognitive neuroscience of alexithymia. *Trends Cogn Sci, 9*(12), 553-555.

Allen, G. V., Saper, C. B., Hurley, K. M., & Cechetto, D. F. (1991). Organization of visceral and limbic connections in the insular cortex of the rat. *J Comp Neurol, 311*(1), 1-16.

Andersson, J. L., Hutton, C., Ashburner, J., Turner, R., & Friston, K. (2001). Modeling geometric deformations in EPI time series. *Neuroimage, 13*(5), 903-919.

Ashburner, J., & Friston, K. J. (1999). Nonlinear spatial normalization using basis functions. *Hum Brain Mapp, 7*(4), 254-266.

Ashburner, J., & Friston, K. J. (2000). Voxel-based morphometry--the methods. *Neuroimage, 11*(6 Pt 1), 805-821.

Ashburner, J., Neelin, P., Collins, D. L., Evans, A., & Friston, K. (1997). Incorporating prior knowledge into image registration. *Neuroimage, 6*(4), 344-352.

Augustine, J. R. (1985). The insular lobe in primates including humans. *Neurol Res, 7*(1), 2-10.

Augustine, J. R. (1996). Circuitry and functional aspects of the insular lobe in primates including humans. *Brain Res Brain Res Rev, 22*(3), 229-244.

Baird, A. A., Fugelsang, J., & Bennett, C. M. (in press). "What were you thinking"? A neural signature associated with reasoning in adolescence.".

Baker, G. P., & Morris, K. J. (2002). *Descartes' dualism*. New York: Routledge.

Banati, R. B., Goerres, G. W., Tjoa, C., Aggleton, J. P., & Grasby, P. (2000). The functional anatomy of visual-tactile integration in man: a study using positron emission tomography. *Neuropsychologia, 38*(2), 115-124.

Bannister, R. (1988). Clinical features of autonomic failure: Symptoms, signs, and special investigations. In R. Bannister (Ed.), *Autonomic failure : a textbook of clinical disorders of the autonomic nervous system* (2nd ed., pp. xv, 783 p.). Oxford ; New York: Oxford University Press.

Bannister, R., Mathias, C. J., & Polinsky, R. (1988). Clinical features of autonomic failure: A comparison between UK and US experience. In R. Bannister (Ed.), *Autonomic failure : a textbook of clinical disorders of the autonomic nervous system* (2nd ed., pp. xv, 783 p.). Oxford ; New York: Oxford University Press.

Bartlett, G., Stewart, J. D., Tamblyn, R., & Abrahamowicz, M. (1998). Normal distributions of thermal and vibration sensory thresholds. *Muscle Nerve, 21*(3), 367-374.

Bartzokis, G., Beckson, M., Lu, P. H., Nuechterlein, K. H., Edwards, N., & Mintz, J. (2001). Age-related changes in frontal and temporal lobe volumes in men: a magnetic resonance imaging study. *Arch Gen Psychiatry, 58*(5), 461-465.

Bechara, A., Damasio, H., & Damasio, A. R. (2000). Emotion, decision making and the orbitofrontal cortex. *Cereb Cortex, 10*(3), 295-307.

Beckmann, C. F., & Smith, S. M. (2004). Probabilistic independent component analysis for functional magnetic resonance imaging. *IEEE Trans Med Imaging, 23*(2), 137-152.

Bekker, E. M., Kenemans, J. L., & Verbaten, M. N. (2005). Source analysis of the N2 in a cued Go/NoGo task. *Brain Res Cogn Brain Res, 22*(2), 221-231.

Benes, F. M., Turtle, M., Khan, Y., & Farol, P. (1994). Myelination of a key relay zone in the hippocampal formation occurs in the human brain during childhood, adolescence, and adulthood. *Arch Gen Psychiatry, 51*(6), 477-484.

Bennett, C. M., & Baird, A. A. (2006). Anatomical changes in the emerging adult brain: a voxel-based morphometry study. *Hum Brain Mapp, 27*(9), 766-777.

Berns, G. S., Chappelow, J., Cekic, M., Zink, C. F., Pagnoni, G., & Martin-Skurski, M. E. (2006). Neurobiological substrates of dread. *Science, 312*(5774), 754-758.

Berthier, M., Starkstein, S., & Leiguarda, R. (1988). Asymbolia for pain: a sensory-limbic disconnection syndrome. *Ann Neurol, 24*, 41-49.

Berthoz, S., Artiges, E., Van De Moortele, P. F., Poline, J. B., Rouquette, S., Consoli, S. M., et al. (2002). Effect of impaired recognition and expression of emotions on frontocingulate cortices: an fMRI study of men with alexithymia. *Am J Psychiatry, 159*(6), 961-967.

Bleuler. (1950). *Dementia Praecox of the group of schizophrenias* (J. Zinkin, Trans.). New York: International Universities Press.

Blomqvist, A., Zhang, E. T., & Craig, A. D. (2000). Cytoarchitectonic and immunohistochemical characterization of a specific pain and temperature relay, the posterior portion of the ventral medial nucleus, in the human thalamus. *Brain, 123 Pt 3*, 601-619.

Boecker, H., Jankowski, J., Ditter, P., & Scheef, L. (2008). A role of the basal ganglia and midbrain nuclei for initiation of motor sequences. *Neuroimage, 39*(3), 1356-1369.

Brody, B. A., Kinney, H. C., Kloman, A. S., & Gilles, F. H. (1987). Sequence of central nervous system myelination in human infancy. I. An autopsy study of myelination. *J Neuropathol Exp Neurol, 46*(3), 283-301.

Brooks, J. C., Zambreanu, L., Godinez, A., Craig, A. D., & Tracey, I. (2005). Somatotopic organisation of the human insula to painful heat studied with high resolution functional imaging. *Neuroimage, 27*(1), 201-209.

Buckner, R. L., & Carroll, D. C. (2007). Self-projection and the brain. *Trends Cogn Sci, 11*(2), 49-57.

Bunzeck, N., & Duzel, E. (2006). Absolute coding of stimulus novelty in the human substantia nigra/VTA. *Neuron, 51*(3), 369-379.

Bush, G., Luu, P., & Posner, M. I. (2000). Cognitive and emotional influences in anterior cingulate cortex. *Trends Cogn Sci, 4*(6), 215-222.

Bydlowski, S., Corcos, M., Jeammet, P., Paterniti, S., Berthoz, S., Laurier, C., et al. (2005).

Emotion-processing deficits in eating disorders. *Int J Eat Disord, 37*(4), 321-329.

Cameron, O. G. (2001). Interoception: the inside story--a model for psychosomatic processes. *Psychosom Med, 63*(5), 697-710.

Cameron, O. G. (2002). *Visceral sensory neuroscience : interoception*. Oxford ; New York: Oxford University Press.

Cannon, W. (1914). The interrelations of emotions as suggested by recent psychophysiological researchers. *American Journal of Psychology*(25), 252-282.

Cannon, W. (1927). The James-Lange theory of emotions: A critical examination and an alternative theory. *American Journal of Psychology*(39), 106-124.

Cannon, W. B. (1932). *The wisdom of the body*. New York,: W.W. Norton & Company.

Casey, B., Trainor, R., Orendi, J., Schubert, A., Nystrom, L., Giedd, J., et al. (1997). A developmental functional MRI study of prefrontal activation during performance of a go-no-go task. *Journal of Cognitive Neuroscience, 9*(6), 835-847.

Casey, B. J., Cohen, J. D., Jezzard, P., Turner, R., Noll, D. C., Trainor, R. J., et al. (1995). Activation of prefrontal cortex in children during a nonspatial working memory task with functional MRI. *Neuroimage, 2*(3), 221-229.

Casey, B. J., Tottenham, N., Liston, C., & Durston, S. (2005). Imaging the developing brain: what have we learned about cognitive development? *Trends Cogn Sci, 9*(3), 104-110.

Casey, K. L., Minoshima, S., Morrow, T. J., & Koeppe, R. A. (1996). Comparison of human cerebral activation pattern during cutaneous warmth, heat pain, and deep cold pain. *J Neurophysiol, 76*(1), 571-581.

Chikama, M., McFarland, N. R., Amaral, D. G., & Haber, S. N. (1997). Insular cortical projections to functional regions of the striatum correlate with cortical cytoarchitectonic organization in the primate. *J Neurosci, 17*(24), 9686-9705.

Chiron, C., Raynaud, C., Maziere, B., Zilbovicius, M., Laflamme, L., Masure, M. C., et al. (1992). Changes in regional cerebral blood flow during brain maturation in children

and adolescents. *J Nucl Med, 33*(5), 696-703.

Christmann, C., Koeppe, C., Braus, D. F., Ruf, M., & Flor, H. (2007). A simultaneous EEG-fMRI study of painful electric stimulation. *Neuroimage, 34*(4), 1428-1437.

Ciesielski, K. T., Lesnik, P. G., Savoy, R. L., Grant, E. P., & Ahlfors, S. P. (2006). Developmental neural networks in children performing a Categorical N-Back Task. *Neuroimage, 33*(3), 980-990.

Coghill, R. C., Gilron, I., & Iadarola, M. J. (2001). Hemispheric lateralization of somatosensory processing. *J Neurophysiol, 85*(6), 2602-2612.

Coghill, R. C., Sang, C. N., Maisog, J. M., & Iadarola, M. J. (1999). Pain intensity processing within the human brain: a bilateral, distributed mechanism. *J Neurophysiol, 82*(4), 1934-1943.

Collins, K. (1988). Autonomic control of sweat glands and disorders of sweating. In R. Bannister (Ed.), *Autonomic failure : a textbook of clinical disorders of the autonomic nervous system* (2nd ed., pp. xv, 783 p.). Oxford ; New York: Oxford University Press.

Corwin, J. (1994). On measuring discrimination and response bias: unequal numbers of targets and idstractors and two classes of distractors. *Neuropsychology, 8*, 110-117.

Cotton, J. (1981). A review of research on Schachter's theory of emotion and the misattribution of arousal. *European Journal of Social Psychology*(11), 365-397.

Craig, A. D. (1995). Distribution of brainstem projections from spinal lamina I neurons in the cat and the monkey. *J Comp Neurol, 361*(2), 225-248.

Craig, A. D. (1996). An ascending general homeostatic afferent pathway originating in lamina I. *Prog Brain Res, 107*, 225-242.

Craig, A. D. (2002). How do you feel? Interoception: the sense of the physiological condition of the body. *Nat Rev Neurosci, 3*(8), 655-666.

Craig, A. D. (2003a). A new view of pain as a homeostatic emotion. *Trends Neurosci,*

26(6), 303-307.

Craig, A. D. (2003b). Interoception: the sense of the physiological condition of the body. *Curr Opin Neurobiol, 13*(4), 500-505.

Craig, A. D. (2004a). Distribution of trigeminothalamic and spinothalamic lamina I terminations in the macaque monkey. *J Comp Neurol, 477*(2), 119-148.

Craig, A. D. (2004b). Human feelings: why are some more aware than others? *Trends Cogn Sci, 8*(6), 239-241.

Craig, A. D., Bushnell, M. C., Zhang, E. T., & Blomqvist, A. (1994). A thalamic nucleus specific for pain and temperature sensation. *Nature, 372*(6508), 770-773.

Craig, A. D., Chen, K., Bandy, D., & Reiman, E. M. (2000). Thermosensory activation of insular cortex. *Nat Neurosci, 3*(2), 184-190.

Craig, A. D., & Dostrovsky, J. O. (2001). Differential projections of thermoreceptive and nociceptive lamina I trigeminothalamic and spinothalamic neurons in the cat. *J Neurophysiol, 86*(2), 856-870.

Critchley, H. D. (2005). Neural mechanisms of autonomic, affective, and cognitive integration. *J Comp Neurol, 493*(1), 154-166.

Critchley, H. D., Corfield, D. R., Chandler, M. P., Mathias, C. J., & Dolan, R. J. (2000). Cerebral correlates of autonomic cardiovascular arousal: a functional neuroimaging investigation in humans. *J Physiol, 523 Pt 1*, 259-270.

Critchley, H. D., Elliott, R., Mathias, C. J., & Dolan, R. J. (2000). Neural activity relating to generation and representation of galvanic skin conductance responses: a functional magnetic resonance imaging study. *J Neurosci, 20*(8), 3033-3040.

Critchley, H. D., Good, C. D., Ashburner, J., Frackowiak, R. S., Mathias, C. J., & Dolan, R. J. (2003). Changes in cerebral morphology consequent to peripheral autonomic denervation. *Neuroimage, 18*(4), 908-916.

Critchley, H. D., Mathias, C. J., & Dolan, R. J. (2001). Neuroanatomical basis for first- and second-order representations of bodily states. *Nat Neurosci, 4*(2), 207-212.

Critchley, H. D., Mathias, C. J., Josephs, O., O'Doherty, J., Zanini, S., Dewar, B. K., et al. (2003). Human cingulate cortex and autonomic control: converging neuroimaging and clinical evidence. *Brain, 126*(Pt 10), 2139-2152.

Critchley, H. D., Rotshtein, P., Nagai, Y., O'Doherty, J., Mathias, C. J., & Dolan, R. J. (2005). Activity in the human brain predicting differential heart rate responses to emotional facial expressions. *Neuroimage, 24*(3), 751-762.

Critchley, H. D., Tang, J., Glaser, D., Butterworth, B., & Dolan, R. J. (2005). Anterior cingulate activity during error and autonomic response. *Neuroimage, 27*(4), 885-895.

Critchley, H. D., Wiens, S., Rotshtein, P., Ohman, A., & Dolan, R. J. (2004). Neural systems supporting interoceptive awareness. *Nat Neurosci, 7*(2), 189-195.

Cross, E., Bennett, C. M., Grafton, S., & Baird, A. A. (2006). *Functional and anatomical differences between the adolescent and young adult brain in primary motor cortex: Evidence from functional neuroimaging and diffusion tensor imaging.* Paper presented at the 12th Annual Meeting of the Organization for Human Brain Mapping, Florence, Italy.

Dalgleish, T. (2004). The emotional brain. *Nat Rev Neurosci, 5*(7), 583-589.

Damasio, A. R. (1994). *Descartes' error : emotion, reason, and the human brain*. New York: Putnam.

Damasio, A. R. (1996). The somatic marker hypothesis and the possible functions of the prefrontal cortex. *Philos Trans R Soc Lond B Biol Sci, 351*(1346), 1413-1420.

Darwin, C. (1859). *On the origin of species by means of natural selection*. London,: J. Murray.

Darwin, C. (1872). *The expression of the emotions in man and animals*. London,: J. Murray.

Decety, J., & Grezes, J. (2006). The power of simulation: imagining one's own and other's behavior. *Brain Res, 1079*(1), 4-14.

Deichmann, R., Gottfried, J. A., Hutton, C., & Turner, R. (2003). Optimized EPI for fMRI studies of the orbitofrontal cortex. *Neuroimage, 19*(2 Pt 1), 430-441.

Della Rocca, M. (1996). *Representation and the mind-body problem in Spinoza*. New York: Oxford University Press.

DelParigi, A., Chen, K., Salbe, A. D., Reiman, E. M., & Tataranni, P. A. (2005). Sensory experience of food and obesity: a positron emission tomography study of the brain regions affected by tasting a liquid meal after a prolonged fast. *Neuroimage, 24*(2), 436-443.

Descartes, R. (1990). *Descartes : selected philosophical writings*. Cambridge ; New York: Cambridge University Press.

Dosenbach, N. U., Fair, D. A., Miezin, F. M., Cohen, A. L., Wenger, K. K., Dosenbach, R. A., et al. (2007). Distinct brain networks for adaptive and stable task control in humans. *Proc Natl Acad Sci U S A, 104*(26), 11073-11078.

Dosenbach, N. U., Visscher, K. M., Palmer, E. D., Miezin, F. M., Wenger, K. K., Kang, H. C., et al. (2006). A core system for the implementation of task sets. *Neuron, 50*(5), 799-812.

Dresel, C., Parzinger, A., Rimpau, C., Zimmer, C., Ceballos-Baumann, A. O., & Haslinger, B. (2008). A new device for tactile stimulation during fMRI. *Neuroimage, 39*(3), 1094-1103.

Dunn, B. D., Dalgleish, T., Ogilvie, A. D., & Lawrence, A. D. (2007). Heartbeat perception in depression. *Behav Res Ther, 45*(8), 1921-1930.

Dupont, S., Bouilleret, V., Hasboun, D., Semah, F., & Baulac, M. (2003). Functional anatomy of the insula: new insights from imaging. *Surg Radiol Anat, 25*(2), 113-119.

Durston, S., Davidson, M. C., Tottenham, N., Galvan, A., Spicer, J., Fossella, J. A., et al. (2006). A shift from diffuse to focal cortical activity with development. *Dev Sci, 9*(1), 1-8.

Durston, S., Tottenham, N. T., Thomas, K. M., Davidson, M. C., Eigsti, I. M., Yang, Y., et al. (2003). Differential patterns of striatal activation in young children with and without ADHD. *Biol Psychiatry, 53*(10), 871-878.

Edwards, J., Pattison, P. E., Jackson, H. J., & Wales, R. J. (2001). Facial affect and affective prosody recognition in first-episode schizophrenia. *Schizophr Res, 48*(2-3), 235-253.

Ehlers, A., & Breuer, P. (1996). How good are patients with panic disorder at perceiving their heartbeats? *Biol Psychol, 42*(1-2), 165-182.

Eickhoff, S. B., Lotze, M., Wietek, B., Amunts, K., Enck, P., & Zilles, K. (2006). Segregation of visceral and somatosensory afferents: an fMRI and cytoarchitectonic mapping study. *Neuroimage, 31*(3), 1004-1014.

Eley, T. C., Stirling, L., Ehlers, A., Gregory, A. M., & Clark, D. M. (2004). Heart-beat perception, panic/somatic symptoms and anxiety sensitivity in children. *Behav Res Ther, 42*(4), 439-448.

Ernst, M., Nelson, E. E., Jazbec, S., McClure, E. B., Monk, C. S., Leibenluft, E., et al. (2005). Amygdala and nucleus accumbens in responses to receipt and omission of gains in adults and adolescents. *Neuroimage, 25*(4), 1279-1291.

Estes, D. (1998). Young children's awareness of their mental activity: the case of mental rotation. *Child Dev, 69*(5), 1345-1360.

Farah, M. J. (1984). The neurological basis of mental imagery: a componential analysis. *Cognition, 18*(1-3), 245-272.

Flechsig, P. (1920). *Anatomie des Menschlichen Gehirns und Rückenmarks auf Myelogenetischer Grundlage*. Leipzig, Germany: Thieme.

Friston, K. J., Ashburner, J., Frith, C. D., Poline, J.-B., Heather, J. D., & Frackowiak, R. S. (1995). Spatial Registration and Normalization of Images. *Human Brain Mapping, 2*, 165-189.

Frot, M., Magnin, M., Mauguiere, F., & Garcia-Larrea, L. (2006). Human SII and Posterior

Insula Differently Encode Thermal Laser Stimuli. *Cereb Cortex*.

Frot, M., Magnin, M., Mauguiere, F., & Garcia-Larrea, L. (2007). Human SII and posterior insula differently encode thermal laser stimuli. *Cereb Cortex, 17*(3), 610-620.

Fulbright, R. K., Troche, C. J., Skudlarski, P., Gore, J. C., & Wexler, B. E. (2001). Functional MR imaging of regional brain activation associated with the affective experience of pain. *AJR Am J Roentgenol, 177*(5), 1205-1210.

Funk, M., Brugger, P., & Wilkening, F. (2005). Motor processes in children's imagery: the case of mental rotation of hands. *Dev Sci, 8*(5), 402-408.

Galvan, A., Hare, T. A., Parra, C. E., Penn, J., Voss, H., Glover, G., et al. (2006). Earlier development of the accumbens relative to orbitofrontal cortex might underlie risk-taking behavior in adolescents. *J Neurosci, 26*(25), 6885-6892.

Ganis, G., Keenan, J. P., Kosslyn, S. M., & Pascual-Leone, A. (2000). Transcranial magnetic stimulation of primary motor cortex affects mental rotation. *Cereb Cortex, 10*(2), 175-180.

Genovese, C. R., Lazar, N. A., & Nichols, T. (2002). Thresholding of statistical maps in functional neuroimaging using the false discovery rate. *Neuroimage, 15*(4), 870-878.

George, M. S., Ketter, T. A., Parekh, P. I., Horwitz, B., Herscovitch, P., & Post, R. M. (1995). Brain activity during transient sadness and happiness in healthy women. *Am J Psychiatry, 152*(3), 341-351.

Giedd, J. N., Blumenthal, J., Jeffries, N. O., Castellanos, F. X., Liu, H., Zijdenbos, A., et al. (1999). Brain development during childhood and adolescence: a longitudinal MRI study. *Nat Neurosci, 2*(10), 861-863.

Gitelman, D. (1998). spm_slice_timing (Version v1.1). Chicago, IL.

Gogtay, N., Giedd, J. N., Lusk, L., Hayashi, K. M., Greenstein, D., Vaituzis, A. C., et al. (2004). Dynamic mapping of human cortical development during childhood through early adulthood. *Proc Natl Acad Sci U S A, 101*(21), 8174-8179.

Golja, P., Tipton, M., & Mekjavic, I. (2003). Cutaneous thermal thresholds-the reproducibility of their measurements and the effect of gender. *Journal of Thermal Biology, 28*(4), 341-346.

Green, M. F., Kern, R. S., Braff, D. L., & Mintz, J. (2000). Neurocognitive deficits and functional outcome in schizophrenia: are we measuring the "right stuff"? *Schizophr Bull, 26*(1), 119-136.

Grefkes, C., & Fink, G. R. (2005). The functional organization of the intraparietal sulcus in humans and monkeys. *J Anat, 207*(1), 3-17.

Grefkes, C., Weiss, P. H., Zilles, K., & Fink, G. R. (2002). Crossmodal processing of object features in human anterior intraparietal cortex: an fMRI study implies equivalencies between humans and monkeys. *Neuron, 35*(1), 173-184.

Guillery, R. W. (2005). Is postnatal neocortical maturation hierarchical? *Trends Neurosci, 28*(10), 512-517.

Hague, K., Lento, P., Morgello, S., Caro, S., & Kaufmann, H. (1997). The distribution of Lewy bodies in pure autonomic failure: autopsy findings and review of the literature. *Acta Neuropathol (Berl), 94*(2), 192-196.

Heims, H. C., Critchley, H. D., Dolan, R., Mathias, C. J., & Cipolotti, L. (2004). Social and motivational functioning is not critically dependent on feedback of autonomic responses: neuropsychological evidence from patients with pure autonomic failure. *Neuropsychologia, 42*(14), 1979-1988.

Heims, H. C., Critchley, H. D., Martin, N. H., Jager, H. R., Mathias, C. J., & Cipolotti, L. (2006). Cognitive functioning in orthostatic hypotension due to pure autonomic failure. *Clin Auton Res, 16*(2), 113-120.

Henderson, L. A., Gandevia, S. C., & Macefield, V. G. (2007). Somatotopic organization of the processing of muscle and cutaneous pain in the left and right insula cortex: a single-trial fMRI study. *Pain, 128*(1-2), 20-30.

Hendry, S., Hsiao, S., & Brown, M. (2003). Fundamentals of Sensory Systems. In L. Squire,

F. Bloom, S. McConnell, J. Roberts, N. Spitzer & M. Zigmond (Eds.), *Fundamental Neuroscience*. San Diego: Academic Press.

Herrmann, M. J., Plichta, M. M., Ehlis, A. C., & Fallgatter, A. J. (2005). Optical topography during a Go-NoGo task assessed with multi-channel near-infrared spectroscopy. *Behav Brain Res, 160*(1), 135-140.

Horan, W. P., Kring, A. M., & Blanchard, J. J. (2006). Anhedonia in schizophrenia: a review of assessment strategies. *Schizophr Bull, 32*(2), 259-273.

Hua le, H., Strigo, I. A., Baxter, L. C., Johnson, S. C., & Craig, A. D. (2005). Anteroposterior somatotopy of innocuous cooling activation focus in human dorsal posterior insular cortex. *Am J Physiol Regul Integr Comp Physiol, 289*(2), R319-R325.

Huang, R. S., & Sereno, M. I. (2007). Dodecapus: An MR-compatible system for somatosensory stimulation. *Neuroimage, 34*(3), 1060-1073.

Hunter, S. F., Leavitt, J. A., & Rodriguez, M. (1997). Direct observation of myelination in vivo in the mature human central nervous system. A model for the behaviour of oligodendrocyte progenitors and their progeny. *Brain, 120 (Pt 11)*, 2071-2082.

Hurliman, E., Nagode, J. C., & Pardo, J. V. (2005). Double dissociation of exteroceptive and interoceptive feedback systems in the orbital and ventromedial prefrontal cortex of humans. *J Neurosci, 25*(18), 4641-4648.

Hyvarinen, A., & Pajunen, P. (1999). Nonlinear independent component analysis: Existence and uniqueness results. *Neural Netw, 12*(3), 429-439.

Iannetti, G. D., Truini, A., Romaniello, A., Galeotti, F., Rizzo, C., Manfredi, M., et al. (2003). Evidence of a specific spinal pathway for the sense of warmth in humans. *J Neurophysiol, 89*(1), 562-570.

James, W. (1890). *The principles of psychology*. New York,: H. Holt and company.

Jeannerod, M., & Decety, J. (1995). Mental motor imagery: a window into the representational stages of action. *Curr Opin Neurobiol, 5*(6), 727-732.

Job, D. E., Whalley, H. C., McConnell, S., Glabus, M., Johnstone, E. C., & Lawrie, S. M.

(2002). Structural gray matter differences between first-episode schizophrenics and normal controls using voxel-based morphometry. *Neuroimage, 17*(2), 880-889.

Johnson, M. (1997). *Developmental Cognitive Neuroscience*. Oxford: Blackwell.

Jones, E. G., & Burton, H. (1976). Areal differences in the laminar distribution of thalamic afferents in cortical fields of the insular, parietal and temporal regions of primates. *J Comp Neurol, 168*(2), 197-247.

Jones, G. (1994). Perception of visceral sensations: A review of recent findings. In J. Jennings, P. Ackles & M. Coles (Eds.), *Advances in Psychophysiology* (Vol. 5, pp. 55-192). London: Jessica Kingsly Publishers.

Kang, H. C., Burgund, E. D., Lugar, H. M., Petersen, S. E., & Schlaggar, B. L. (2003). Comparison of functional activation foci in children and adults using a common stereotactic space. *Neuroimage, 19*(1), 16-28.

Kano, M., Fukudo, S., Gyoba, J., Kamachi, M., Tagawa, M., Mochizuki, H., et al. (2003). Specific brain processing of facial expressions in people with alexithymia: an H2 15O-PET study. *Brain, 126*(Pt 6), 1474-1484.

Kaufmann, H., Hague, K., & Perl, D. (2001). Accumulation of alpha-synuclein in autonomic nerves in pure autonomic failure. *Neurology, 56*(7), 980-981.

Kleber, B., Birbaumer, N., Veit, R., Trevorrow, T., & Lotze, M. (2007). Overt and imagined singing of an Italian aria. *Neuroimage, 36*(3), 889-900.

Kohlberg, L. (1984). *The psychology of moral development : the nature and validity of moral stages* (1st ed.). San Francisco: Harper & Row.

Kohler, C. G., Bilker, W., Hagendoorn, M., Gur, R. E., & Gur, R. C. (2000). Emotion recognition deficit in schizophrenia: association with symptomatology and cognition. *Biol Psychiatry, 48*(2), 127-136.

Kosslyn, S. M., Ganis, G., & Thompson, W. L. (2001). Neural foundations of imagery. *Nat Rev Neurosci, 2*(9), 635-642.

Kosslyn, S. M., Margolis, J. A., Barrett, A. M., Goldknopf, E. J., & Daly, P. F. (1990). Age

differences in imagery abilities. *Child Dev, 61*(4), 995-1010.

Kosslyn, S. M., Thompson, W. L., Costantini-Ferrando, M. F., Alpert, N. M., & Spiegel, D. (2000). Hypnotic visual illusion alters color processing in the brain. *Am J Psychiatry, 157*(8), 1279-1284.

Kosslyn, S. M., Thompson, W. L., Kim, I. J., & Alpert, N. M. (1995). Topographical representations of mental images in primary visual cortex. *Nature, 378*(6556), 496-498.

Kraemer, D. J., Macrae, C. N., Green, A. E., & Kelley, W. M. (2005). Musical imagery: sound of silence activates auditory cortex. *Nature, 434*(7030), 158.

Kringelbach, M. L. (2005). The human orbitofrontal cortex: linking reward to hedonic experience. *Nat Rev Neurosci, 6*(9), 691-702.

Kucian, K., von Aster, M., Loenneker, T., Dietrich, T., Mast, F. W., & Martin, E. (2007). Brain activation during mental rotation in school children and adults. *J Neural Transm, 114*(5), 675-686.

Kuhtz-Buschbeck, J. P., van der Horst, C., Pott, C., Wolff, S., Nabavi, A., Jansen, O., et al. (2005). Cortical representation of the urge to void: a functional magnetic resonance imaging study. *J Urol, 174*(4 Pt 1), 1477-1481.

Lacerda, A. L., Hardan, A. Y., Yorbik, O., Vemulapalli, M., Prasad, K. M., & Keshavan, M. S. (2007). Morphology of the orbitofrontal cortex in first-episode schizophrenia: relationship with negative symptomatology. *Prog Neuropsychopharmacol Biol Psychiatry, 31*(2), 510-516.

Lane, R. D., Sechrest, L., Reidel, R., Weldon, V., Kaszniak, A., & Schwartz, G. E. (1996). Impaired verbal and nonverbal emotion recognition in alexithymia. *Psychosom Med, 58*(3), 203-210.

Lane, R. D., Sechrest, L., Riedel, R., Shapiro, D. E., & Kaszniak, A. W. (2000). Pervasive emotion recognition deficit common to alexithymia and the repressive coping style. *Psychosom Med, 62*(4), 492-501.

Lange, C. G., James, W., & Haupt, I. A. (1922). *The Emotions*. Baltimore,: Williams & Wilkins Company.

Le Bihan, D. (2003). Looking into the functional architecture of the brain with diffusion MRI. *Nat Rev Neurosci, 4*(6), 469-480.

Leone, M., Proietti Cecchini, A., Mea, E., Tullo, V., Curone, M., & Bussone, G. (2006). Neuroimaging and pain: a window on the autonomic nervous system. *Neurol Sci, 27 Suppl 2*, S134-137.

Loewenstein, G., & Lerner, J. (Eds.). (2003). *The role of affect in decision making*. Oxford: Oxford University Press.

Ludwick-Rosenthal, R., & Neufeld, R. W. (1985). Heart beat interoception: a study of individual differences. *Int J Psychophysiol, 3*(1), 57-65.

Luna, B., & Sweeney, J. A. (2004). The emergence of collaborative brain function: FMRI studies of the development of response inhibition. *Ann N Y Acad Sci, 1021*, 296-309.

Luna, B., Thulborn, K. R., Munoz, D. P., Merriam, E. P., Garver, K. E., Minshew, N. J., et al. (2001). Maturation of widely distributed brain function subserves cognitive development. *Neuroimage, 13*(5), 786-793.

Macmillan, N., & Creelman, C. (1991). *Detection theory: a user's guide*. Cambridge, England: Cambridge University Press.

Macwhinney, B., Cohen, J., & Provost, J. (1997). The PsyScope experiment-building system. *Spat Vis, 11*(1), 99-101.

Magnifico, F., Misra, V. P., Murray, N. M., & Mathias, C. J. (1998). The sympathetic skin response in peripheral autonomic failure--evaluation in pure failure, pure cholinergic dysautonomia and dopamine-beta-hydroxylase deficiency. *Clin Auton Res, 8*(3), 133-138.

Mantani, T., Okamoto, Y., Shirao, N., Okada, G., & Yamawaki, S. (2005). Reduced activation of posterior cingulate cortex during imagery in subjects with high degrees

of alexithymia: a functional magnetic resonance imaging study. *Biol Psychiatry, 57*(9), 982-990.

Marmor, G. (1975). Development of kinetic images: when does the child first represent movement in mental images? *Cognitive Psychology, 7*, 548-559.

Mason, O., Startup, M., Halpin, S., Schall, U., Conrad, A., & Carr, V. (2004). Risk factors for transition to first episode psychosis among individuals with 'at-risk mental states'. *Schizophr Res, 71*(2-3), 227-237.

May, J. C., Delgado, M. R., Dahl, R. E., Stenger, V. A., Ryan, N. D., Fiez, J. A., et al. (2004). Event-related functional magnetic resonance imaging of reward-related brain circuitry in children and adolescents. *Biol Psychiatry, 55*(4), 359-366.

Mazaika, P., Whitfield, S., & Cooper, J. (2005). *Detection and Repair of Transient Artifacts in fMRI Data*. Paper presented at the Human Brain Mapping conference.

Mazaika, P., Whitfield-Gabrieli, S., & Reiss, A. (2007). *Artifact Repair for fMRI Data from High Motion Clinical Subjects*. Paper presented at the Human Brain Mapping conference.

Mazziotta, J. C., Toga, A. W., Evans, A., Fox, P., & Lancaster, J. (1995). A probabilistic atlas of the human brain: theory and rationale for its development. The International Consortium for Brain Mapping (ICBM). *Neuroimage, 2*(2), 89-101.

McGivern, R. F., Andersen, J., Byrd, D., Mutter, K. L., & Reilly, J. (2002). Cognitive efficiency on a match to sample task decreases at the onset of puberty in children. *Brain Cogn, 50*(1), 73-89.

McGlone, F., Kelly, E. F., Trulsson, M., Francis, S. T., Westling, G., & Bowtell, R. (2002). Functional neuroimaging studies of human somatosensory cortex. *Behav Brain Res, 135*(1-2), 147-158.

McKinley, M. J., Denton, D. A., Oldfield, B. J., De Oliveira, L. B., & Mathai, M. L. (2006). Water intake and the neural correlates of the consciousness of thirst. *Semin Nephrol, 26*(3), 249-257.

Mesulam, M. M., & Mufson, E. J. (1982). Insula of the old world monkey. I. Architectonics in the insulo-orbito-temporal component of the paralimbic brain. *J Comp Neurol, 212*(1), 1-22.

Minka, T. (2000). Automatic choice of dimensionality for PCA, *Technica Report 514*. MIT Media Laboratory, Perceptual Computing Section.

Mochizuki, H., Sadato, N., Saito, D. N., Toyoda, H., Tashiro, M., Okamura, N., et al. (2007). Neural correlates of perceptual difference between itching and pain: a human fMRI study. *Neuroimage, 36*(3), 706-717.

Mori, S., & van Zijl, P. C. (2002). Fiber tracking: principles and strategies - a technical review. *NMR Biomed, 15*(7-8), 468-480.

Morrison, S. F. (2001). Differential regulation of brown adipose and splanchnic sympathetic outflows in rat: roles of raphe and rostral ventrolateral medulla neurons. *Clin Exp Pharmacol Physiol, 28*(1-2), 138-143.

Moulton, E. A., Keaser, M. L., Gullapalli, R. P., & Greenspan, J. D. (2005). Regional intensive and temporal patterns of functional MRI activation distinguishing noxious and innocuous contact heat. *J Neurophysiol, 93*(4), 2183-2193.

Mukherjee, P., & McKinstry, R. C. (2006). Diffusion tensor imaging and tractography of human brain development. *Neuroimaging Clin N Am, 16*(1), 19-43, vii.

Murray, W. B., & Foster, P. A. (1996). The peripheral pulse wave: information overlooked. *J Clin Monit, 12*(5), 365-377.

Naidich, T. P., Kang, E., Fatterpekar, G. M., Delman, B. N., Gultekin, S. H., Wolfe, D., et al. (2004). The insula: anatomic study and MR imaging display at 1.5 T. *AJNR Am J Neuroradiol, 25*(2), 222-232.

Naqvi, N. H., Rudrauf, D., Damasio, H., & Bechara, A. (2007). Damage to the insula disrupts addiction to cigarette smoking. *Science, 315*(5811), 531-534.

Nauta, W. J. (1971). The problem of the frontal lobe: a reinterpretation. *J Psychiatr Res, 8*(3), 167-187.

Neafsey, E. J., Hurley-Gius, K. M., & Arvanitis, D. (1986). The topographical organization of neurons in the rat medial frontal, insular and olfactory cortex projecting to the solitary nucleus, olfactory bulb, periaqueductal gray and superior colliculus. *Brain Res, 377*(2), 561-570.

Nelson, A. J., Staines, W. R., Graham, S. J., & McIlroy, W. E. (2004). Activation in SI and SII: the influence of vibrotactile amplitude during passive and task-relevant stimulation. *Brain Res Cogn Brain Res, 19*(2), 174-184.

Paulus, M. P., Feinstein, J. S., Leland, D., & Simmons, A. N. (2005). Superior temporal gyrus and insula provide response and outcome-dependent information during assessment and action selection in a decision-making situation. *Neuroimage, 25*(2), 607-615.

Paulus, M. P., Rogalsky, C., Simmons, A., Feinstein, J. S., & Stein, M. B. (2003). Increased activation in the right insula during risk-taking decision making is related to harm avoidance and neuroticism. *Neuroimage, 19*(4), 1439-1448.

Penfield, W., & Faulk, M. (1955). The insula: Further observations on its function. *Brain, 78*(December), 445-470.

Perl, E. R. (2007). Ideas about pain, a historical view. *Nat Rev Neurosci, 8*(1), 71-80.

Peterson, B. S., Skudlarski, P., Gatenby, J. C., Zhang, H., Anderson, A. W., & Gore, J. C. (1999). An fMRI study of Stroop word-color interference: evidence for cingulate subregions subserving multiple distributed attentional systems. *Biol Psychiatry, 45*(10), 1237-1258.

Piaget, J. (1954). *Das moralische Urteil beim Kinde*. [Zürich]: Rascher.

Ploner, M., Freund, H.-J., & Schnitzler, A. (1999). Pain affect without pain sensation in a patient with a postcentral lesion. *Pain*(81), 211-214.

Pollatos, O., Herbert, B. M., Matthias, E., & Schandry, R. (2007). Heart rate response after emotional picture presentation is modulated by interoceptive awareness. *Int J Psychophysiol, 63*(1), 117-124.

Pollatos, O., Kirsch, W., & Schandry, R. (2005). On the relationship between interoceptive awareness, emotional experience, and brain processes. *Brain Res Cogn Brain Res, 25*(3), 948-962.

Pollatos, O., Traut-Mattausch, E., Schroeder, H., & Schandry, R. (2007). Interoceptive awareness mediates the relationship between anxiety and the intensity of unpleasant feelings. *J Anxiety Disord, 21*(7), 931-943.

Pollock, R. A., Carter, A. S., Amir, N., & Marks, L. E. (2006). Anxiety sensitivity and auditory perception of heartbeat. *Behav Res Ther, 44*(12), 1739-1756.

Price, D. D. (2002). Central neural mechanisms that interrelate sensory and affective dimensions of pain. *Mol Interv, 2*(6), 392-403, 339.

Ramnani, N., Behrens, T. E., Penny, W., & Matthews, P. M. (2004). New approaches for exploring anatomical and functional connectivity in the human brain. *Biol Psychiatry, 56*(9), 613-619.

Reed, S., Harver, A., & Katkin, E. (1990). Interoception. In J. Cacioppo & L. Tassinary (Eds.), *Principles of psychophysiology: Physiocal, social, an inferential elements* (pp. 253-291). New York: Cambridge University Press.

Reisenzein, R. (1983). The Schachter theory of emotion: two decades later. *Psychol Bull, 94*(2), 239-264.

Reiss, A. L., Abrams, M. T., Singer, H. S., Ross, J. L., & Denckla, M. B. (1996). Brain development, gender and IQ in children. A volumetric imaging study. *Brain, 119 (Pt 5)*, 1763-1774.

Rolls, E. T. (2006). Brain mechanisms underlying flavour and appetite. *Philos Trans R Soc Lond B Biol Sci, 361*(1471), 1123-1136.

Romanski, L. M. (2007). Representation and integration of auditory and visual stimuli in the primate ventral lateral prefrontal cortex. *Cereb Cortex, 17 Suppl 1*, i61-69.

Rowe, M. J., Turman, A. B., Murray, G. M., & Zhang, H. Q. (1996). Parallel organization of somatosensory cortical areas I and II for tactile processing. *Clin Exp Pharmacol*

Physiol, 23(10-11), 931-938.

Rypma, B., Berger, J. S., Prabhakaran, V., Martin Bly, B., Kimberg, D. Y., Biswal, B. B., et al. (2006). Neural correlates of cognitive efficiency. *Neuroimage, 33*(3), 969-979.

Saleem, K. S., Kondo, H., & Price, J. L. (2008). Complementary circuits connecting the orbital and medial prefrontal networks with the temporal, insular, and opercular cortex in the macaque monkey. *J Comp Neurol, 506*(4), 659-693.

Saper, C. B. (2002). The central autonomic nervous system: conscious visceral perception and autonomic pattern generation. *Annu Rev Neurosci, 25*, 433-469.

Saze, T., Hirao, K., Namiki, C., Fukuyama, H., Hayashi, T., & Murai, T. (2007). Insular volume reduction in schizophrenia. *Eur Arch Psychiatry Clin Neurosci, 257*(8), 473-479.

Schachter, S., & Singer, J. E. (1962). Cognitive, social, and physiological determinants of emotional state. *Psychol Rev, 69*, 379-399.

Schachter, S., & Wheeler, L. (1962). Epinephrine, chlorpromazine, and amusement. *J Abnorm Soc Psychol, 65*, 121-128.

Schilder, P., & Stengel, E. (1931). Asymbolia for pain. *Arch Neurol Psychiatry, 25*, 598-600.

Schreckenberger, M., Siessmeier, T., Viertmann, A., Landvogt, C., Buchholz, H. G., Rolke, R., et al. (2005). The unpleasantness of tonic pain is encoded by the insular cortex. *Neurology, 64*(7), 1175-1183.

Seeley, W. W., Menon, V., Schatzberg, A. F., Keller, J., Glover, G. H., Kenna, H., et al. (2007). Dissociable intrinsic connectivity networks for salience processing and executive control. *J Neurosci, 27*(9), 2349-2356.

Sherrington, C. S. (1906). *The integrative action of the nervous system*. New York,: C. Scribner's sons.

Shi, C. J., & Cassell, M. D. (1998). Cortical, thalamic, and amygdaloid connections of the anterior and posterior insular cortices. *J Comp Neurol, 399*(4), 440-468.

Shumeiko, N. S. (1998). Age-related changes in the cytoarchitectonics of the human sensorimotor cortex. *Neurosci Behav Physiol, 28*(4), 345-348.

Sifneos, P. E. (1972). *Short-term psychotherapy and emotional crisis*. Cambridge, Mass.,: Harvard University Press.

Simons, J. S., Davis, S. W., Gilbert, S. J., Frith, C. D., & Burgess, P. W. (2006). Discriminating imagined from perceived information engages brain areas implicated in schizophrenia. *Neuroimage, 32*(2), 696-703.

Sowell, E. R., Thompson, P. M., Holmes, C. J., Jernigan, T. L., & Toga, A. W. (1999). In vivo evidence for post-adolescent brain maturation in frontal and striatal regions. *Nat Neurosci, 2*(10), 859-861.

Sowell, E. R., Thompson, P. M., Tessner, K. D., & Toga, A. W. (2001). Mapping continued brain growth and gray matter density reduction in dorsal frontal cortex: Inverse relationships during postadolescent brain maturation. *J Neurosci, 21*(22), 8819-8829.

Sowell, E. R., Thompson, P. M., & Toga, A. W. (2004). Mapping changes in the human cortex throughout the span of life. *Neuroscientist, 10*(4), 372-392.

Spinoza, B. d., Boyle, A., & Parkinson, G. H. R. (1989). *Ethics*. London: J.M. Dent; C.E. Tuttle.

Stenger, V. A., Boada, F. E., & Noll, D. C. (2000). Three-dimensional tailored RF pulses for the reduction of susceptibility artifacts in T(*)(2)-weighted functional MRI. *Magn Reson Med, 44*(4), 525-531.

Stewart, S. H., Buffett-Jerrott, S. E., & Kokaram, R. (2001). Heartbeat awareness and heart rate reactivity in anxiety sensitivity: a further investigation. *J Anxiety Disord, 15*(6), 535-553.

Symonds, L. L., Gordon, N. S., Bixby, J. C., & Mande, M. M. (2006). Right-lateralized pain processing in the human cortex: an FMRI study. *J Neurophysiol, 95*(6), 3823-3830.

Tamm, L., Menon, V., & Reiss, A. L. (2002). Maturation of brain function associated with response inhibition. *J Am Acad Child Adolesc Psychiatry, 41*(10), 1231-1238.

Taylor, G. J., Bagby, R. M., & Parker, J. D. A. (1997). *Disorders of affect regulation : alexithymia in medical and psychiatric illness*. Cambridge ; New York: Cambridge University Press.

Terreberry, R. R., & Neafsey, E. J. (1983). Rat medial frontal cortex: a visceral motor region with a direct projection to the solitary nucleus. *Brain Res, 278*(1-2), 245-249.

Thompson, P. M., Giedd, J. N., Woods, R. P., MacDonald, D., Evans, A. C., & Toga, A. W. (2000). Growth Patterns in the Developing Brain Detected by Using Continuum Mechanical Tensor Maps. *Nature, 404*, 190-193.

Tohka, J., Foerde, K., Aron, A. R., Tom, S. M., Toga, A. W., & Poldrack, R. A. (2008). Automatic independent component labeling for artifact removal in fMRI. *Neuroimage, 39*(3), 1227-1245.

Ture, U., Yasargil, D. C., Al-Mefty, O., & Yasargil, M. G. (1999). Topographic anatomy of the insular region. *J Neurosurg, 90*(4), 720-733.

Van Bogaert, P., Wikler, D., Damhaut, P., Szliwowski, H. B., & Goldman, S. (1998). Regional changes in glucose metabolism during brain development from the age of 6 years. *Neuroimage, 8*(1), 62-68.

Varnavas, G. G., & Grand, W. (1999). The insular cortex: morphological and vascular anatomic characteristics. *Neurosurgery, 44*(1), 127-136; discussion 136-128.

Vogt, B. A. (2005). Pain and emotion interactions in subregions of the cingulate gyrus. *Nat Rev Neurosci, 6*(7), 533-544.

Waber, D. P., Carlson, D., & Mann, M. (1982). Developmental and differential aspects of mental rotation in early adolescence. *Child Dev, 53*(6), 1614-1621.

Wilson, J. L., Jenkinson, M., & Jezzard, P. (2002). Optimization of static field homogeneity in human brain using diamagnetic passive shims. *Magn Reson Med, 48*(5), 906-914.

Yakovlev, P. I., & Lecours, A. R. (1967). The Myelogenetic Cycles of Regional Maturation of the Brain. In A. Minkowski (Ed.), *Regional Development of the Brain in Early Life* (pp. 3-70). Oxford: Blackwell.

Yoo, S. S., Freeman, D. K., McCarthy, J. J., 3rd, & Jolesz, F. A. (2003). Neural substrates of tactile imagery: a functional MRI study. *Neuroreport, 14*(4), 581-585.

Zatorre, R. J., & Halpern, A. R. (2005). Mental concerts: musical imagery and auditory cortex. *Neuron, 47*(1), 9-12.

Zoellner, L. A., & Craske, M. G. (1999). Interoceptive accuracy and panic. *Behav Res Ther, 37*(12), 1141-1158.